



ELSEVIER

Available online at www.sciencedirect.com

SCIENCE @ DIRECT®

Progress in Oceanography 58 (2003) 43–114

**Progress in
Oceanography**

www.elsevier.com/locate/pocean

A new extended Gibbs thermodynamic potential of seawater

Rainer Feistel *

Baltic Sea Research Institute, D-18119 Warnemünde, Germany

Received 3 February 2003; revised 5 May 2003; accepted 5 June 2003

Abstract

A new and extended Gibbs thermodynamic potential function of seawater is proposed to overcome generally known weaknesses of the International Equation of State of Seawater 1980 and its associated formulas (EOS80). It is valid for applied pressures up to 100 MPa (10,000 dbar), temperatures from -2 – 40°C , and practical salinities up to 42. At ambient pressure, it is applicable in heat capacity and density up to salinity 50. It includes the triple point of water for reference and is, over its range of validity, fully consistent with the current 1995 international scientific pure water standard, IAPWS95. In conjunction with an improved Gibbs potential of ice, it provides freezing temperatures of seawater for pressures up to 50 MPa (5000 dbar). It is compiled from an extensive set of experimental seawater data, rather than being derived from EOS80 equations. Older seawater data were specifically recalibrated for compatibility with the recent pure water standard. By this procedure, experimental high-pressure densities proved consistent with sound speeds confirmed by deep-sea travel time measurements. Temperatures of maximum density are described within their experimental uncertainty. For very low salinities, Debye-Hückel limiting laws are recompiled using latest physical and chemical constants. The potential function is expressed in the 1990 International Temperature Scale ITS-90.

© 2003 Elsevier Ltd. All rights reserved.

Contents

| | |
|---|----|
| 1. Introduction | 44 |
| 2. Heat capacity of water | 51 |
| 3. Thermal expansion of water | 53 |
| 4. Density of water | 54 |
| 5. Compressibility of water | 58 |
| 6. Free enthalpy of water | 63 |

* Tel.: +49-381-5197-152; fax: +49-381-5197-4818.

E-mail address: rainer.feistel@io-warnemuende.de (R. Feistel).

| | | |
|-----|---|----|
| 7. | Density of seawater | 64 |
| 8. | Heat capacity of seawater | 68 |
| 9. | Thermal expansion of seawater | 70 |
| 10. | Sound speed in seawater | 70 |
| 11. | High-pressure density of seawater | 75 |
| 12. | Limiting laws | 79 |
| 13. | Freezing point of seawater | 82 |
| 14. | Mixing heat of seawater | 85 |
| 15. | Conclusion | 89 |

1. Introduction

At present, the most important international standard formulas for seawater are those described in the collection of nine FORTRAN algorithms by Fofonoff & Millard (1983). Two of them are devoted to the relation between electrical conductivity of seawater and the Practical Salinity Scale 1978 (PSS-78, Unesco, 1981b). Both will not be discussed later because conductivity is not an equilibrium property of electrolytic solutions.

Three other formulas cover basic equilibrium properties of seawater as functions of practical salinity, S , Celsius temperature, t , expressed in IPTS-68 scale (Barber, 1969), and applied pressure, p :

- Density of seawater, $\rho(S, t, p)$, representing the International Equation of State of Seawater 1980 (Unesco, 1981c), termed in short EOS80, assembled by Millero, Chen, Bradshaw & Schleicher (1980) and Millero & Poisson (1981a).
- Specific heat capacity of seawater at constant pressure, $c_p(S, t, p)$, as proposed by Millero, Perron & Desnoyers (1973a).
- Sound speed of seawater, $U(S, t, p)$, after the formula of Chen & Millero (1977).

We shall refer to this triple of functions later jointly as ‘EOS80’ for convenience.

Three more algorithms refer to properties important under the influence of gravity, hydrostatic pressure–depth conversion, adiabatic lapse rate, and potential temperature. They will not further be discussed in the current paper. All of them could in principle have been derived from the EOS80 set, but in fact the latter two are based on the formulas of Bryden (1973).

Finally, a formula for the freezing point temperature of seawater, $t_f(S, p)$, is defined as specified by Millero (1978), and recommended by the Joint Panel on Oceanographic Tables and Standards (Unesco, 1981a). It additionally exploits certain properties of ice (Millero & Leung, 1976b).

Several weaknesses of the well-established EOS80 and associated equations have been revealed over the two decades of their successful use in oceanography. They can be summarized under four aspects:

1. Agreement with experiments

- (i) EOS80 does not properly describe high-pressure sound speed as derived from deep-sea travel times (Spiesberger & Metzger, 1991, Dushaw, Worcester, Cornuelle & Howe, 1993, Millero & Li, 1994, Meinen & Watts, 1997)
- (ii) Due to (i), there is evidently a pending potential conflict between abyssal travel-time measurements and EOS80 high-pressure densities, which are considered consistent with EOS80 sound speed.
- (iii) EOS80 does not properly describe temperatures of maximum density determined experimentally, especially for brackish waters under pressure (Caldwell, 1978, Siedler & Peters, 1986)

2. Consistency with international standards

- (iv) EOS80 is not expressed in terms of the international temperature scale ITS-90 (Blanke, 1989, Preston-Thomas, 1990, Saunders, 1990)
- (v) At zero salinity, EOS80 shows systematic deviations from the international pure water standard IAPWS95 (Wagner & Pruß, 2002), especially in compressibility, thermal expansion, and sound speed (sections 2–6 of this paper)
- (vi) EOS80 is derived from seawater measurements relative to or calibrated with fresh water properties which are partly obsolete with respect the new pure water standard IAPWS95
- (vii) EOS80 range of validity does not include the triple point of water which is a standard reference point for thermodynamic descriptions of water

3. Internal consistency

- (viii) EOS80 is redundant and contradictory, as certain thermodynamic properties like heat capacity can be computed by combining other equations of EOS80, sometimes leading to very different results, especially near the density maximum
- (ix) EOS80 obeys thermodynamic cross-relations (Maxwell relations) only approximately but not identically
- (x) Freezing point temperatures are valid for air-saturated water, while other EOS80 formulas are defined for air-free water, thus causing systematic offsets

4. Completeness

- (xi) EOS80 does not provide specific enthalpy which is required for the hydrodynamic energy balance by means of the enthalpy flux (Landau & Lifschitz, 1974, Bacon & Fofonoff, 1996, Warren, 1999) or the Bernoulli function (Gill, 1982, Saunders, 1995). Specific enthalpy is further necessary for the calculation of mixing heat (Fofonoff, 1962) or of conservative quantities like potential enthalpy (McDougall, 2003)
- (xii) EOS80 does not provide specific entropy as an unambiguous alternative for potential temperature (Feistel & Hagen, 1994). It allows e.g. for an effective and accurate computation of potential temperature and potential density (Bradshaw, 1978, Feistel, 1993), especially in numerical ocean models (McDougall, Jackett, Wright & Feistel, 2003)
- (xiii) EOS80 does not provide specific internal energy, which like enthalpy is required for proper energy balances, and e.g. elucidates the changing thermal water and seawater properties when being compressed
- (xiv) EOS80 does not provide chemical potentials which allow the computation of properties of vapour pressure or osmotic pressure (Millero and Leung, 1976b), or properties of sea ice (Feistel & Hagen, 1998), or as indicators for oceanic actively mixing layers (Feistel and Hagen, 1994)
- (xv) EOS80 density was only later extended to salinity $S = 50$ at ambient pressure by another separate high-salinity equation of state (Poisson, Gadhomi & Morcos, 1991)
- (xvi) Existing freezing point temperatures are valid up to pressures of 5 MPa (500 dbar), which is insufficient for extreme polar systems like Lake Vostok (Siegert, Ellis-Evans, Tranter, Mayer, Petits, Salamantin, et al., 2001)

The thermodynamic potential proposed in the current paper, referred to as ‘F03’ later, overcomes all the problems mentioned above. In the last case, (xvi), it is to be used in conjunction with a compatible Gibbs potential of ice, as specified in section 13.

A proper potential function constitutes a very compact, practical, mathematically elegant and physically consistent way of representing and computing all thermodynamic equilibrium properties of a given substance. Many books and articles treat various aspects of this classical method, like e.g. Fofonoff (1962), Landau & Lifschitz (1966, 1974), Falkenhagen & Ebeling (1971), Tillner-Roth (1998), or, quite recently, the comprehensive review by Alberty (2001).

For pure water, thermodynamic potential functions were quantitatively defined as a standard as early as 1968 by an International Formulation Committee, leading finally to IAPWS95, the current “IAPWS Formulation 1995 for the Thermodynamic Properties of Ordinary Water Substance for General and Scientific Use” (IAPWS, 1996, Wagner and Pruß, 2002). Despite a similar proposal for seawater made by Fofonoff (1962), and even though all necessary additional ingredients for its construction were available at the time when EOS80 was specified (Millero and Leung, 1976b, Millero, 1982, 1983), it took another decade until a first version was assembled, called here ‘F93’ (Feistel, 1993) and improved later, referred to as ‘FH95’ (Feistel and Hagen, 1995). The recently published equation of state of McDougall et al. (2003) is a computationally faster but numerically equivalent formulation of FH95 for use in numerical models, restricted to naturally occurring combinations of salinity, temperature and pressure, so-called ‘Neptunian’ waters, and formulated in terms of potential density as function of salinity, potential temperature, and pressure.

Specific free enthalpy (also called Gibbs function, Gibbs energy, Gibbs free energy, or free energy in the literature) of seawater, $g(S, t, p)$, is assumed to be a polynomial-like function of the independent variables practical salinity (PSS-78) (Lewis & Perkin, 1981, Unesco, 1981b), $S = 40 \cdot x^2$, temperature (ITS-90) (Blanke, 1989, Preston-Thomas, 1990), $t = 40^\circ\text{C} \cdot y$, and applied pressure, $p = 100 \text{ MPa} \cdot z$, as,

$$g(S, t, p) = 1 \text{ J/kg} \cdot \sum_{j,k} \left\{ g_{0jk} + g_{1jk} x^2 \ln x + \sum_{i>1} g_{ijk} x^i \right\} y^j z^k \quad (1)$$

We shall use capital symbols $T = T_0 + t$ for absolute temperatures, with $T_0 = 273.15 \text{ K}$, and $P = P_0 + p$ for absolute pressures, with $P_0 = 0.101325 \text{ MPa}$, in the following text. IAPWS95 formulas are expressed in density, absolute temperature or absolute pressure as independent variables, and will later be written this way if used in mathematical expressions. The logarithmic term in Eq. (1) follows from Planck’s theory of ideal solutions; it is a pressure-independent linear function of temperature, as shown in Table 1 (compare Eq. (47)). The series expansion with respect to the salinity root results from the Debye-Hückel theory of dilute electrolytes. Both are required for correct behaviour in the limit of infinite dilution (Landau and Lifschitz, 1966, Falkenhagen and Ebeling, 1971).

The structure of the right-hand side of Eq. (1) is convenient for the analytical execution and numerical implementation of partial derivatives by suitable index shifting in the array of coefficients. These derivatives serve for the compilation of all thermodynamic properties in terms of the potential function, Eq. (1), either in explicit form, or by Newton iteration of implicit expressions like those in Eqs. (16)–(21). We list the most relevant oceanographic quantities here for easy reference, as being expressed by the potential function, $g(S, t, p)$, and its partial derivatives.

There are three first derivatives of g with respect to its independent variables p , t , and S .

Density, ρ , density anomaly, γ (also called σ_t), and specific volume, v :

$$\frac{1}{\rho} = \frac{1}{1000 \text{ kg/m}^3 + \gamma} = v = \left(\frac{\partial g}{\partial p} \right)_{S,t} \quad (2)$$

Specific entropy, σ :

Table 1

Coefficients of the free enthalpy polynomial being determined in this paper. Variables x , y , z represent salinity root, temperature and pressure in dimensionless form. Numbers in the cells are the sections where the computation of the particular coefficient is described

| g_{ijk} | x^0 | $x^2 \ln x$ | x^2 | x^3 | x^4 | x^5 | x^6 | x^7 |
|-----------|-------|-------------|-------|-------|-------|-------|-------|-------|
| $y^0 z^0$ | 6 | 12 | 12 | 12 | 13,14 | 13,14 | 13,14 | 13,14 |
| $y^1 z^0$ | 6 | 12 | 12 | 12 | 13,14 | 13,14 | 13,14 | 13,14 |
| $y^2 z^0$ | 2 | | 7–11 | 7–11 | | | | |
| $y^3 z^0$ | 2 | | 7–11 | 7–11 | | | | |
| $y^4 z^0$ | 2 | | 7–11 | 7–11 | | | | |
| $y^5 z^0$ | 2 | | 7–11 | | | | | |
| $y^6 z^0$ | 2 | | | | | | | |
| $y^7 z^0$ | 2 | | | | | | | |
| $y^0 z^1$ | 3–5 | | 7–11 | 7–11 | 7–11 | 7–11 | | |
| $y^1 z^1$ | 3–5 | | 7–11 | 7–11 | 7–11 | | | |
| $y^2 z^1$ | 3–5 | | 7–11 | 7–11 | | | | |
| $y^3 z^1$ | 3–5 | | 7–11 | 7–11 | | | | |
| $y^4 z^1$ | 3–5 | | 7–11 | 7–11 | | | | |
| $y^5 z^1$ | 3–5 | | | | | | | |
| $y^6 z^1$ | 3–5 | | | | | | | |
| $y^7 z^1$ | 3–5 | | | | | | | |
| $y^0 z^2$ | 3–5 | | 7–11 | 7–11 | 7–11 | | | |
| $y^1 z^2$ | 3–5 | | 7–11 | 7–11 | | | | |
| $y^2 z^2$ | 3–5 | | 7–11 | 7–11 | | | | |
| $y^3 z^2$ | 3–5 | | 7–11 | | | | | |
| $y^4 z^2$ | 3–5 | | 7–11 | | | | | |
| $y^5 z^2$ | 3–5 | | | | | | | |
| $y^6 z^2$ | 3–5 | | | | | | | |
| $y^0 z^3$ | 3–5 | | 7–11 | 7–11 | 7–11 | | | |
| $y^1 z^3$ | 3–5 | | 7–11 | 7–11 | | | | |
| $y^2 z^3$ | 3–5 | | 7–11 | 7–11 | | | | |
| $y^3 z^3$ | 3–5 | | 7–11 | | | | | |
| $y^4 z^3$ | 3–5 | | 7–11 | | | | | |
| $y^5 z^3$ | 3–5 | | | | | | | |
| $y^6 z^3$ | 3–5 | | | | | | | |
| $y^0 z^4$ | 3–5 | | 7–11 | 7–11 | | | | |
| $y^1 z^4$ | 3–5 | | 7–11 | | | | | |
| $y^2 z^4$ | 3–5 | | 7–11 | | | | | |
| $y^3 z^4$ | 3–5 | | 7–11 | | | | | |
| $y^4 z^4$ | 3–5 | | | | | | | |
| $y^5 z^4$ | 3–5 | | | | | | | |
| $y^0 z^5$ | 3–5 | | 7–11 | | | | | |
| $y^1 z^5$ | 3–5 | | 7–11 | | | | | |
| $y^2 z^5$ | 3–5 | | 7–11 | | | | | |
| $y^3 z^5$ | 3–5 | | | | | | | |
| $y^0 z^6$ | 3–5 | | | | | | | |

$$\sigma = -\left(\frac{\partial g}{\partial t}\right)_{s,p} \quad (3)$$

Relative chemical potential, μ :

$$\mu = \left(\frac{\partial g}{\partial S}\right)_{t,p} \quad (4)$$

Note that the density anomaly (Eqs. (2), (17)) was originally defined by the Knudsen parameter, $\rho/\rho_{\max}-1$, relative to the maximum density of pure water at atmospheric pressure, ρ_{\max} , and, $\gamma = \rho - 1000 \text{ kg/m}^3$, was proposed later as its more practical substitute (Unesco, 1985, 1986, Mamayev, Dooley, Millard, Taira & Morcos, 1991). But, the symbol γ was not accepted by the oceanographic community, and therefore the traditional letter was redefined as, $\sigma = \rho - 1000 \text{ kg/m}^3$ (Siedler, 1998).

Several thermodynamic coefficients require second derivatives of g .

Isothermal compressibility, K :

$$K = -\frac{1}{v} \left(\frac{\partial v}{\partial p} \right)_{S,t} = -\frac{(\partial^2 g / \partial p^2)_{S,t}}{(\partial g / \partial p)_{S,t}} \quad (5)$$

Isobaric thermal expansion coefficient, α :

$$\alpha = \frac{1}{v} \left(\frac{\partial v}{\partial t} \right)_{S,p} = \frac{(\partial^2 g / \partial t \partial p)_S}{(\partial g / \partial p)_{S,t}} \quad (6)$$

Isobaric specific heat capacity, c_p :

$$c_p = T \left(\frac{\partial \sigma}{\partial t} \right)_{S,p} = -T \left(\frac{\partial^2 g}{\partial t^2} \right)_{S,p} \quad (7)$$

Isothermal haline contraction coefficient, β :

$$\beta = -\frac{1}{v} \left(\frac{\partial v}{\partial S} \right)_{t,p} = -\frac{(\partial^2 g / \partial p \partial S)_t}{(\partial g / \partial p)_{S,t}} \quad (8)$$

Adiabatic compressibility, κ , and sound speed, U :

$$\kappa = -\frac{1}{v} \left(\frac{\partial v}{\partial p} \right)_{S,\sigma} = \frac{v}{U^2} = \frac{(\partial^2 g / \partial t \partial p)_S^2 - (\partial^2 g / \partial t^2)_{S,p} (\partial^2 g / \partial p^2)_{S,t}}{(\partial g / \partial p)_{S,t} (\partial^2 g / \partial t^2)_{S,p}} \quad (9)$$

Adiabatic lapse rate, Γ :

$$\Gamma = \left(\frac{\partial t}{\partial p} \right)_{S,\sigma} = -\frac{(\partial^2 g / \partial t \partial p)_S}{(\partial^2 g / \partial t^2)_{S,p}} \quad (10)$$

Adiabatic haline contraction coefficient, β' :

$$\beta' = -\frac{1}{v} \left(\frac{\partial v}{\partial S} \right)_{\sigma,p} = \frac{(\partial^2 g / \partial S \partial t)_p (\partial^2 g / \partial t \partial p)_S - (\partial^2 g / \partial t^2)_{S,p} (\partial^2 g / \partial S \partial p)_t}{(\partial g / \partial p)_{S,t} (\partial^2 g / \partial t^2)_{S,p}} \quad (11)$$

Further thermodynamic functions are defined by mathematical Legendre transforms (Alberty, 2001).

Specific free energy (also called Helmholtz energy or Helmholtz free energy), f :

$$f = g - Pv = g - P \cdot \left(\frac{\partial g}{\partial p} \right)_{S,t} \quad (12)$$

Specific enthalpy, h :

$$h = g + T\sigma = g - T \cdot \left(\frac{\partial g}{\partial t} \right)_{S,p} \quad (13)$$

Specific internal energy, e :

$$e = g + T\sigma - Pv = g - T \cdot \left(\frac{\partial g}{\partial t} \right)_{S,p} - P \cdot \left(\frac{\partial g}{\partial p} \right)_{S,t} \quad (14)$$

Chemical potential of water in seawater, μ^w :

$$\mu^w = g - S\mu = g - S \cdot \left(\frac{\partial g}{\partial S} \right)_{t,p} \quad (15)$$

Oceanographic so-called ‘potential’ quantities can be obtained by formally replacing in-situ temperature t and in-situ pressure p by potential temperature θ and reference pressure p_r . They describe the property a water parcel would take if moved from in-situ pressure p to reference pressure p_r without exchange of matter and heat. Due to the latter, by definition of θ , specific entropy is equal to ‘potential’ specific entropy.

Potential temperature, $\theta(S, t, p, p_r)$, is implicitly given by (Bradshaw, 1978, Feistel, 1993):

$$\sigma(S, t, p) = \sigma(S, \theta, p_r) \quad (16)$$

Potential density, ρ_θ , and potential density anomaly, γ_θ (also called σ_θ):

$$\rho_\theta(S, t, p, p_r) = 1000 \text{ kg/m}^3 + \gamma_\theta = \rho(S, \theta(S, t, p, p_r), p_r) \quad (17)$$

Potential specific enthalpy, h_θ (McDougall, 2003):

$$h_\theta(S, t, p, p_r) = h(S, \theta(S, t, p, p_r), p_r) \quad (18)$$

Equilibria between seawater and other aqueous phases are controlled by equal chemical potentials of water in both.

Osmotic pressure, $\pi(S, t, p)$, is implicitly given by:

$$\mu^w(S, t, p + \pi) = \mu^w(0, t, p) \quad (19)$$

Freezing point temperature, $t_f(S, p)$, is implicitly given by (requiring additionally free enthalpy of water ice, g^{Ice} , see section 13):

$$\mu^w(S, t_f, p) = g^{Ice}(t_f, p) \quad (20)$$

Vapour pressure, $p_v(S, t, p)$, above seawater at pressure p , is implicitly given by (requiring additionally free enthalpy of water vapour, g^{Vapour} , as available by IAPWS95):

$$\mu^w(S, t, p) = g^{Vapour}(t, p_v) \quad (21)$$

The functions defined by Eqs. (12)–(15) can serve as alternative thermodynamic potentials if formulated in terms of their particular natural independent variables (Alberty, 2001). This may lead to more compact and effective expressions, like e.g. the use of enthalpy (13) as a function of salinity, entropy, and pressure for the description of adiabatic processes, but it may require e.g. an additional temperature-entropy conversion formula because entropy cannot be directly measured experimentally (Feistel and Hagen, 1995, Tillner-Roth, 1998, McDougall et al., 2003).

A Gibbs potential of sea ice is immediately available from a suitable combination of the Gibbs potentials of seawater and of ice (Feistel and Hagen, 1998). It provides all equilibrium properties of sea ice like e.g. brine salinity, isochoric pressure coefficient, or its exceptionally large heat capacity, which results from the addition of the latent and dilution heats of internal phase transition processes to the heat capacities of brine and ice.

The physico-chemical properties of seawater listed above are sometimes distinguished between so-called ‘PVT’ and ‘thermochemical’ properties (Millero, 1982, 1983). The first is an abbreviation for ‘Pressure-Volume-Temperature’ and comprises quantities mostly related to mechanical forces and dimensions like

density and sound speed, as well as their combinations or derivatives. They are available from measurements, do not contain freely adjustable constants, and do not possess the logarithm term of Eq. (1). The second group of properties deals with energy, entropy, enthalpy, and chemical potentials, as well as quantities derived thereof. In many cases, only their differences, but not the quantities themselves are available from experiments. Therefore they can depend on freely adjustable gauge constants like the absolute energy and absolute entropy of water and of every single dissolved component. The so-called ‘colligative’ properties like freezing point depression or osmotic pressure of a solution are assigned to the thermochemical group. This classification is not unique; heat capacity is often counted in the second category for obvious reasons, but it can be expressed by density and sound speed using thermodynamic rules. Therefore, we consider here the EOS80 triple as a complete description of seawater PVT properties, and the related freezing point formula as its incomplete thermochemical counterpart.

The four free constants of F03 are defined, as opposed to FH95 and F93, by the conditions of vanishing internal energy and entropy of the liquid phase at the triple point of water at $S = 0$, $T_t = 273.16$ K, $P_t = 611.657$ Pa, and vanishing enthalpy and entropy of standard ocean seawater at $S = 35$, $T = T_0 = 273.15$ K, $P = P_0 = 101325$ Pa.

The equilibrium properties of seawater depicted by the actual Gibbs potential are, in the strict sense, only valid for gravity-free conditions. Seawater exposed to a centrifugal or gravity force is at thermodynamic equilibrium if temperature and all chemical potentials are constant throughout the volume. Under such circumstances other quantities like pressure or entropy, however, will exhibit spatial gradients proportional to the external field (Landau and Lifschitz, 1966, 1974, Alberty, 2001). The chemical potentials of the various components forming seasalt depend on pressure in different ways, consequently, the equilibrium stoichiometric composition of seasalt will vary with the pressure level in the water column. Practically this is not observed in the ocean because the relaxation time towards this equilibrium significantly exceeds time scales of oceanic processes, especially turbulent mixing, as well as reasonable observation periods. Molecular baro-diffusion is slow and terrestrial gravity is weak enough to make gravity-free thermodynamics the much better approximation for natural oceanographic conditions, thus allowing for a greatly simplified description with formally only seasalt as single solute (Fofonoff, 1962, 1985).

Variations in the chemical composition of seasalt are observed in regions suffering from reduced water exchange with the world ocean, like in the North Sea (Krümmel, 1893), the Baltic Sea (Rohde, 1966), the Bering Sea (Tsunogai, Kusakabe, Iizumi, Koike & Hattori, 1979), or the Red Sea (Poisson, Lebel & Brunet, 1981). In such cases, true densities may deviate up to 0.1 kg/m^3 from those formally derived by means of conductivity measurements (Brewer & Bradshaw, 1975, Millero & Kremling, 1976c, Millero & Sohn, 1992, Feistel, 1998, Millero, 2000). Their impact on ocean dynamics is usually only small because the anomalies vary smoothly in space, or are masked by strong absolute density gradients (McDougall et al., 2003). Composition anomalies will not further be considered in this paper.

It is obvious from Eqs. (2)–(21) that a particular coefficient of the thermodynamic potential function portrays itself through various different thermodynamic quantities. Vice versa, any kind of measured equilibrium property can be included into the determination of the potential function from experiments. The method used here for this purpose, multi-variable linear and nonlinear regression, has to achieve suitable compromises between the overlapping requirements posed by the different data and their particular scatter. For this goal, we have systematically specified numerical weights by estimated or reported experimental errors, called ‘required r.m.s.’ in the further text, where r.m.s. stands for root mean square deviation. The abbreviation ppm denotes ratios in parts per million ($1/1,000,000$).

The computation of coefficients belonging to the pure water part is described in sections 2 to 6 of this paper, compare Table 1. One fit was carried out for heat capacity at ambient pressure (section 2), another one for all high-pressure properties (sections 3 to 5), and two coefficients are implied by the reference state definition (section 6). A single regression was run for all PVT properties of seawater (sections 7 to 11), another one for thermochemical properties (sections 13, 14), after the required Debye-Hückel limiting

laws had been evaluated in section 12. For details of the regression algorithm we refer to the former papers about F93 and FH95.

2. Heat capacity of water

Isobaric specific heat capacity, c_p , of water in EOS80 was taken from the paper of [Millero et al. \(1973a\)](#), who used as pure water reference the data of de Haas, composed of several measurements between 1902 and 1927, published by [Stimson \(1955\)](#). FH95 was computed from exactly the same function. The accuracy of these data is not given, but is likely in the range of several J/(kg K), as suggested by [Millero et al. \(1973a\)](#), who found a deviation of 2 J/(kg K) from the earlier measurements of [Cox & Smith \(1959\)](#), [Bromley \(1968\)](#) and [Bromley, Diamond, Salami & Wilkins \(1970\)](#). The precision of seawater measurements relative to pure water is, however, much better with their typical deviations up to only 0.5 J/(kg K) ([Millero et al., 1973a](#)).

IAPWS95 heat capacities deviate up to 6 J/(kg K) from the recent measurements of [Archer & Carter \(2000\)](#), thus obeying the experimental accuracy of 13 J/(kg K) of the latter, see [Fig. 1](#). EOS80 and FH95 heat capacities are systematically lower by about 2 J/(kg K). Data reported by [Bromley et al. \(1970\)](#), maximum error given there is 2.2 cal/(kg K), converted 9 J/(kg K), are in very good agreement with EOS80 and FH95 after transforming temperatures from IPTS-48 to ITS-90 and calories to Joule by 4.1840 J/cal. They are a smoothed version of seawater measurements published by [Bromley, Desaussure, Clipp & Wright \(1967\)](#), based on pure water data of [Osborne, Stimson & Ginnings \(1939\)](#).

New coefficients g_{0j0} , $j > 1$ have been determined by fitting the least square integral

$$\int \left\{ T \left(\frac{\partial^2 g}{\partial t^2} \right)_{S=0, p=0} + c_p^{IAPWS95}(T, P_0) \right\}^2 dt = \text{Min} \quad (22)$$

with respect to IAPWS95 heat capacities at atmospheric pressure between the freezing point and 45 °C, as given in the appendix. The r.m.s. of the fit was 0.01 J/(kg K), which is well below the experimental uncertainty. High pressure heat capacities computed after performing the density regression as described in sections 3–5, by $c_p = -T \left(\frac{\partial^2 g}{\partial t^2} \right)_{S=0, p}$, show a stronger deviation of up to 0.1 J/(kg K) at high temperatures, see [Fig. 2](#).

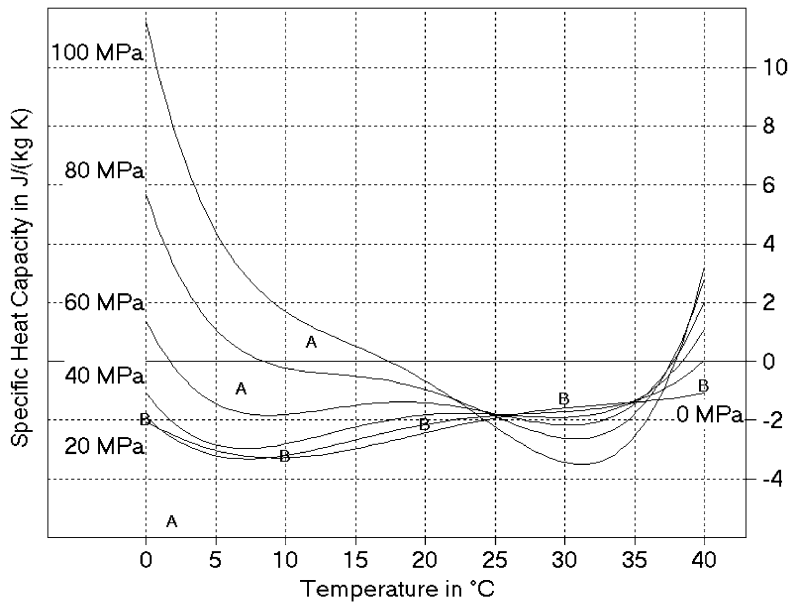
The estimated experimental uncertainty Δc_p of about 10 J/(kg K) even in latest measurements of heat capacities is remarkably high and significantly exceeds the scatter between different accurate experiments. This value does not only apply to pure water, but to seawater as well since the most reliable measurements of the latter ([Millero et al., 1973a](#)) precisely detected their readings only relative to a pure water reference. We can estimate the possible influence of changes Δc_p on other important properties.

Uncertainties in the determination of the adiabatic lapse rate $\Gamma = \left(\frac{\partial t}{\partial p} \right)_{s, \sigma} = \frac{\alpha T v}{c_p}$ ([Fofonoff and Millard, 1983](#)) are given by,

$$\frac{\Delta \Gamma}{\Gamma} = \frac{\Delta \alpha}{\alpha} + \frac{\Delta v}{v} - \frac{\Delta c_p}{c_p} \quad (23)$$

Typical seawater values are e.g. $\Delta \alpha \approx 0.6$ ppm/K, $\alpha = 100$ ppm/K, $\Delta v/v \approx 1$ ppm, $\Delta c_p \approx 10$ J/(kg K), $c_p = 4000$ J/(kg K), $\Gamma = 10$ mK/MPa. Here, $\Delta \alpha/\alpha \approx 0.6\%$ and $\Delta c_p/c_p \approx 0.3\%$ contribute the biggest shares to the total error. Reported experimental accuracies of lapse rates $\Delta \Gamma/\Gamma \approx 0.4\%$ ([Rögner & Soll, 1980](#), [Wagner and Pruß, 2002](#)) or $\Delta \Gamma/\Gamma \approx 0.2\%$ ([Caldwell & Eide, 1980](#)) are of similar size. These estimates agree quite

(a) Isobaric Specific Heat Capacity: Difference EOS80 - IAPWS95



(b) Isobaric Specific Heat Capacity: Difference FH95 - IAPWS95

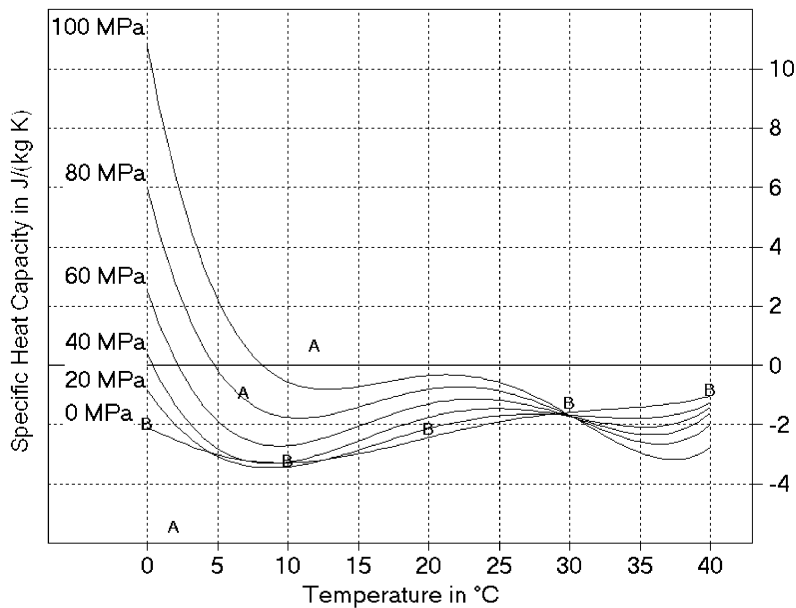


Fig. 1. Deviation of a) EOS80, above, and b) FH95, below, isobaric specific heat capacities, $c_p(0, t, p)$, from IAPWS95 at applied pressures p between 0 MPa and 100 MPa. Measurements at atmospheric pressure ($P = 0.101325$ MPa) of [Archer and Carter \(2000\)](#) with accuracy 13 J/(kg K) are shown as points “A”, those reported by [Bromley et al. \(1970\)](#) with accuracy 9 J/(kg K), as “B”, taken originally from [Osborne et al. \(1939\)](#), with precision 100 ppm.

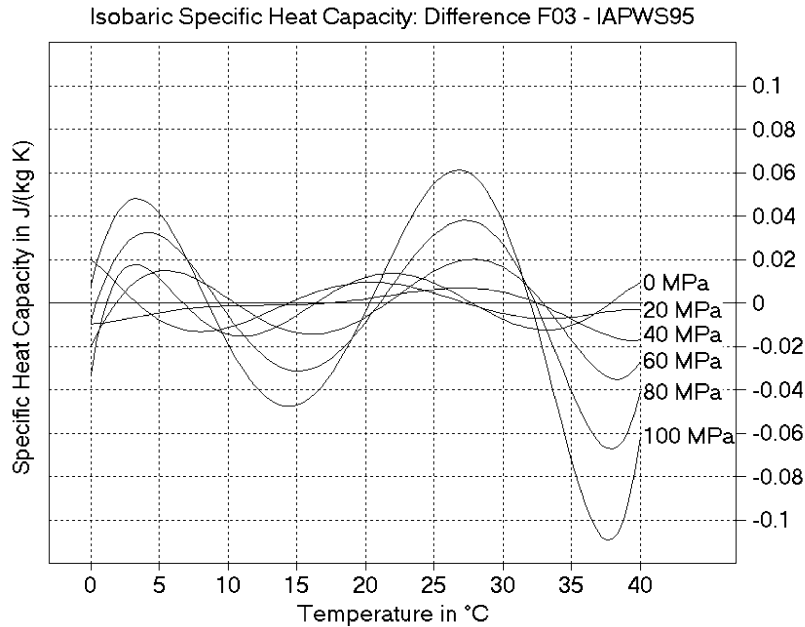


Fig. 2. Deviation between isobaric heat capacity, $c_p(0, t, p)$, of F03 from IAPWS95 at various applied pressures between 0 and 100 MPa (10,000 dbar). Note that only data at atmospheric pressure were used for the fit.

well with a potential temperature error of 6 mK over a pressure change of 100 MPa (Fofonoff and Millard, 1983).

3. Thermal expansion of water

The isobaric thermal expansion coefficient of water α can be expressed in terms of temperature t and pressure p by first and second derivatives of free enthalpy g , as given by Eq. (6). Due to the density anomaly of water, α becomes negative below the temperature of maximum density, t_{MD} . By definition, thermal expansion is theoretically zero at the t_{MD} points determined experimentally by Caldwell (1978).

From his accuracy of $\Delta t = 40$ mK follows $\left| \Delta \frac{\partial v}{\partial t} \right| \approx \left| \frac{\partial^2 v}{\partial t^2} \right| \Delta t \approx 0.6 \text{ mm}^3/(\text{kg K})$ or $|\Delta \alpha| \approx 0.6 \text{ ppm/K}$ at the

measured t_{MD} (Feistel and Hagen, 1995). At other temperatures, this error range may be considered as a quality criterion of density formulas in general (McDougall et al., 2003). This value is in good agreement with the deviation of 0.4 ppm/K (Millero, Chen, Bradshaw & Schleicher, 1981c) between the thermal expansion coefficients of Bigg (1967) and Kell (1975), and with the measurements of Bradshaw & Schleicher (1970).

In the IAPWS95 formulation, the thermal expansion coefficient is expressed as,

$$\alpha(T, \rho) = \frac{1(\partial P / \partial T)_\rho}{\rho(\partial P / \partial \rho)_T} \quad (24)$$

with $P(T, \rho) = \rho^2 \left(\frac{\partial f}{\partial \rho} \right)_T$ and its inverse “backward” function provided, $\rho = \rho(T, P)$.

The deviations of thermal expansion coefficients of EOS80 and FH95 from IAPWS95 are shown in Fig.

3(a) and (b). Only at pressures below 20 MPa do the residuals remain within the desired error range. The strongest differences appear at low temperatures and high pressures and exceed this range by more than a factor of 10.

The coefficients g_{0jk} , $j > 0$, $k > 0$, have been determined by a least-square fit of

$$\int \left\{ \left(\frac{\partial^2 g}{\partial t \partial p} \right)_{s=0} - \frac{1}{\rho^2} \frac{(\partial P / \partial T)_\rho}{(\partial P / \partial \rho)_T} \right\}^2 dp dt = \text{Min} \quad (25)$$

with respect to the functions $\rho(T, P)$ and $P(T, \rho)$ provided by IAPWS95, together with the fits of density (section 4) and compressibility (section 5). Thermal expansion was treated in two data groups, the first group contains values at $p = 0$ MPa and temperatures between the freezing point and 45 °C with a required r.m.s. deviation of 0.6 mm³/(kg K), the second at pressures between triple point and 110 MPa and temperatures between the pressure-dependent freezing points and 45 °C with the same r.m.s. Note that $t = 0$ °C at atmospheric pressure is below the freezing temperature of air-free water ($t_f = 0.0026$ °C, Wagner and Pruß, 2002) and is beyond validity of IAPWS95, see also section 13 of this paper. The resulting r.m.s. deviation was 0.005 mm³/(kg K) for the first and 0.010 mm³/(kg K) for the second group, as shown in Fig. 4, which is significantly better than the required precision. Determined coefficients are listed in the appendix.

At Caldwell's t_{MD} points, thermal expansion coefficients at various pressures are plotted in Fig. 5, computed with either EOS80 (A), FH95 (B), or IAPWS95 (C). Data of F03 are virtually identical with IAPWS95 in this plot. Above about 3.5 °C (or 2 MPa), IAPWS95 is almost identical with FH95 and slightly higher than EOS80. From 3.5–2 °C (10 MPa), IAPWS95 is in between FH95 and EOS80. From then on, IAPWS95 values are systematically lower than the other two and even exceed the range of 0.6 ppm/K. The comprehensive and consistent description of IAPWS95, however, suggests its higher reliability than Caldwell's measurements in this comparison. Data below the freezing point, where IAPWS95 is not valid (Wagner and Pruß, 2002), are shown in brackets. Despite these details, all four data sets remain on average within the error limit with r.m.s. deviations of 0.55 ppm/K (EOS80), 0.52 ppm/K (FH95) and 0.63 ppm/K (IAPWS95, F03).

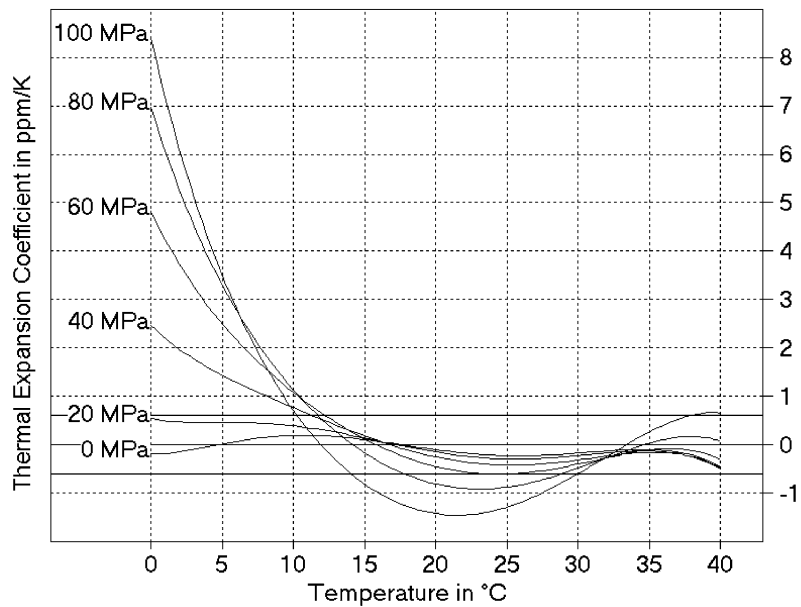
The currently best experimental value for the t_{MD} at $p = 0$ MPa is $t_{MD} = 3.983\,035 \pm 0.000\,67$ °C (Tanaka, Girard, Davis, Peuto & Bignell, 2001, Wagner and Pruß, 2002), while Caldwell (1978) had determined $t_{MD} = 4.02 \pm 0.04$ °C. The t_{MD} values computed as zeroes of the corresponding thermal expansion formulas are given in Table 2, all are about 2–5 mK lower than Tanaka's et al. t_{MD} . This corresponds to an error in thermal expansion of 0.03–0.08 ppm/K.

4. Density of water

The density of air-free water at atmospheric pressure is described very accurately by EOS80, based on the equation of Bigg (Bigg, 1967, Millero and Poisson, 1981a) within an error limit of $\Delta\rho/\rho \approx 3$ ppm to 6 ppm (Wagenbreth & Blanke, 1971), and consequently by FH95 as well. Near 20 °C, it deviates about 2 ppm from the IAPWS95 standard and 1.5 ppm from the currently recommended density formula of Tanaka et al. (2001) with accuracy better than 1 ppm, see Fig. 6. Thus, the recent measurements are within the error range of EOS80, but EOS80 is not entirely in the range of these measurements.

At higher pressures, densities of Kell & Whalley (1975) with accuracy about 20 ppm are considered the best (Wagner and Pruß, 2002) and have served as reference data for IAPWS95 in the region $t = 0$ –50 °C, $p = 0$ –100 MPa. The pure water part of EOS80, however, is based on the work of Millero et al. (1980, 1981c) with claimed accuracy of 4.3 ppm. The deviation between EOS80 and IAPWS95 is less than 10 ppm at temperatures above 25 °C but exceeds 20 ppm between 0 and 17 °C, see Fig. 7. Thus,

(a) Thermal Expansion Coefficient: Difference EOS80 - IAPWS95



(b) Thermal Expansion Coefficient: Difference FH95 - IAPWS95

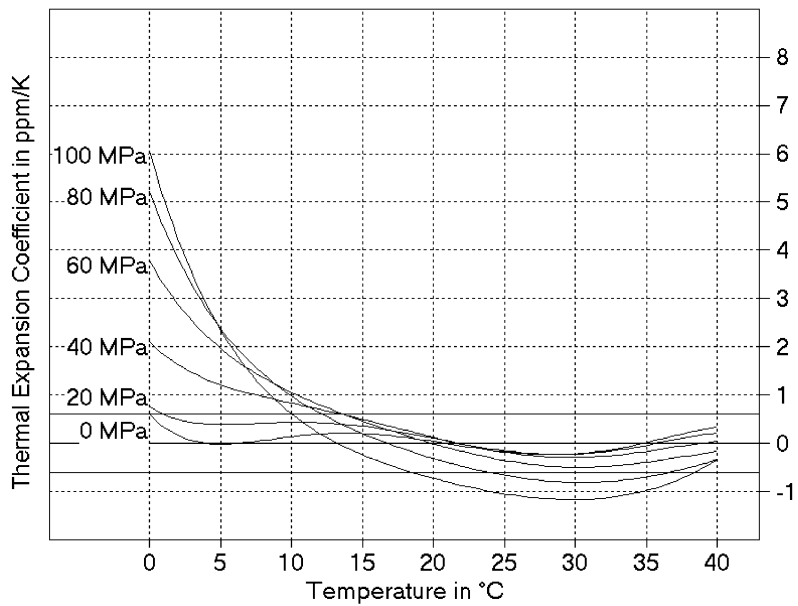


Fig. 3. Comparison of isobaric thermal expansion coefficients, $\alpha(0,t,p)$, of (a) EOS80, above and (b) FH95, below, with IAPWS95 at applied pressures p between 0 and 100 MPa (0 and 10,000 dbar). The anticipated error range of 0.6 ppm/K is shown by solid lines.

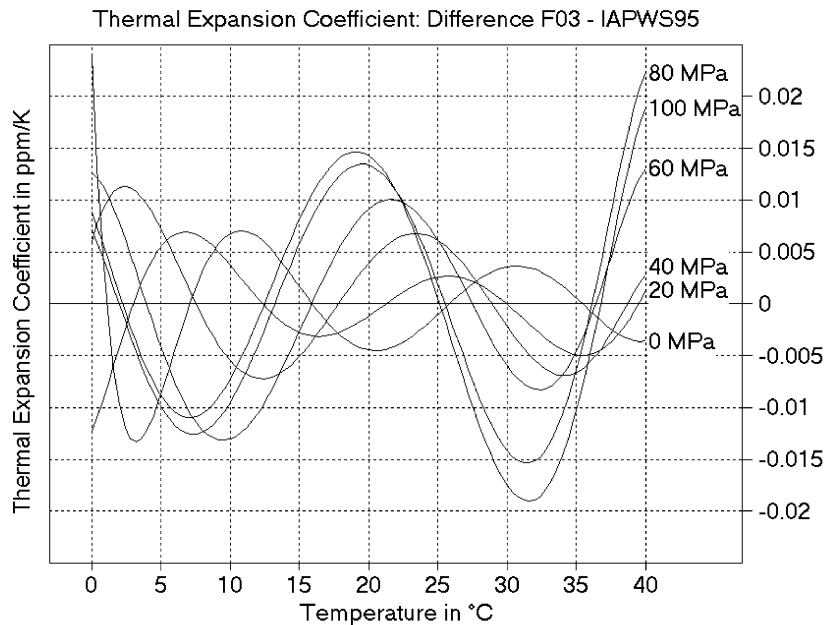


Fig. 4. Deviation of isobaric thermal expansion coefficients, $\alpha(0, t, p)$, of F03 from IAPWS95 at applied pressures between 0 and 100 MPa (0 and 10,000 dbar).

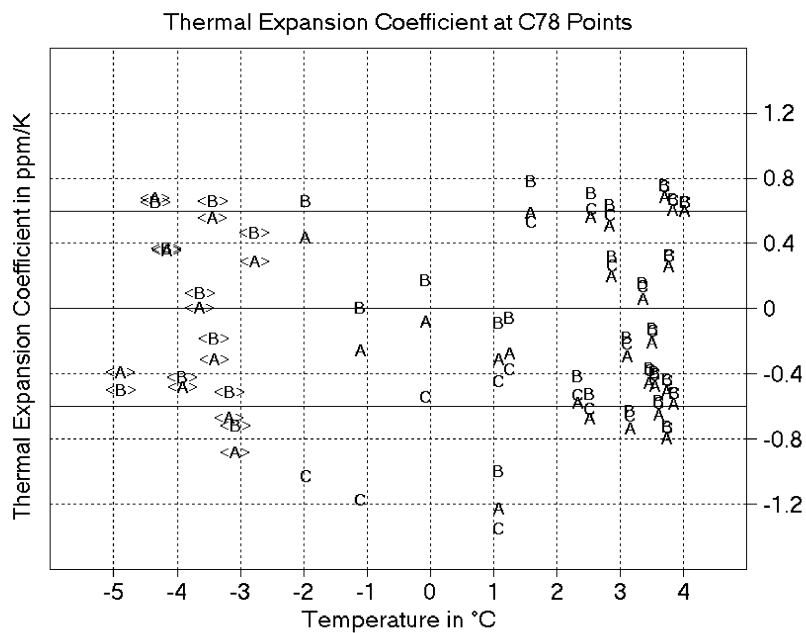


Fig. 5. Isobaric thermal expansion coefficients, $\alpha(0, t_{MD}, p)$, at Caldwell's (1978) measured points of maximum density, t_{MD} , of water, computed with EOS80 (A), FH95 (B), and IAPWS95/F03 (C). Symbols in brackets are below the freezing temperature. The experimental error of Caldwell's measurements is 0.6 ppm/K, shown as solid lines.

Table 2

Comparison of temperatures (t_{MD} , ITS-90) and densities of pure water at its density maximum under atmospheric pressure taken from several sources or formulas

| Source/Formula | t_{MD} /°C | ρ /(kg/m ³) |
|-------------------------------|--------------|------------------------------|
| F03 | 3.978 890 | 999.974 877 |
| Tanaka et al., 2001 | 3.983 035 | 999.974 950 |
| IAPWS95 | 3.978 121 | 999.974 873 |
| FH95 | 3.978 102 | 999.974 657 |
| Bradshaw and Schleicher, 1986 | 3.969 783 | 999.972 604 |
| EOS80 | 3.980 759 | 999.974 961 |
| Caldwell, 1978 | 4.02 | – |
| Menaché, 1976 | near to 4 | 999.975 |
| Wagenbreth and Blanke, 1971 | 3.979 080 | 999.972 0 |

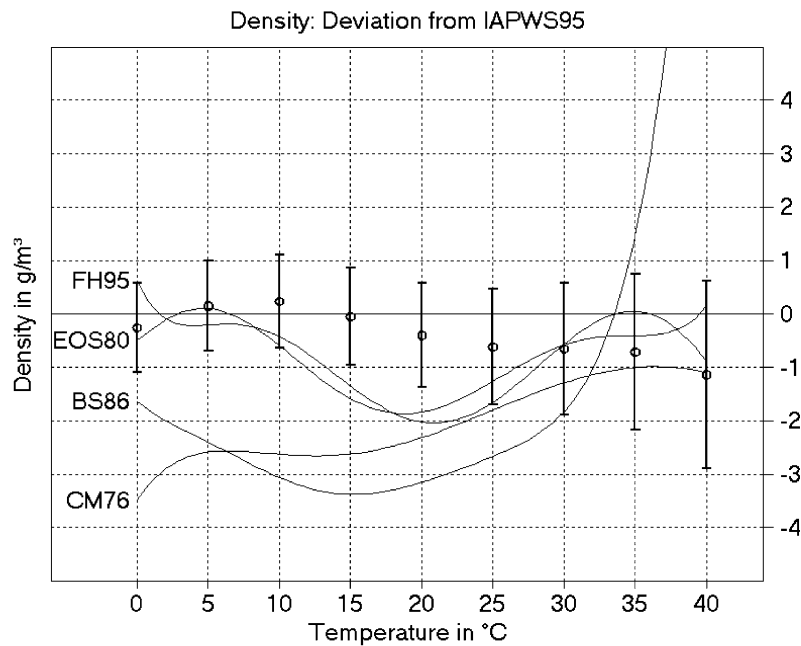


Fig. 6. Deviation of several water density formulas from IAPWS95 at atmospheric pressure ($P = 0.101325$ MPa). BS86 is the equation of state derived from specific volume measurements by Bradshaw and Schleicher (1986). CM76 describes related experiments of Chen and Millero (1976). Data points with error bars are values recently recommended by Tanaka et al. (2001).

EOS80 is within the error interval 30 ppm of IAPWS95, but IAPWS95 is clearly outside the range 4 ppm of EOS80 for pressures above 20 MPa.

The coefficients g_{00k} , $k > 0$ have been determined by fitting specific volume, Eq. (2), as,

$$\int \left\{ \left(\frac{\partial g}{\partial p} \right)_{S=0,t} - \frac{1}{\rho^{IAPWS95}(T,P)} \right\}^2 dt dp = \text{Min} \quad (26)$$

with respect to reciprocal density given by IAPWS95, as given in appendix. The fit was jointly done with those for thermal expansion (section 3) and compressibility (section 5). The least-square integrals were

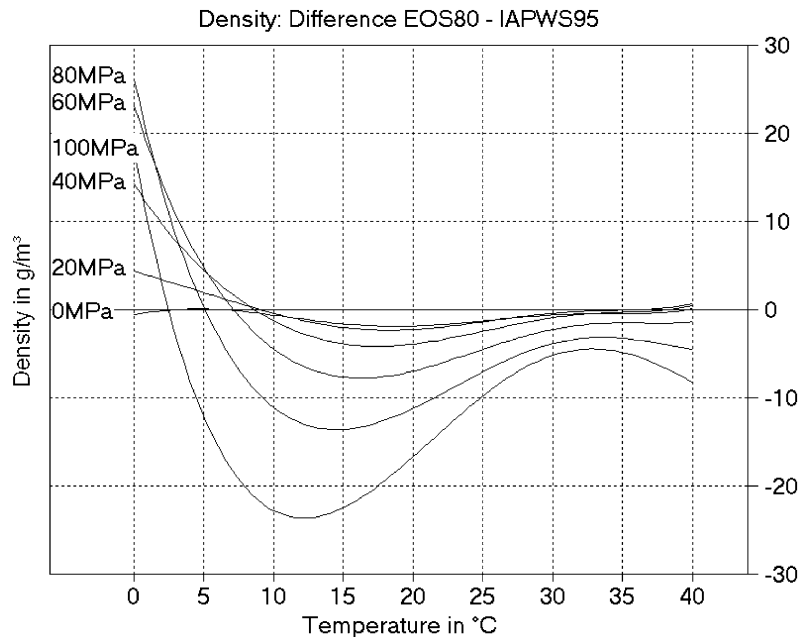


Fig. 7. Comparison of the high pressure equations of state EOS80 (claimed accuracy 4 ppm) and IAPWS95 (claimed accuracy 30 ppm) for applied pressures from 0–100 MPa (0–10,000 dbar).

extended between triple point and 110 MPa in applied pressure and from freezing points to 45 °C in temperature. Two data groups were used, one at $p = 0$ MPa with required variance of 1 ppm (resulting r.m.s. 0.021 ppm), and the other one for all pressures, requiring 30 ppm (resulting r.m.s. 0.032 ppm). The final maximum deviation between both functions is below 0.1 ppm, see Fig. 8, which is significantly less than the experimental uncertainty.

Maximum densities are preferably used for absolute calibration of density formulas. Table 2 is a list of densities computed or measured at their t_{MD} . The currently best value is $t_{MD} = 3.983\,035 \pm 0.000\,67$ °C with the density $\rho_{MD} = 999.974\,950 \pm 0.000\,84$ kg/m³ (Tanaka et al., 2001, Wagner and Pruß, 2002). While their agreement in densities is excellent, all t_{MD} values are below that of Tanaka et al. and beyond its uncertainty. In the computation of F03, full compatibility with IAPWS95 was preferred over a better agreement with Tanaka's et al. data.

5. Compressibility of water

The new IAPWS95 formulation deviates from EOS80 and FH95 in isothermal compressibilities, Eq. (5), up to $\Delta K \approx 0.8$ ppm/MPa, which is twice the estimated experimental error (Kell and Whalley, 1975), see Fig. 9. Consequently, deviations in sound speeds about $\Delta U \approx 1$ m/s must be expected for high pressures and low temperatures, compare Eq. (29) and Fig. 11.

Compressibilities were adjusted to IAPWS95 by minimizing the least-square integral

$$\int \left\{ \left(\frac{\partial^2 g}{\partial p^2} \right)_{S=0,t} + \frac{1}{(\rho^{IAPWS95})^2 \cdot (\partial P^{IAPWS95} / \partial \rho)_T} \right\}^2 dt dp = \text{Min} \quad (27)$$

in a common fit together with thermal expansion coefficients (section 3) and densities (section 4). The

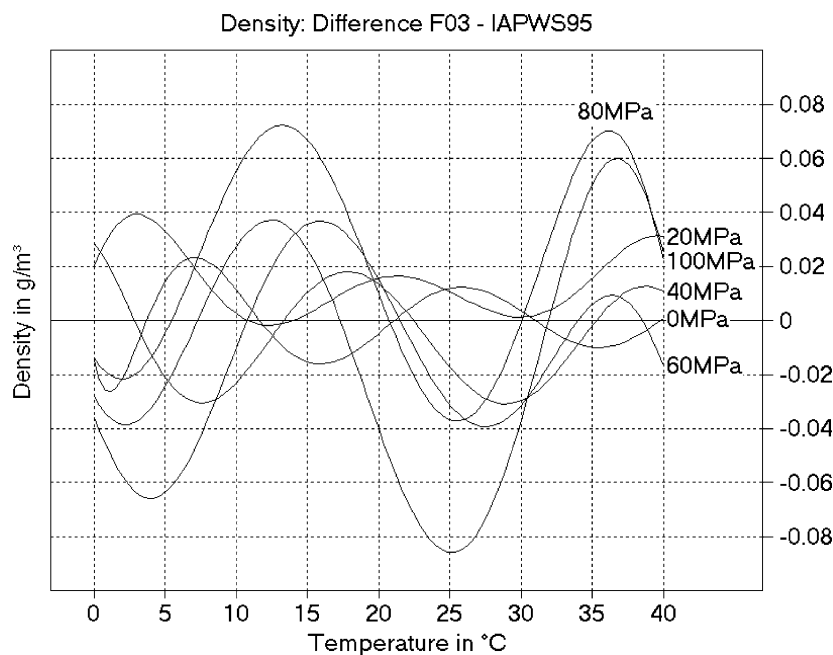


Fig. 8. Deviation between high pressure densities of F03 and IAPWS95 at applied pressures from 0–100 MPa (0–10,000 dbar).

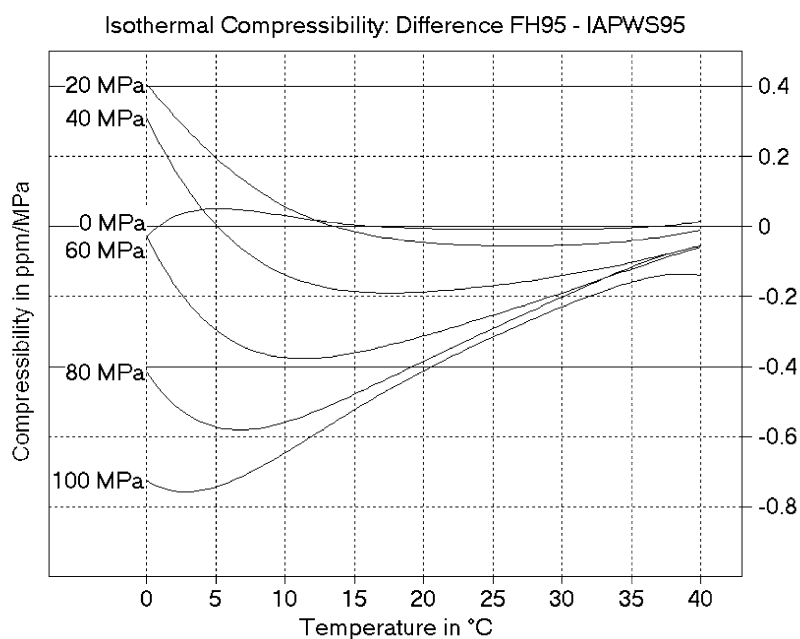


Fig. 9. Difference in isothermal compressibilities of water, $K(0,t,p)$, computed by FH95 and IAPWS95, for applied pressures p between 0–100 MPa (0–10,000 dbar). Estimated experimental accuracy is 0.4 ppm/MPa, shown by solid lines. Deviations between EOS80 and IAPWS95 are very similar.

integral was extended in pressure from the triple point to 110 MPa and from freezing temperatures up to 45 °C with required r.m.s. of 0.4 mm³/(kg MPa), resulting in a residual of 0.003 mm³/(kg MPa), Fig.10.

The regression runs done so far have determined all coefficients required for the so-called PVT properties of water. Other quantities like the adiabatic lapse rate or sound speed can now be directly computed by means of the corresponding thermodynamic relations.

For computed sound speed U , derived from adiabatic compressibility, Eq. (9),

$$U^{-2} = \left(\frac{\partial \rho}{\partial p} \right)_{s,\sigma} = K\rho + \frac{\alpha^2 T}{c_p} \quad (28)$$

the possible error can be estimated as,

$$\frac{\Delta U}{U} = 0.5 \cdot U^2 \left\{ K\rho \left(\frac{\Delta v}{v} - \frac{\Delta K}{K} \right) + \frac{\alpha^2 T}{c_p} \left(\frac{\Delta c_p}{c_p} - \frac{2\Delta\alpha}{\alpha} \right) \right\} \quad (29)$$

or, with $U = 1500$ m/s, $T = 300$ K, $K = 500$ ppm/MPa, and the other values chosen as in Eq. (23),

$$\frac{\Delta U}{U} \approx 0.5 \cdot \left(\frac{\Delta v}{v} - \frac{\Delta K}{K} \right) + 0.001 \cdot \left(\frac{\Delta c_p}{c_p} - \frac{2\Delta\alpha}{\alpha} \right) \quad (30)$$

The biggest uncertainty of $\Delta U/U \approx 400$ ppm or $\Delta U \approx 0.6$ m/s is caused here by isothermal compressibility K with assumed accuracy $\Delta K \approx 0.4$ ppm/MPa (Kell and Whalley, 1975), while the possible heat capacity error contributes only to negligible $\Delta U/U \approx 3$ ppm.

Some error estimates applicable to EOS80 and FH95 sound speeds are 0.2 m/s (Wilson, 1959), 0.3 m/s (Barlow & Yazgan, 1967, Kell and Whalley, 1975), and for low pressures 0.03–0.04 m/s (Wille, 1986)

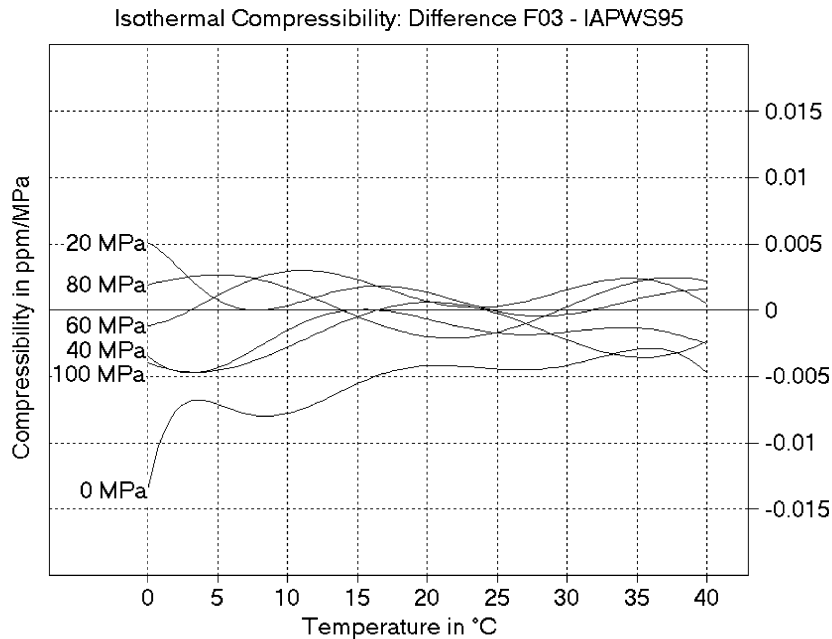


Fig. 10. Isothermal compressibility of water, $K(0,t,p)$, of F03 compared to IAPWS95 for applied pressures p between 0 and 100 MPa (0 and 10,000 dbar) as indicated at the curves. Experimental uncertainty is about 0.4 ppm/MPa.

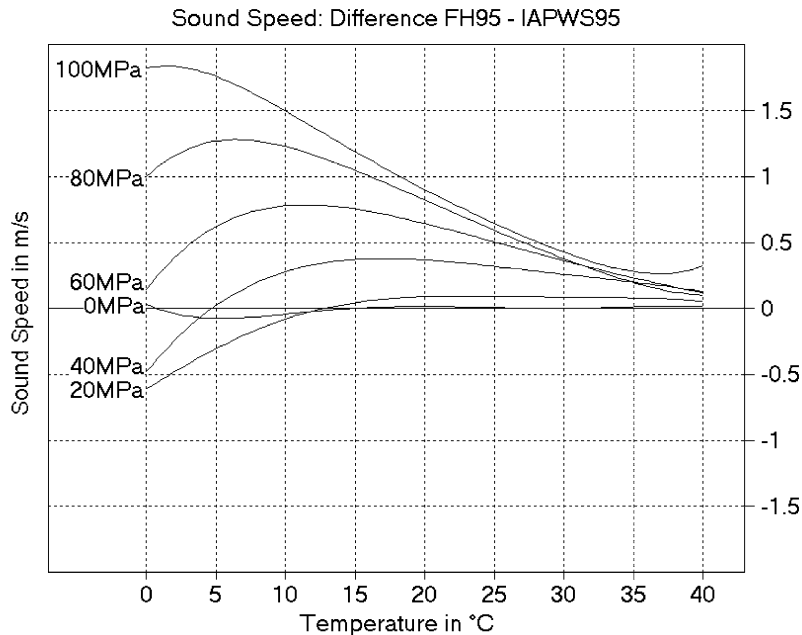


Fig. 11. Difference between the sound speeds of water, $U(0,t,p)$, computed by the FH95 and IAPWS95 formulas for applied pressures p between 0 and 100 MPa (0 and 10,000 dbar). Corresponding curves for the EOS80 or Kell and Whalley (1975) formulas look quite similar to FH95.

or 0.015 m/s (Del Grosso & Mader, 1972). They evidently underestimate the corrections required for EOS80 and FH95 at pressures above 40 MPa to meet the new IAPWS95 standard.

The sound speed equation of EOS80 is derived from measurements of Chen and Millero, (1977), who used as pure water reference the one atmosphere measurements of Del Grosso (1970) and Del Grosso and Mader (1972) together with the high pressure measurements of Wilson (1959). The latter ones are questionable (Del Grosso, 1974) and are mainly blamed (Millero and Li, 1994) to be the cause for discrepancies between computed and measured sound travel times in the ocean (Dushaw et al., 1993), which amount for about 0.5 m/s and are partly reduced but not overcome by the correction proposed by Millero and Li (1994), as was pointed out again by Meinen and Watts (1997). The sound speed formula of Del Grosso (1974), however, is in agreement with travel-time data within only 0.05 m/s. The new IAPWS95 sound speed formula suggested the hope that these problems with Chen-Millero sound speeds may now be eventually resolved in a natural way, but unfortunately this could not be achieved by a simple replacement of the pure water parts (see Fig. 12 and Table 3).

In the region of interest here, IAPWS95 sound speed can be considered as accurate as $\Delta U/U \approx 1000$ ppm (Wagner and Pruß, 2002) compared to measurements of Mamedov (1979) and Petitot, Tufeu & Le Neindre (1983). The precise measurements of Fujii (1994) between 303 and 323 K, and between 10 and 200 MPa, are even covered within $\Delta U/U \approx 250$ ppm (or 0.5 m/s). The one atmosphere measurements of Del Grosso and Mader (1972) and Fujii & Masui (1993) are reproduced with maximum errors of only 10 ppm (or 0.02 m/s) resp. 30 ppm (or 0.05 m/s).

While the high-pressure data of Wilson (1959), which are suspected as erratic (Del Grosso, 1974, Millero and Li, 1994), are the only basis for the high pressure formulas of Kell and Whalley (1975), EOS80, or FH95, the new IAPWS95 standard is derived from more than 600 sound speed data points of 12 studies including only 32 from Wilson (Wagner and Pruß, 2002) and can therefore be considered as being much more reliable.

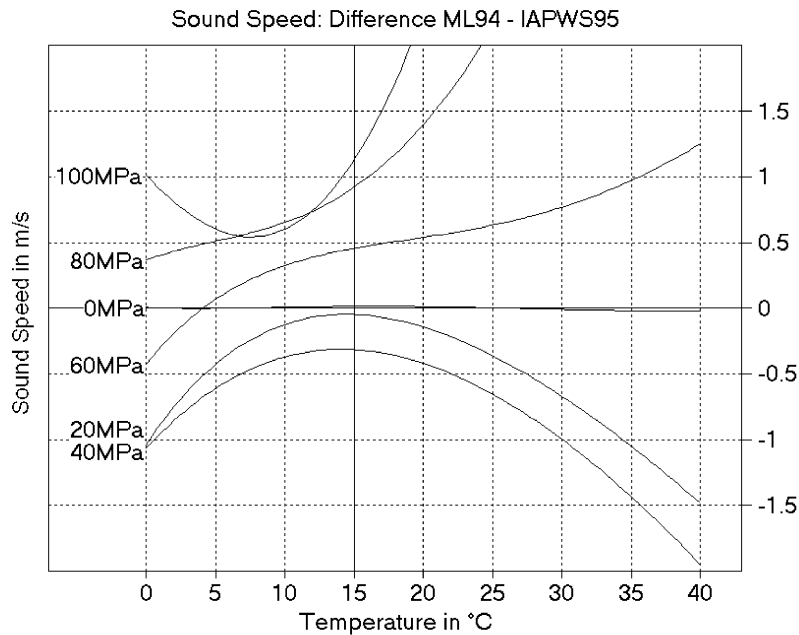


Fig. 12. Difference between the sound speeds of water, $U(0, t, p)$, computed by the ML94 equation (i.e. EOS80 with correction after [Millero and Li, 1994](#)) and IAPWS95 formulas, for applied pressures p between 0 and 100 MPa (0 and 10,000 dbar). ML94 is only applicable for temperatures t below 15 °C (solid line).

Table 3

Deviations of sound speed formulas from DG74 ([Del Grosso, 1974](#)) in the ranges of his Tables I to VII with different intervals of salinity, temperature and pressure. “ML94” is the correction of EOS80 sound speeds due to [Millero and Li \(1994\)](#). “Eq. (40)” means EOS80 sound speeds with its pure water part tentatively replaced by IAPWS95 sound speed (which is not valid for $t = 0$ °C at $p = 0$ MPa), as given in Eq. (40)

| DG74 data | S | t_{68} °C | p MPa | EOS80 m/s | ML94 m/s | Eq. (40) m/s |
|-----------|-------|----------------|------------|--------------|-------------|-----------------|
| Table I | 29–41 | 0–35 | 0 | 0.086 | 0.086 | 0.101 |
| Table II | 33–37 | 0–35 | 2 | 0.205 | 0.102 | 0.236 |
| Table III | 29–43 | 0–30 | 0 | 0.066 | 0.066 | 0.074 |
| Table IVa | 29–43 | 0 | 5 | 0.221 | 0.094 | 0.483 |
| Table IVb | 29–43 | 10 | 2 | 0.068 | 0.030 | 0.110 |
| Table IVc | 29–43 | 20 | 1 | 0.026 | 0.036 | 0.030 |
| Table IVd | 29–43 | 30 | 0.1 | 0.138 | 0.129 | 0.164 |
| Table V | 33–37 | 0 | 0–100 | 0.601 | 0.070 | 0.813 |
| Table VI | 33–37 | 5 | 0–100 | 0.692 | 0.120 | 0.485 |
| Table VII | 0 | 0–30 | 0 | 0.036 | 0.036 | 0.039 |

Deviations between FH95 and IAPWS95 are small at atmospheric pressure but grow to almost 2 m/s for high pressures, as shown in [Fig. 11](#). Very similar pictures (not shown here) arise for EOS80 or [Kell-Whalley \(1975\)](#) formulas if drawn instead of FH95 because all of them are derived from [Wilson’s \(1959\)](#) high-pressure data.

The correction to Wilson (1959) as proposed by Millero and Li (1994) for temperatures up to 15 °C is shown in Fig. 12. Especially at pressures above 60 MPa the deviations are smaller by a factor of about 2 than those of FH95 (and EOS80), but still beyond the error of 0.5 m/s as discussed for seawater, above.

Sound speeds computed by Eq. (28) using the Gibbs potential derived in this paper deviate from IAPWS95 by typically 0.01 m/s or 10 ppm for all temperatures and pressures considered here, see Fig. 13, which is a well tolerable error.

6. Free enthalpy of water

Free enthalpy, $g(S, t, p)$, as proposed by Feistel and Hagen (1995) can immediately be compared with the corresponding expression derived from IAPWS95 free energy, $f(T, p)$, by $g = f + P/\rho$ after alignment of their reference states. While IAPWS95 entropy σ and internal energy e of the liquid water phase are supposed to vanish at the triple point $T_t = 273.16$ K, $P_t = 611.657$ Pa (Wagner and Pruß, 2002), entropy and enthalpy of FH95 are zero for standard seawater, $t_0 = 0$ °C ($T_0 = 273.15$ K), $p_0 = 0$ MPa ($P_0 = 0.101325$ MPa), compare Feistel and Hagen (1995). Both free enthalpies can differ by an arbitrary linear function of temperature,

$$g^{IAPWS95} = g^{FH95} + A + B \cdot T \quad (31)$$

The coefficients A and B can e.g. be determined by comparing entropies and enthalpies at a specified mutual reference point (T, P) , which we have chosen at triple point temperature, $T = T_t$, and atmospheric pressure, $P = P_0$, to obtain the relative gauge constants $A = 61.034755$ J/kg and $B = 0.147566807$ J/(kg K).

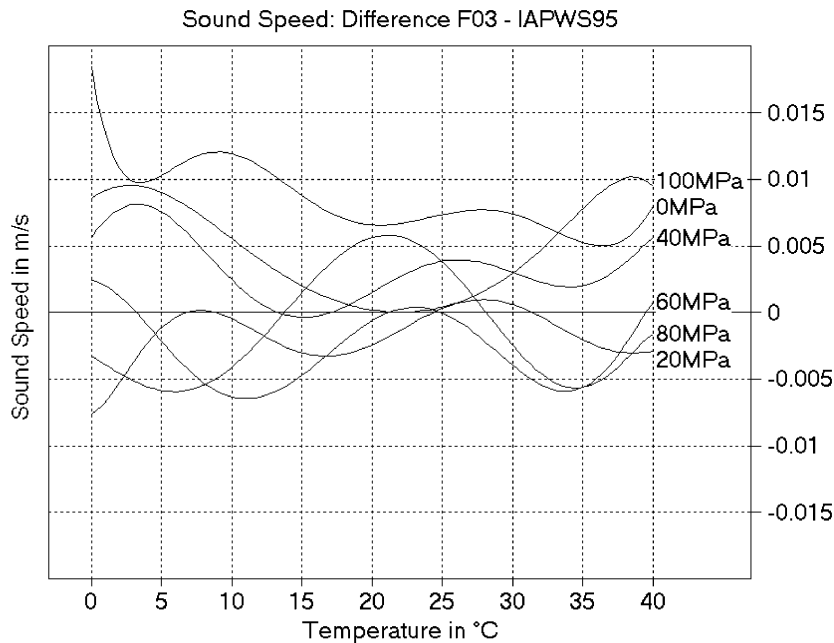


Fig. 13. Deviation between sound speeds of water, $U(0, t, p)$, computed by F03 and IAPWS95, for applied pressures p between 0 and 100 MPa (0 and 10,000 dbar).

The difference between both sides of Eq. (31) is shown in Fig. 14(a). While the curves belonging to different applied pressures between $p = 0$ and $p = 100$ MPa look very similar, both free enthalpies differ systematically and much stronger in their dependencies on temperature. This is caused by the offset in heat capacities as discussed in section 2.

Deviations in enthalpy $h = g - T \frac{\partial g}{\partial T}$ between the two sides of Eq. (32),

$$h^{IAPWS95} = h^{FH95} + A \quad (32)$$

see Fig. 14(b), following from the heat capacity offset as well, are in the order of $\Delta h \approx 100$ J/kg or $\Delta h/h \approx 0.1\%$, with only small consequences to be expected for e.g. oceanographic energy budgets.

Two coefficients g_{000} , g_{010} have been determined by adopting the pure water reference state of IAPWS95, which is vanishing entropy and internal energy at the triple point (t_t , p_t):

$$\left(\frac{\partial g(0, t_t, p_t)}{\partial t} \right)_{s,p} = 0 \quad (33)$$

$$g(0, t_t, p_t) - T_t \left(\frac{\partial g(0, t_t, p_t)}{\partial t} \right)_{s,p} - p_t \left(\frac{\partial g(0, t_t, p_t)}{\partial p} \right)_{s,t} = 0 \quad (34)$$

Although not mandatory, it is reasonable here to substitute the pure water reference state used in FH95 by a description consistent with the IAPWS95 standard. This change has become possible now because the F03 is valid at the triple point, while FH95 was not. The resulting maximum deviations over the whole range of pressures and temperatures are about 0.003 J/kg in free enthalpies, and 0.3 J/kg in enthalpies, see Fig. 15. These coefficients are required if computations are performed for typical cases like phase equilibria in freezing point or vapour pressure investigations.

7. Density of seawater

The EOS80 density equation $\rho^{EOS80}(S, t, p)$ of seawater at one atmosphere ($p = 0$ MPa) was determined by Millero and Poisson (1981a) with precision $\Delta\rho/\rho \approx 3.6$ ppm relative to pure water density, ρ_0 , using the IPTS-68 temperature scale. They had used 122 data points of Millero, Gonzalez & Ward (1976a) and 345 data points from Poisson, Brunet & Brun-Cottan (1980). We have used here their normalized data $\Delta\rho = \rho - \rho_0$ as reported in Millero & Poisson (1981b), and minimized the corresponding expression

$$\sum \left\{ \left(\frac{\partial g}{\partial p} \right)_{s,t} - \frac{1}{\Delta\rho(S, t_{68}, 0) + \rho^{IAPWS95}(T, P_0)} \right\}^2 = Min \quad (35)$$

with required r.m.s. deviation of 4 mm³/kg to determine the coefficients g_{ij1} , $i > 0$, as shown in the appendix. At temperatures below the fresh water freezing point, IAPWS95 density is not valid and was extrapolated from $t = 0.0026$ °C by means of the thermal expansion coefficient. The latter correction is small (0.3 ppm). The temperatures t_{68} were converted into ITS-90 temperatures, t , by the formula given by Blanke (1989). The results of the fit are shown in Fig. 16. The regression polynomial fits well within the experimental scatter of 4 ppm. The r.m.s. deviation of the fits was 4 mm³/kg for both the data sets of Poisson et al. (1980) and of Millero et al. (1976a). The relative densities $\Delta\rho = \rho(S, t, 0) - \rho(0, t, 0)$ of seawater to water computed by either EOS80 or F03 are shown in Fig. 17. Except some edge effects, both formulas agree fairly well within 4 ppm.

For higher salinities, the density measurements of Poisson & Gadhoumi (1993), see also Poisson et al. (1991), at temperatures 15–30 °C and salinities 34–50 have been included in a similar manner. EOS80

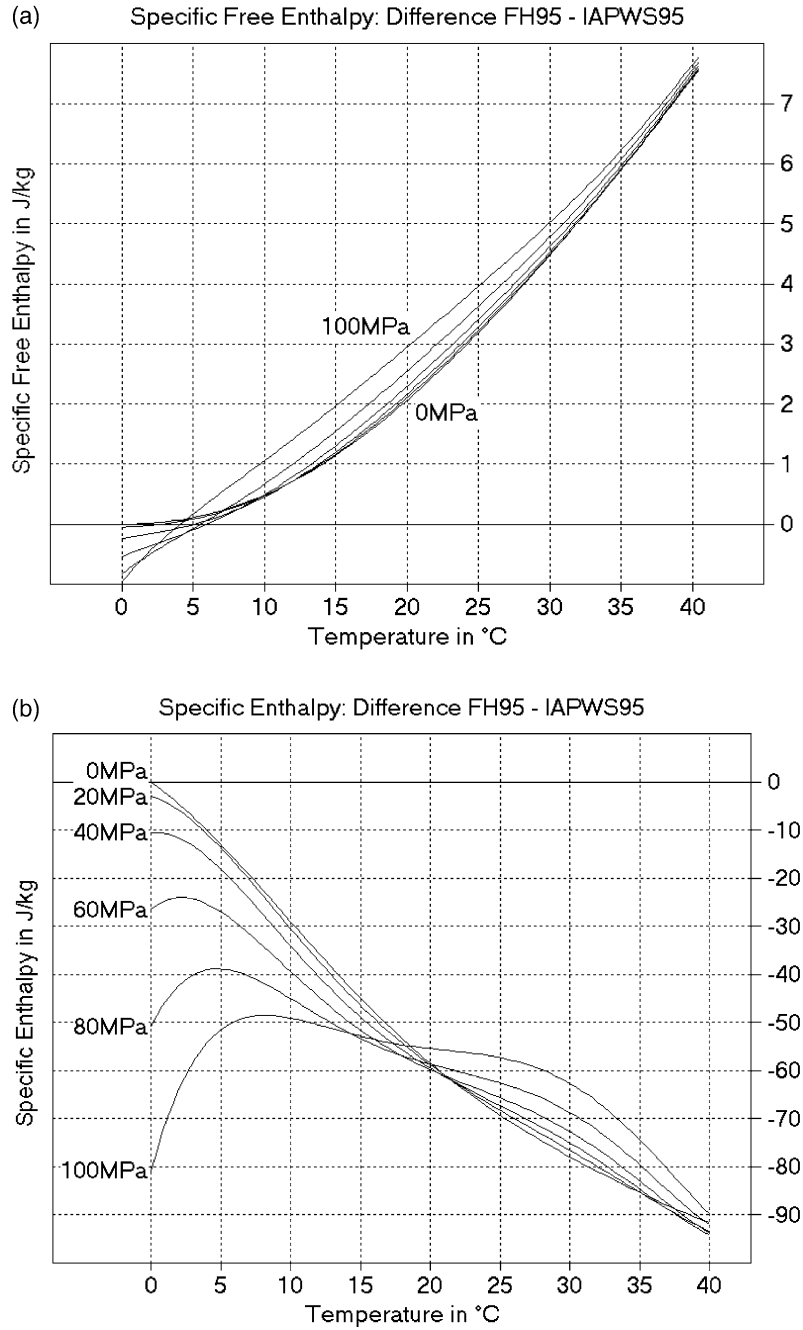


Fig. 14. Difference between pure water (a) free enthalpies, $g(0, t, p)$, above, and (b) enthalpies, $h(0, t, p)$, below, of FH95 and IAPWS95, after alignment to the same reference state, Eq. (31). The different curves belong to applied pressures p between 0 and 100 MPa. Neither enthalpy nor free enthalpy are available from EOS80. The striking differences in curvature of $g(0, t, p)$ and in slope of $h(0, t, p)$ are due to the different heat capacities involved.

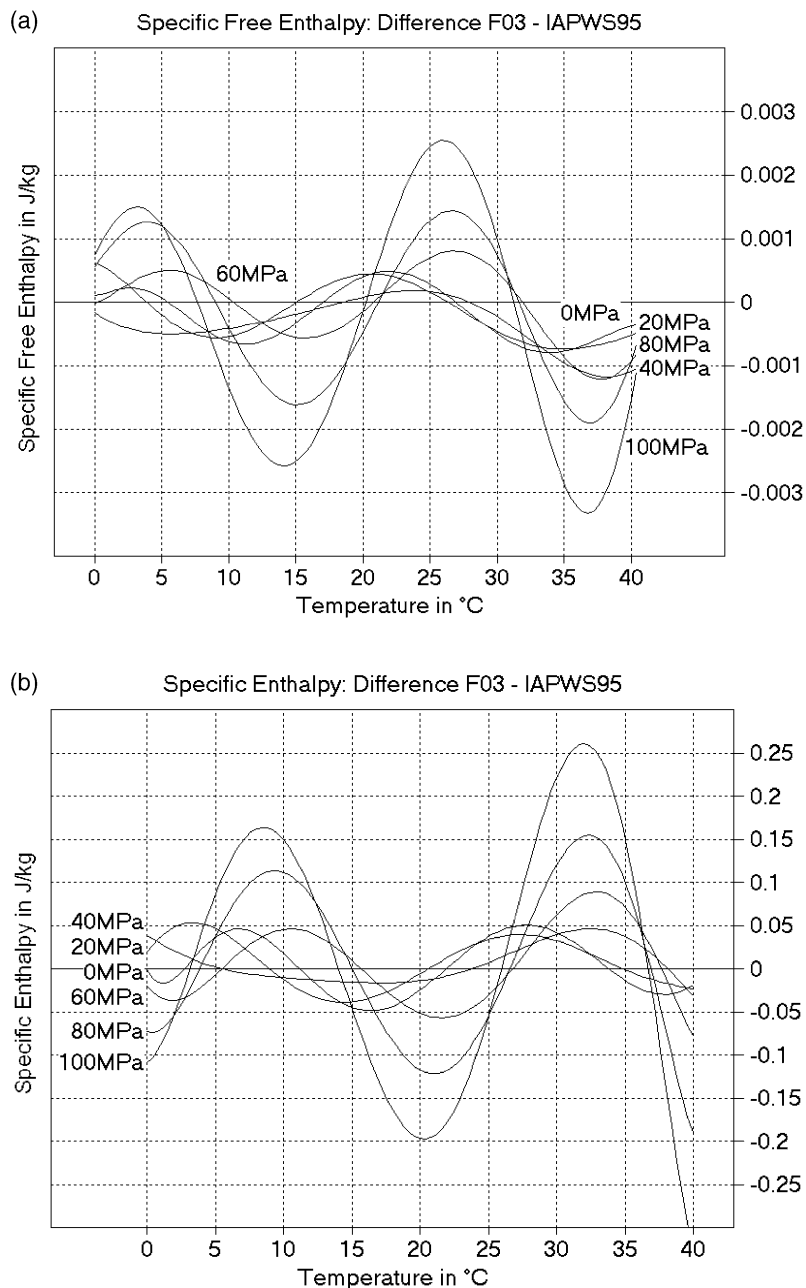


Fig. 15. Difference between (a) free enthalpies, $g(0, t, p)$, above, and (b) enthalpies, $h(0, t, p)$, below, of F03 and IAPWS95 for water at the applied pressures p as indicated at the curves. All functions refer to the same reference state, zero energy and zero entropy at the triple point.

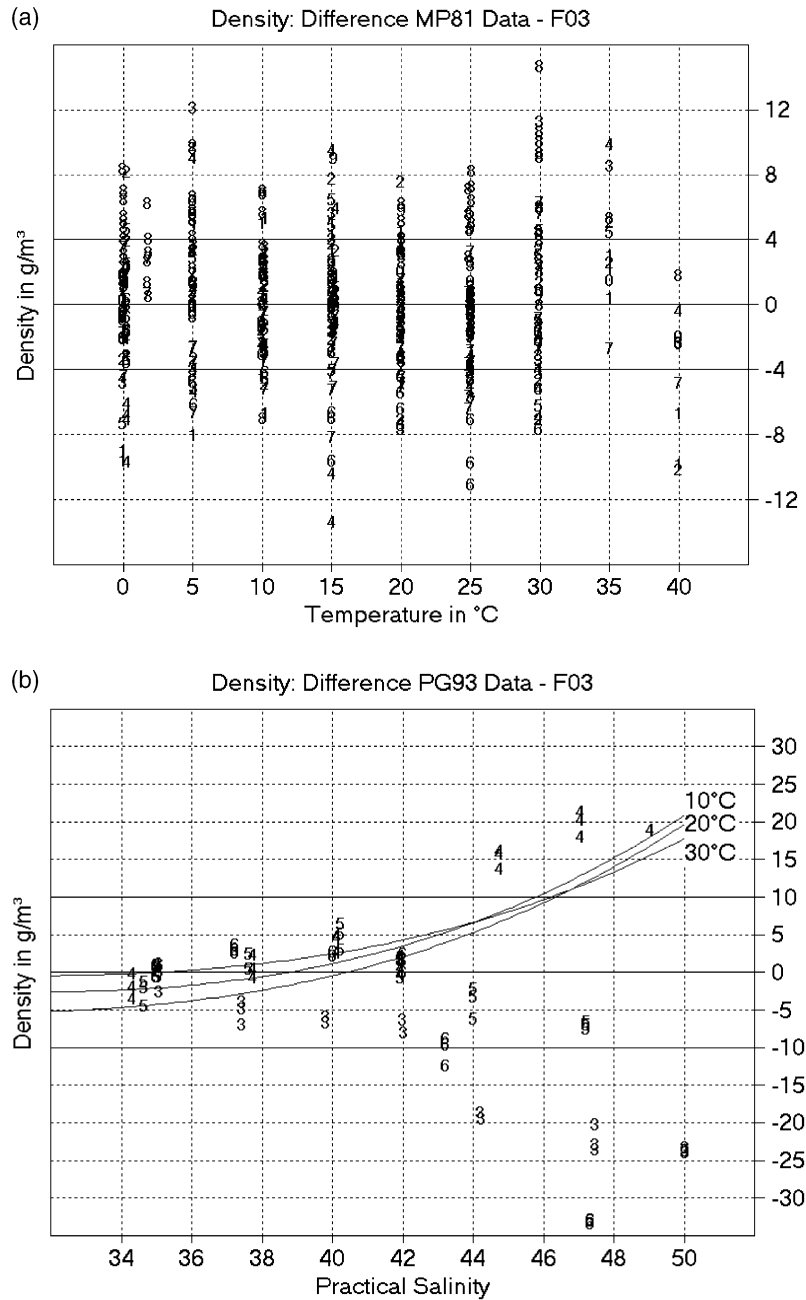


Fig. 16. Deviation of recalibrated density measurements at atmospheric pressure ($P = 0.101325$ MPa) from computed densities of F03: (a) MP81 data, above, as reported by [Millero and Poisson \(1981b\)](#). Symbols 0–8 represent salinities by $S/5$ rounded to integers. Experimental uncertainty of 4 ppm is indicated by horizontal lines. (b) PG93 data, below, as reported by [Poisson and Gadhoumi \(1993\)](#). Symbols 3–6 represent temperatures by $t/5$ rounded to integers. Data with $S > 44$ at 20 °C (“4”) appear about 30 ppm denser than the rest. Required tolerance 10 ppm of the fit is indicated by horizontal lines. Curves are computed by EOS80 for temperatures 10, 20 and 30 °C, called the ‘Red Sea extension’ up to $S = 43$ ([Mamayev et al., 1991](#)).

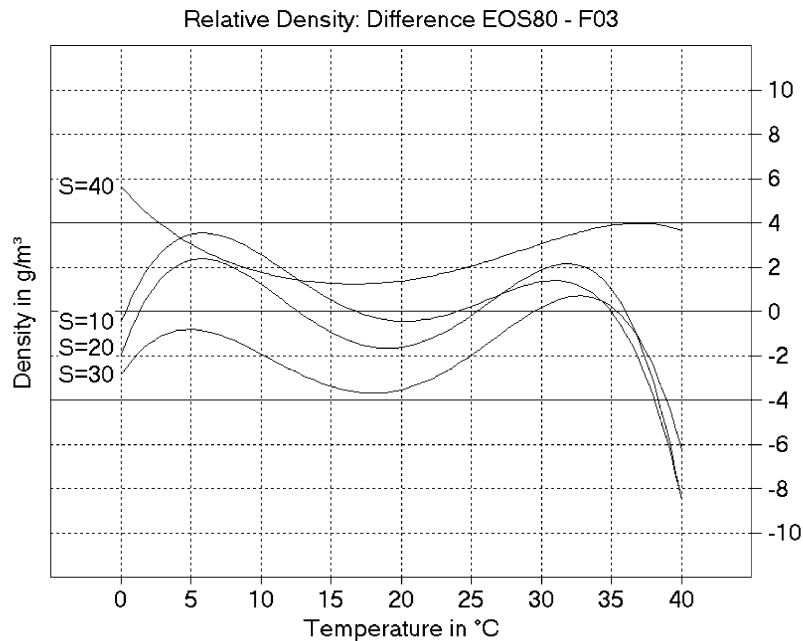


Fig. 17. Relative densities $\Delta\rho = \rho(S,t,0) - \rho(0,t,0)$ of seawater to pure water have been computed by EOS80 and by F03 for various salinities S (as indicated at the curves) as functions of temperature t .

pure water densities have first been subtracted from densities reported in the paper, and the resulting relative densities were treated as in Eq. (35). The error range of 4 ppm claimed by the authors had to be relaxed to merely required 10 ppm due to apparent conflicts with other data groups in this fit, which finally achieved an r.m.s. of 11 ppm. The data at 20 °C and salinities above 44 seem to be responsible for this discrepancy since they form a separate cluster in Fig. 16(b).

Because the same coefficients also influence heat capacities, density maxima, sound speeds, and high-pressure densities, a simultaneous regression of all these quantities was performed. The other fits are discussed in the following sections.

8. Heat capacity of seawater

The EOS80 heat capacity equation is derived from measurements of Millero et al. (1973a). They determined the power ratios $r(S,t) = \Delta P/P$ of their Picker calorimeter with an overall uncertainty of 0.5% and computed heat capacities $c_P(S,t,0)$ of seawater at atmospheric pressure by the formula,

$$\frac{c_P(S,t,0)}{c_P(0,t,0)} = (1 + r(S,t)) \cdot \frac{\rho(0,t,0)}{\rho(S,t,0)} \quad (36)$$

using densities $\rho(S,t,0)$ and $\rho(0,t,0)$ of EOS80 and pure water heat capacities $c_P(0,t,0)$ as reported by Stimson (1955). Fortunately, in their paper they have made available their measured power ratios such that a recalibration of their heat capacities could easily be done. We have minimized the corresponding sum over all reported points $r(S,t_{68})$, as,

$$\sum \left\{ T \left(\frac{\partial^2 g}{\partial t^2} \right)_{S,p=0} + c_P^{IAPWS95}(T,P_0) \cdot (1 + r(S,t_{68})) \cdot \rho^{IAPWS95}(T,P_0) \cdot v(S,t,0) \right\}^2 = \text{Min} \quad (37)$$

with a required r.m.s. deviation of 0.5 J/(kg K) (Millero et al., 1973a) using specific volume $v = \left(\frac{\partial g}{\partial p}\right)_{S,t}$ available after Eq. (35) to determine the coefficients g_{ij0} , $i > 0, j > 1$. The fit was carried out simultaneously with further heat capacity data, below, as well as the ones for density, sound speed and density maxima due to commonly required coefficients of the thermodynamic potential. The results are shown in Fig. 18. The current fit reproduces the recalibrated measurements with an r.m.s. of 0.5 J/(kg K). Former equations EOS80 and FH95 deviate from it up to 5 J/(kg K), or 0.1%.

Bromley et al. (1970) have determined heat capacities at atmospheric pressure for seawater over a wide range of temperatures and salinities. These data can be assumed to be very accurate, compare Fig. 6. The authors estimated the maximum error to be 0.22% or 9 J/(kg K). Systematic thermal causes may possibly contribute one half to it. We have selected 25 points from $t = 0$ –40 °C and from $S = 10$ –50. The latter ones were used especially to support the high salinity density data of Poisson and Gadhoumi (1993), see section 7. Assuming that systematic thermal errors of the calorimeter bomb are likely independent of sample salinities, they may be diminished by using as reference the heat capacities of pure water reported by Bromley et al. (1970) in comparison to IAPWS95. Therefore, we have adjusted their seawater data, $c_p^{BDSW70}(S, t_{48}, 0)$, supposing IPTS-48 temperature scale, prior to regression as,

$$\sum \left\{ T \cdot \left(\frac{\partial^2 g}{\partial t^2} \right)_{S,p=0} + c_p^{BDSW70}(S, t_{48}, 0) \cdot \frac{c_p^{IAPWS95}(T, P_0)}{c_p^{BDSW70}(0, t_{48}, 0)} \right\}^2 = \text{Min} \quad (38)$$

These recalibration corrections remain between 0.02 and 0.08% of the measured values, thus, the function $c_p^{BDSW70}(0, t_{48}, 0)$, based on data of Osborne et al. (1939), agrees quite well with IAPWS95 heat capacities.

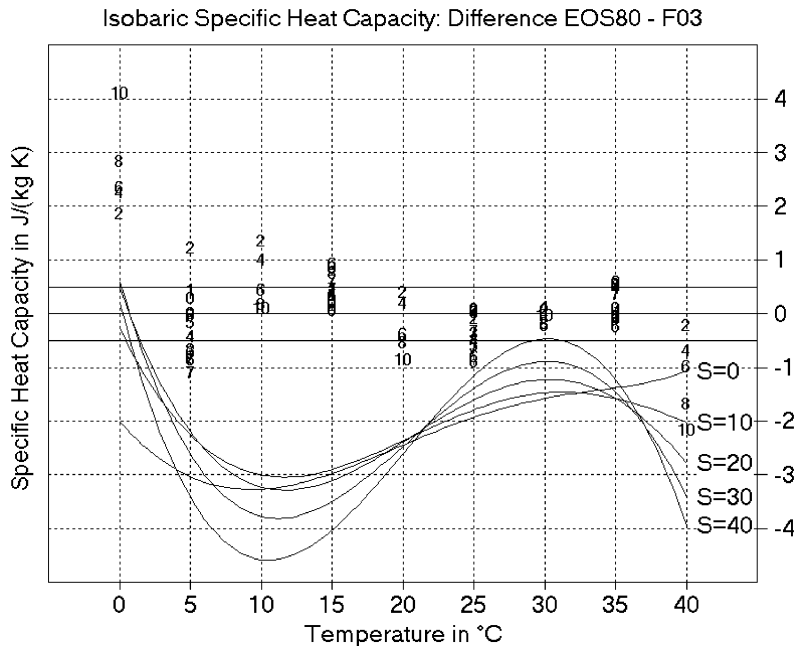


Fig. 18. Comparison of EOS80 isobaric specific heat capacities at atmospheric pressure ($P = 0.101325$ MPa), $c_p(S, t, 0)$, with F03 for salinities $S = 0$ –50 as indicated at the curves. Symbols 1–10 indicate, by salinities as $S/5$ rounded to integers, the recalibrated measurements at atmospheric pressure of Millero et al. (1973a) at temperatures $t = 5, 15, 25, 35$ °C and of Bromley et al. (1970) at $t = 0, 10, 20, 30$ and 40°C. Estimated precision of relative heat capacity measurements is marked by solid lines. FH95 heat capacities, not shown, are very similar to the EOS80 curves.

For the fit, we have required an r.m.s. deviation of 2 J/(kg K) (or 0.05%), which was met by an even less resulting mean residual of 1.4 J/(kg K) (or 0.01%), compare Fig. 18. The data seem to possess a systematic, almost linear temperature trend in the plot, which contributes most of the scatter at the interval edges of 0 and 40 °C.

For higher pressures, computed heat capacities of EOS80 and FH95 deviate up to 3 times as much, see Fig. 19, although still obeying the typical accuracy of 10 J/(kg K) of specific heat measurements. These stronger differences are mainly a result of a modified determination of high pressure densities in comparison to FH95, see section 11 for details.

9. Thermal expansion of seawater

Temperatures of maximum density, t_{MD} , determined by Caldwell (1978) for seawater of various pressures and salinities, correspond to zeroes of the thermal expansion coefficient. The experimental temperature uncertainty of 40 mK leads to a limitation of thermal expansion in between ± 0.6 ppm/K (Feistel and Hagen, 1995). The fit was done to minimize the sum over all reported triples (S , t_{MD} , p), assuming IPTS-68,

$$\sum_{t_{MD}} \left\{ \frac{\partial^2 g}{\partial t \partial p} \right\}^2 = \text{Min} \quad (39)$$

with a required r.m.s. deviation of 0.6 mm³/(kg K), jointly with density, heat capacity and sound speed of seawater. The fit achieved the desired goal with a resulting r.m.s. of 0.7 mm³/(kg K), compare Fig. 20. The current F03 formula reproduces the t_{MD} data as good as FH95, but visibly better than EOS80.

For higher temperatures and salinity $S = 35$, EOS80 thermal expansion coefficients deviate from the current ones up to 10 times the estimated experimental error, see Fig. 21. FH95 deviations are of similar magnitude, but happen already at lower temperatures. The main reason for this difference is the fact that FH95 high pressure densities outside the naturally encountered combinations of S , t and p are exclusively determined from EOS80 sound speeds, while EOS80 high-pressure densities are mainly based on measured thermal expansion data. On the other hand, for temperatures up to 20 °C and pressures up to 40 MPa (4000 dbar), all three formulas agree well within the tolerance range.

10. Sound speed in seawater

Sound speed measurements of seawater are used here to determine its compressibilities and high pressure densities. The function of Del Grosso (1974), briefly DG74, can immediately be used for this purpose after converting temperatures from IPTS-68 to ITS-90 scales. It is only valid for Neptunian waters, in form of his “tables” I–VI with accuracy 0.05 m/s, see Table 3. Due to this small error, these data are the preferred means for the determination of high-pressure densities since the precision of the results can be expected to be one order of magnitude more accurate than the direct density measurements (see Eq. (29)). Measurements of Chen and Millero (1977), briefly CM77, cover the entire range of salinities $S = 0$ –40, temperatures 0–40 °C and pressures 0–100 MPa, but they were found to be in error up to 0.5 m/s (Dushaw et al., 1993, Millero and Li, 1994, Meinen and Watts, 1997). Millero and Li (1994), briefly ML94, pointed out that Chen and Millero had measured only sound speed differences to pure water, for which they had used the formula of Wilson (1959), and proposed a pressure correction valid below 15 °C.

We have studied a possible (simply additive) replacement of pure water sound speed in the EOS80 (CM77) formula by IAPWS95 sound speeds. The comparison made within the different tables of DG74 is shown in Table 3. We see that in the oceanographically important high-pressure regions of tables V and

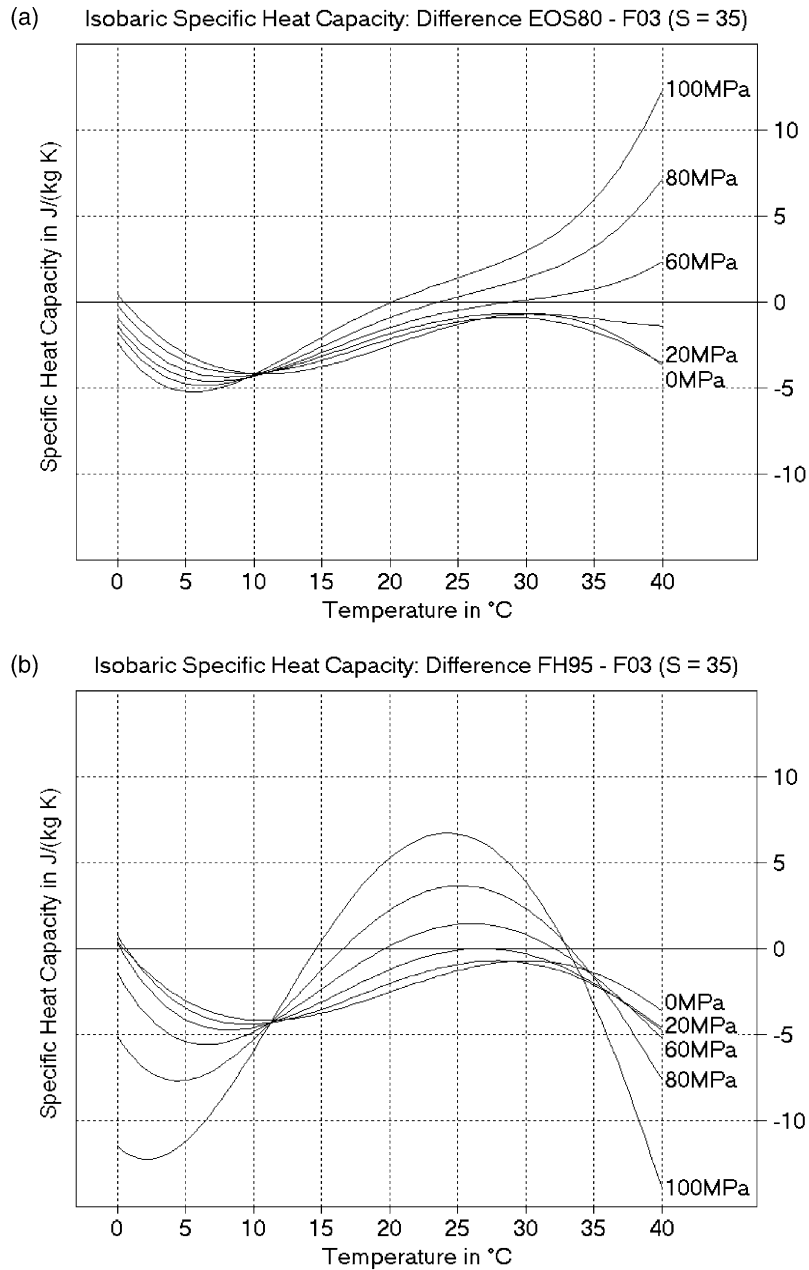


Fig. 19. High pressure isobaric specific heat capacities, $c_p(S, t, p)$, computed with (a) EOS80, above, and (b) FH95, below, compared with F03, for salinity $S = 35$ and applied pressures p between 0 and 100 MPa (0 and 10,000 dbar).

VI the mean deviation between DG74 and EOS80 exceeds 0.6 m/s, which is reduced by the ML94 correction to about 0.1 m/s. A tentative replacement of the pure water part, as suggested by the discussion of [Millero and Li \(1994\)](#), of EOS80 by IAPWS95 due to the formula,

$$U^{tent}(S, t, p) = U^{EOS80}(S, t_{68}, p) - U^{EOS80}(0, t_{68}, p) + U^{IAPWS95}(T, P) \quad (40)$$

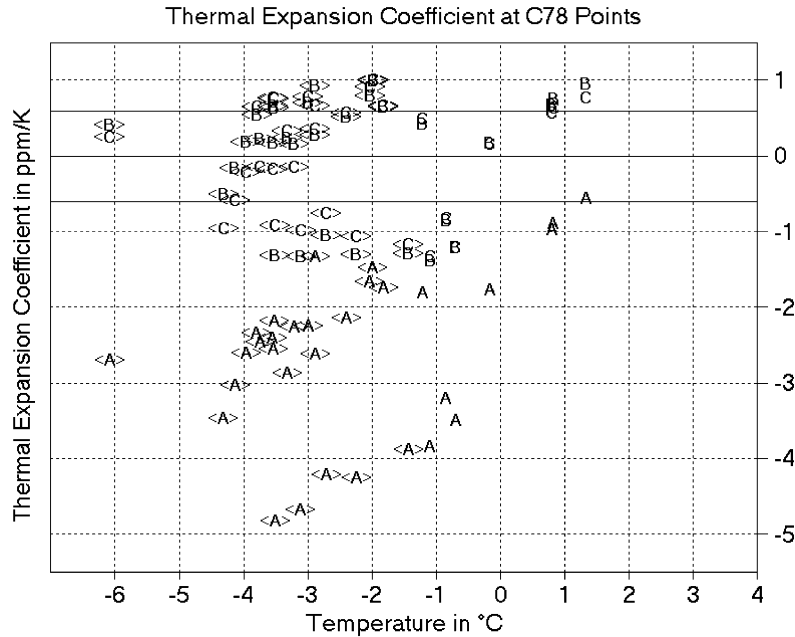


Fig. 20. Isobaric thermal expansion coefficients of seawater, $\alpha(S, t_{MD}, p)$, at Caldwell's (1978) temperatures of maximum density, t_{MD} , for various pressures p and salinities S , computed with EOS80 (A), FH95 (B) and F03 (C). Experimental error bounds are indicated by solid lines. Symbols in brackets are below the freezing temperature.

does not improve the data quality relative to DG74, see Table 3.

For the regression determining the coefficients $g_{i,j,k}$, $i > 0$, we have used DG74 in the regions in S - t - p space of his tables (Table 3) to solve the nonlinear problem,

$$\int dS dt dp \left\{ \frac{(\partial g / \partial p)^2 \cdot \partial^2 g / \partial t^2}{(\partial^2 g / \partial t \partial p)^2 - \partial^2 g / \partial t^2 \cdot \partial^2 g / \partial p^2} - U^2(S, t_{68}, p) \right\}^2 = \text{Min} \quad (41)$$

with required r.m.s. of 0.05 m/s.

In distinction to the previous FH95 Gibbs function computation, we have completely refrained this time from using CM77 sound speeds because of the virtual impossibility to recalibrate them properly to the IAPWS95 standard as shown in Table 3. The correction formula ML94 is neither covering the entire S - t - p region, nor is it sufficiently precise (Meinen and Watts, 1997). Instead, sound speeds of the regions in the S - t - p space outside of Del Grosso's Neptunian waters were indirectly determined here from high-pressure density data. These data proved as very well compatible with DG74 in their overlapping S - t - p domains, as shown in Fig. 22, and in section 11. The fit was carried out in one single run together with densities, heat capacities, and maximum density temperatures. As results, we obtained r.m.s. values for tables I–III of 0.017 m/s, for table IV of 0.012 m/s, and for tables V–VI of 0.035 m/s.

Fig. 22 shows the comparison of the current F03 fit with DG74, EOS80/CM77, SM91 (Spiesberger and Metzger, 1991), ML94 and FH95 formulas for the oceanographically most interesting tables V and VI of Del Grosso. SM91 is a pressure correction to DG74, presumably valid up to 40 MPa, derived from acoustic pulse travel times in the deep Pacific. Deviations from DG74 and FH95 remain in the negligible range of 0.05 m/s, while ML94 provides systematically higher values which exceed even 0.1 m/s. However, for the less interesting conditions of high pressures and high temperatures, not shown here, the situation is still unsatisfactory: deviations between different formulas exceed several m/s in extreme cases. The only system-

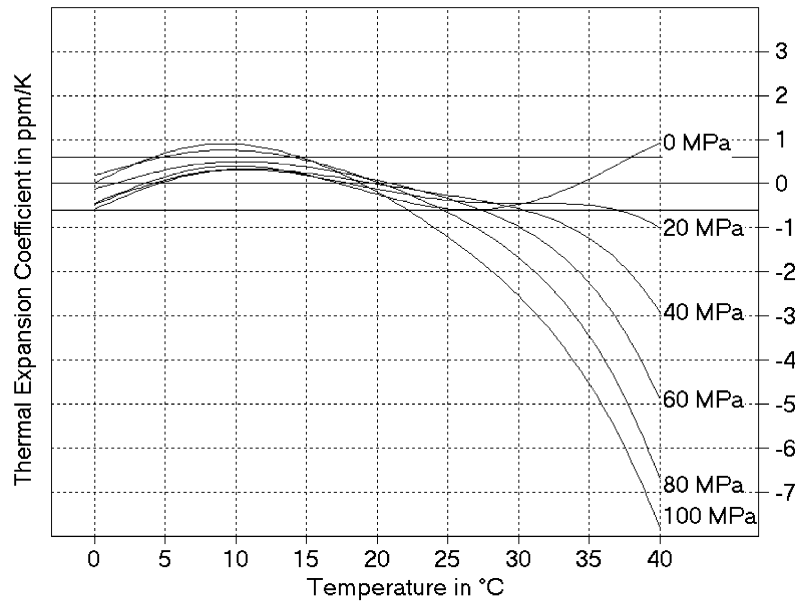
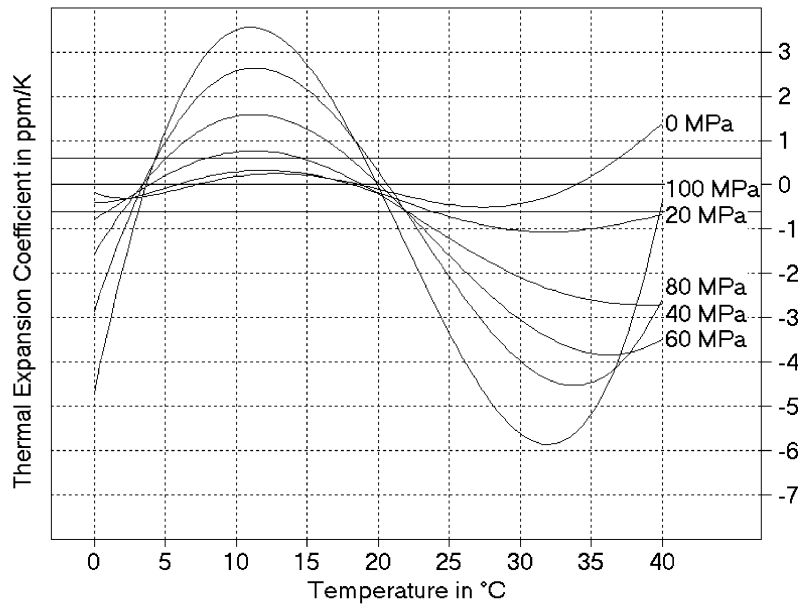
(a) Thermal Expansion Coefficient: Difference EOS80 - F03 ($S = 35$)(b) Thermal Expansion Coefficient: Difference FH95 - F03 ($S = 35$)

Fig. 21. Isobaric thermal expansion coefficients, $\alpha(S, t, p)$, of (a) EOS80, above, and (b) FH95, below, compared to F03, for seawater with salinity $S = 35$ and various pressures p , as indicated at the curves. Experimental uncertainty of 0.6 ppm/K is marked by horizontal lines.

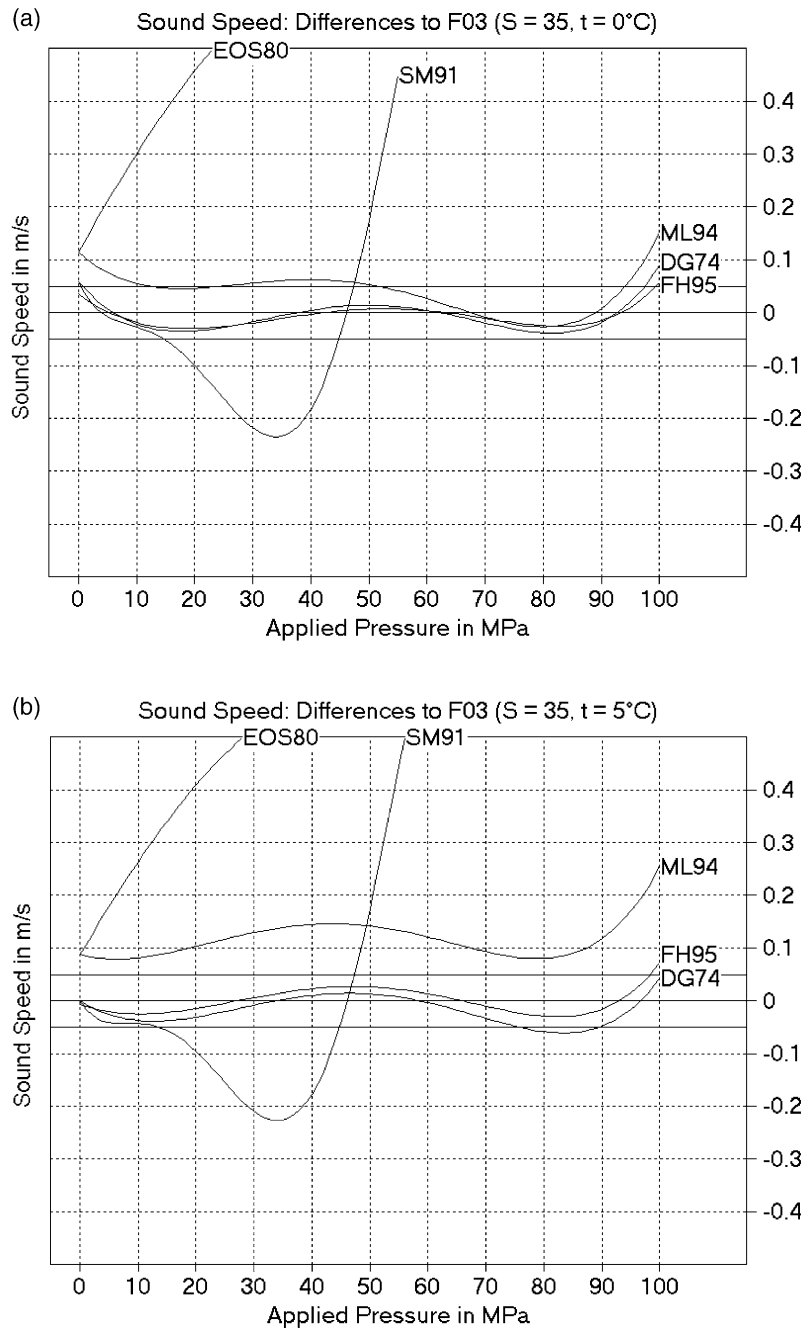


Fig. 22. Comparison of high pressure sound speeds, $U(S, t, p)$, of DG74 (Del Grosso, 1974), EOS80 (Chen and Millero, 1977), SM91 (Spiesberger and Metzger, 1991), ML94 (Millero and Li, 1994) and FH95 (Feistel and Hagen, 1995), with F03, for (a) table V, $S = 35$, $t = 0^\circ\text{C}$, above, and (b) table VI, $S = 35$, $t = 5^\circ\text{C}$, below, of Del Grosso. Estimated accuracy of 5 cm/s is indicated by solid lines.

atic measurements here are still the data of [Chen and Millero \(1977\)](#) which apparently lack of a proper calibration to high-pressure sound speeds of pure water ([Millero and Li, 1994](#)).

11. High-pressure density of seawater

The specific volumes of seawater at high pressures have been measured by [Chen & Millero \(1976\)](#) and were used for the construction of the EOS80 pressure dependence ([Millero et al., 1980](#)). They reported 558 readings from 0–40 °C, 0–100 MPa and $S = 5$ –40 together with a regression polynomial $v^{CM76}(S, t_{68}, p)$, which reproduces their data within an error range of 8.6 ppm, as shown in [Fig. 23\(b\)](#). The authors explicitly describe how the data are gauged to specific volumes of pure water, such that a new calibration with respect to the actual IAPWS95 water properties is relatively obvious. Requiring a mean deviation of 10 ppm, we have minimized the sum over all their data samples v^{meas} in the form of,

$$\sum \left\{ \left(\frac{\partial g}{\partial p} \right)_{S,t} - \frac{v^{meas}(S, t_{68}, p)}{v^{CM76}(0, t_{68}, p) \cdot \rho^{IAPWS95}(T, P)} \right\}^2 = Min \quad (42)$$

The idea behind this correction is the assumption that the most significant errors come from the temperature-pressure calibration of the measuring device, and that these errors are independent of the salinity of the sample under study. Considering IAPWS95 pure water densities as “truth”, Eq. (42) removes all errors of this kind from the measured data since they appear equally in v^{meas} and v^{CM76} . The regression returned an r.m.s. of 11 ppm, as shown in [Fig. 23\(a\)](#), which is nearly as small as the experimental scatter itself. Thus, F03 describes these recalibrated measurements almost equivalently well as the regression polynomial of the authors, and at the same time consistently with [Del Grosso’s \(1974\)](#) sound speeds. Note that the r.m.s. deviation of the v^{meas} data from EOS80 is even bigger (17 ppm, [Fig. 23\(c\)](#)). EOS80 is considered as accurate as 9 ppm ([Millero et al., 1980](#)).

A second extended data set on high-pressure densities used for EOS80 was the thermal expansion experiment by [Bradshaw and Schleicher \(1970\)](#). They reported 221 specific volume data $\Delta v^{meas}(S, t, p) = v(S, t, p) - v(S, 0, p)$ relative to 0 °C from -2 – 30 °C (IPTS-48 scale), 1–100 MPa and $S = 30$ –40. Their equipment was calibrated with mercury. With a required precision of 4 ppm as in the case of one-atmosphere densities (section 7) we have minimized the expression,

$$\sum \left\{ \left(\frac{\partial g}{\partial p} \right)_{S,t} - \left(\frac{\partial g}{\partial p} \right)_{S,t=0} - \Delta v^{meas}(S, t_{48}, p) \right\}^2 = Min \quad (43)$$

resulting in an r.m.s. deviation of only 2.6 ppm of the fit, as shown in [Fig. 24](#). This scatter is comparable to that relative to the thermal expansion polynomial of those authors (3.2 ppm). The r.m.s. deviation of 6 ppm of these data from EOS80 is twice as big. We may conclude that by the current formulation F03, these data of [Bradshaw and Schleicher \(1970\)](#) could be brought into good agreement with recalibrated specific volumes of [Chen and Millero \(1976\)](#), with [Del Grosso’s \(1974\)](#) sound speeds, and with [Caldwell’s \(1978\)](#) t_{MD} data.

In the paper of [Bradshaw & Schleicher \(1976\)](#) the changes of volumes $V_i(S, t, P)$ due to pressure P of given seawater samples (i) with unknown amounts are reported. These data were not included into the fit of F03. For comparison of these measurements with the current formulas, we have first determined the sample masses M_i by regression with respect to the actual specific volume polynomial, $v = \partial g / \partial p$, as,

$$\sum \left\{ \left(\frac{\partial g}{\partial p} \right)_{S,t} \cdot M_i - \frac{V_i(S, t_{48}, P)}{v^{BS86}(t_{68}, p)} \cdot \left(\frac{\partial g}{\partial p} \right)_{S=0,t} \right\}^2 = Min \quad (44)$$

The resulting specimen masses are shown in [Table 4](#).

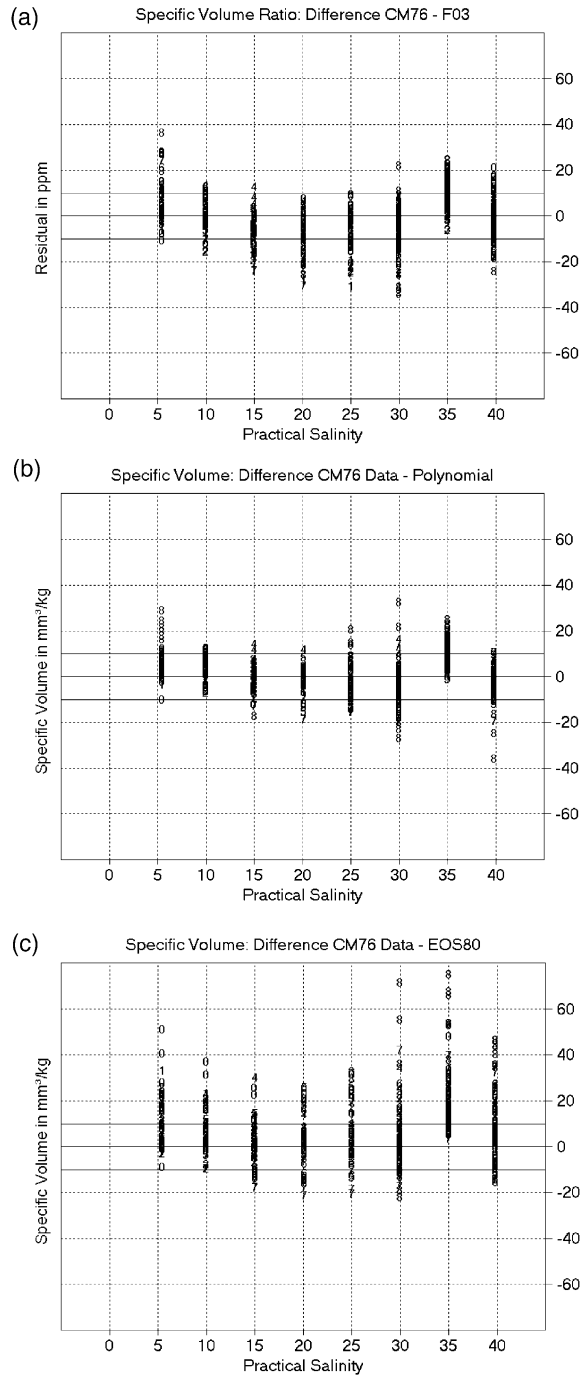


Fig. 23. Specific volume data of [Chen and Millero \(1976\)](#), $v^{meas}(S, t_{68}, p)$, (a) above, compared with F03 after recalibration to pure water, in the way used in Eq. (42), $\frac{v^{meas}(S, t_{68}, p)}{v^{CM76}(0, t_{68}, p)} - \frac{v(S, t, p)}{v(0, t, p)}$, (b) middle, compared with the regression polynomial, $v^{CM76}(S, t_{68}, p)$, of [Chen and Millero \(1976\)](#), (c) below, compared with EOS80. Symbols 0–8 used reflect temperatures by $t/5$ rounded to integers. Horizontal lines at 10 ppm indicate the r.m.s. required for the current fit.

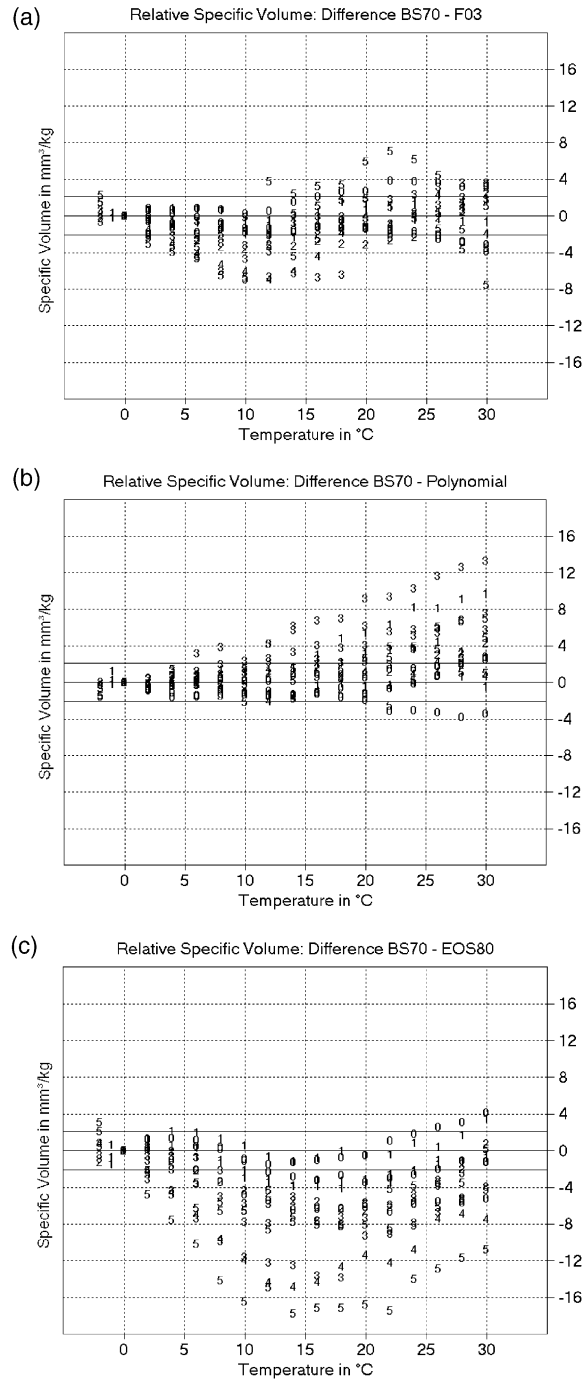


Fig. 24. Comparison of relative specific volume measurements of Bradshaw and Schleicher (1970), $\Delta v^{meas}(S, t, p) = v(S, t, p) - v(S, 0, p)$, with (a) F03, above, (b) the polynomial of Bradshaw and Schleicher (1970), middle, and (c) EOS80, below. The r.m.s. error range of 2 ppm required for the current fit is indicated by horizontal lines. Symbols represent the pressure as $p/20\text{MPa}$ rounded to integers.

Table 4

Seawater samples 1–7 of Bradshaw and Schleicher (1976) used for compression measurements with their masses determined by regression

| BS76 # <i>i</i> | <i>S</i> | <i>t</i> ₄₈ /°C | <i>M_i</i> /g |
|-----------------|----------|----------------------------|-------------------------|
| sample #1 | 0 | 10 | 43.2085 |
| sample #2 | 30.705 | 10 | 47.7841 |
| sample #3 | 34.891 | 10 | 48.2614 |
| sample #4 | 38.884 | 10 | 49.0071 |
| sample #5 | 34.897 | 10 | 48.3196 |
| sample #6 | 34.897 | 25 | 48.3203 |
| sample #7 | 34.912 | 25 | 48.3041 |

A good agreement with r.m.s. 4.8 ppm as shown in Fig. 25 was achieved after readjustment of the pressure dependence of pure water, in analogy to Eqs. (42) and (44), as,

$$v^{recalib}(S, t, p) = \frac{V_i(S, t_{48}, P) / M_i}{v^{BS86}(t_{68}, p) \cdot \rho^{IAPWS95}(T, P)} \quad (45)$$

Here, $v^{BS86}(t_{68}, p)$ is the specific volume of pure water proposed by Bradshaw & Schleicher (1986).

The comparison of seawater densities with $S = 35$ from EOS80 and from FH95 with densities from this paper over the entire intervals of temperatures and pressures shows maximum deviations of 40 ppm, see

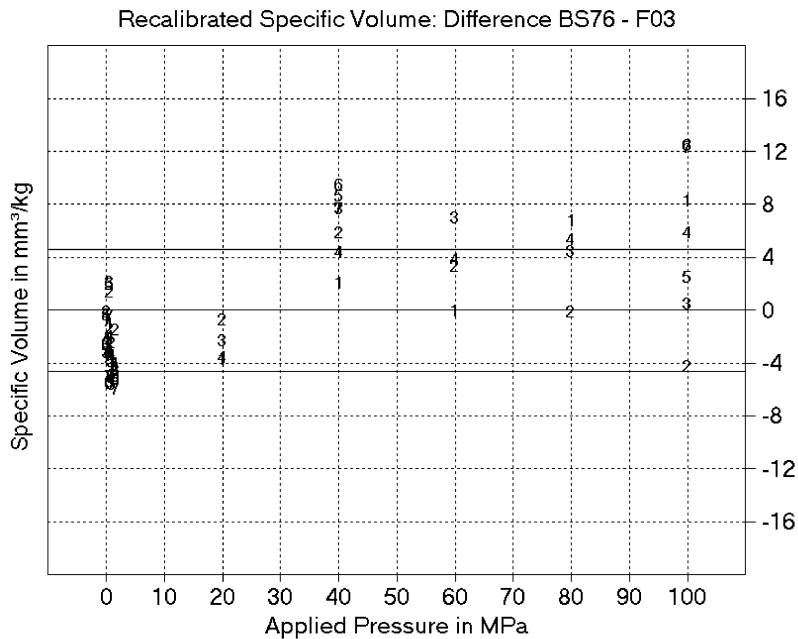


Fig. 25. Specific volume of compressed seawater samples reported by Bradshaw and Schleicher (1976), recalibrated after Eqs. (44), (45), $v^{recalib}(S, t, p)$, in comparison to F03. Symbols are sample numbers as given in Table 4. The r.m.s. deviation of 4.8 ppm is indicated by horizontal lines.

Fig. 26. Biggest errors appear in FH95 for high temperatures and pressures, while FH95 curves between 0 and 7 °C agree within 7 ppm with the current formula for all pressures. Deviations of EOS80 are more evenly distributed over temperatures and grow systematically with pressure. At atmospheric pressure, both formulas agree with the current one for all temperatures within a 4 ppm error limit.

The Gibbs potential is completely determined now by specific volume, $v(S, t, p)$, and heat capacity, $c_P(S, t, 0)$, except for enthalpy, $h(S, 0, 0)$, and entropy, $\sigma(S, 0, 0)$, of seawater at $t = 0$ °C and atmospheric pressure, $p = 0$ MPa, as,

$$g(S, t, p) = h(S, 0, 0) - \sigma(S, 0, 0) \cdot T - \int_0^t dt' \int_0^p dp' \frac{c_P(S, t', 0)}{T_0 + t'} + \int_0^p dp' v(S, t, p') \quad (46)$$

Sections 12–14 describe the computation of these two remaining unknown functions of salinity.

12. Limiting laws

At very low salt concentrations, the Debye–Hückel limiting laws govern the deviations of thermodynamic properties from those of pure water. Their exact measurement is technically difficult; however, they are required for proper fits of experimental data like freezing point depression or mixing heat (Bromley, 1968, Millero, Hansen & Hoff, 1973b) to the Gibbs potential. Fortunately, they can be derived sufficiently easily from the statistical theory of dilute mixed electrolytes (e.g. Lewis & Randall, 1961, Landau and Lifschitz, 1966, Falkenhagen and Ebeling, 1971). The following consideration briefly repeats the formulas given in FH95 except for a number of newer fundamental and molecular constants adopted here.

Up to terms $O(S^{3/2})$, the theoretical series expansion with respect to S of free enthalpy at atmospheric pressure takes the form (Landau and Lifschitz, 1966, Falkenhagen and Ebeling, 1971, Feistel and Hagen, 1995),

$$g(S, t, 0) = c_{00} + c_{01}T + N_S kT S \ln S + (c_{20} + c_{21}T) \cdot S - \frac{kT v(t, 0)}{12\pi} \cdot \kappa(S, t, 0)^3 \quad (47)$$

Its several particular quantities are explained in the following. The Debye parameter κ (the reciprocal Debye radius of the ion cloud, not to be confused here with adiabatic compressibility) of seawater is given by,

$$\kappa(S, t, p)^2 = \frac{\langle Z^2 \rangle e^2}{\epsilon(t, p) \epsilon_0 kT v(t, p)} \cdot N_S S \quad (48)$$

All four free constants, c_{ij} , are to be determined e.g. by the choice of arbitrary reference states (Fofonoff, 1962, Feistel and Hagen, 1995). $c_{00} = h(0, 0, 0)$ is the enthalpy of pure water at atmospheric pressure and 0 °C, and $-c_{01} = \sigma(0, 0, 0)$ is its entropy. Both are determined by the conditions (Eqs. (33) and (34)) prescribed for the triple point. The other two, c_{20} and c_{21} , are to be fixed by a similar condition for standard seawater of salinity $S = 35$, as, $h(35, 0, 0) = 0$ and $\sigma(35, 0, 0) = 0$, after all other remaining coefficients of F03 have finally been evaluated. c_{20} and c_{21} are not required for the agreement with experimental data of seawater.

Eqs. (47) and (48) depend on the explicit details of the dissolved salt components only in compact form via two different quantities, the valence factor $\langle Z^2 \rangle$ and the particle number N_S . We are going to explicitly determine these two figures now from the molecular properties of the electrolytic solution. For the required stoichiometric definition of seasalt we use the specification given in Table 5. The mutual ratios of mass fractions W_a were taken from Millero (1982), except for sodium, which was derived from the electro-neutrality condition using ion charges Z_a ,

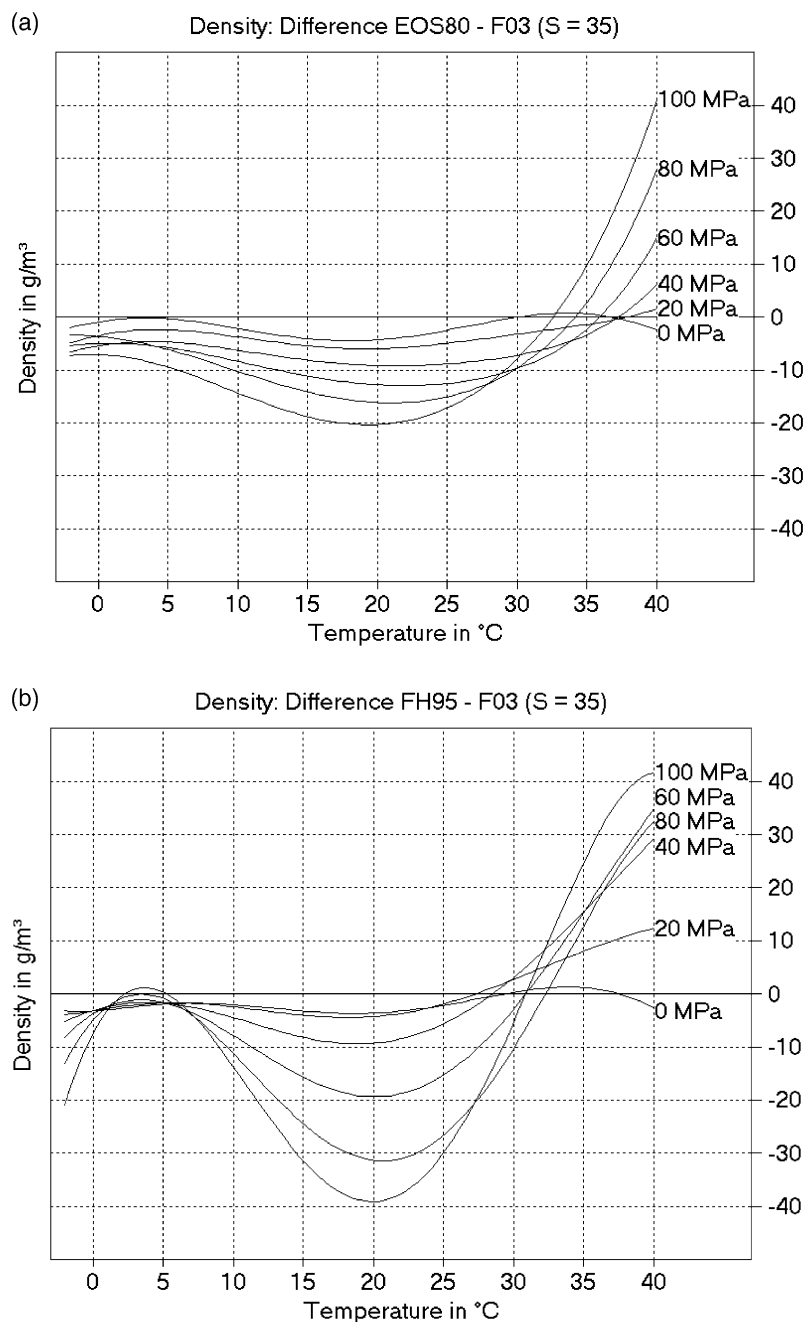


Fig. 26. Comparison of seawater densities, $\rho(S, t, p)$, at applied pressures p between 0 and 100 MPa (0 and 10,000 dbar) computed by (a) EOS80, above, and (b) FH95, below, with F03. FH95 high-pressure densities were derived from CM77 sound speeds for non-Neptunian waters and exhibit strong deviations from the direct density measurements used for F03.

Table 5

Average seawater composition and additional relevant atomic weights. Components and mass fractions from [Millero \(1982\)](#), mole fractions recomputed with IUPAC 99 mole masses ([Coplen, 2001](#)). Molecular weights are computed as sums over their atomic parts. Z: ion charge, A: atomic weight, W: weight fraction, X: mole fraction

| kind (a) | Z _a | A _a /(g/mol) | W _a /ppm | X _a /ppm |
|--------------------------------|----------------|-------------------------|---------------------|---------------------|
| Na | +1 | 22.989 77 | 306 563.3 | 418 791.8 |
| Mg | +2 | 24.305 | 36 499.9 | 47 163.7 |
| Ca | +2 | 40.078 | 11 716.8 | 9 181.5 |
| K | +1 | 39.098 3 | 11 347.7 | 9 115.1 |
| Sr | +2 | 87.62 | 225.9 | 81.0 |
| Cl | −1 | 35.453 | 550 257.7 | 487 445.1 |
| SO ₄ | −2 | 96.062 6 | 77 120.1 | 25 213.1 |
| HCO ₃ | −1 | 61.016 84 | 3 228.0 | 1 661.5 |
| Br | −1 | 79.904 | 1 911.5 | 751.3 |
| CO ₃ | −2 | 60.008 9 | 330.5 | 173 |
| B(OH) ₄ | −1 | 78.840 36 | 187.3 | 74.6 |
| F | −1 | 18.998 403 2 | 33.1 | 54.6 |
| H ₃ BO ₃ | 0 | 61.833 02 | 578.4 | 293.8 |
| H | | 1.007 94 | | |
| B | | 10.811 | | |
| C | | 12.010 7 | | |
| O | | 15.999 4 | | |
| S | | 32.065 | | |
| Ag | | 107.868 2 | | |
| H ₂ O | | 18.015 28 | | |

$$\sum_a X_a \cdot Z_a = 0 \quad (49)$$

The mole fractions X_a were recomputed using IUPAC-99 mole masses ([Coplen, 2001](#)), A_a , by,

$$X_a = \frac{W_a / A_a}{\sum_b W_b / A_b} \quad (50)$$

We get for the average molar mass $\langle A \rangle = \sum X_a \cdot A_a = 31.4060$ g/mol and for the valence factor $\langle Z^2 \rangle = \sum X_a \cdot Z_a^2 = 1.245143$.

N_s is the number of dissolved particles in 1 kg seawater with practical salinity $S = 1$. The link between both these descriptions of salinity is provided by chlorinity Cl , which is defined as the mass of silver needed to precipitate all chlorine and bromine in 328.5233 g of seawater ([Millero and Leung, 1976b](#), [Millero and Sohn, 1992](#)),

$$Cl = 328.5233 \text{ kg} \cdot c \cdot A_{Ag} \cdot \left(\frac{W_{Cl}}{A_{Cl}} + \frac{W_{Br}}{A_{Br}} \right) \quad (51)$$

Here, c is the absolute salinity in grams of salt per kg of seawater. On the other hand, Cl can approximately related to practical salinity by the old conversion formula ([Millero and Leung, 1976b](#), [Lewis and Perkin, 1981](#)),

$$S = 1.80655 \cdot Cl / \text{g} \quad (52)$$

Eliminating Cl , we obtain the desired relation between practical and absolute salinity,

$$S = 1.004867 \cdot c / (\text{g/kg}) \quad (53)$$

The values of the fundamental physical constants (Table 6) we have taken from the recent review of Mohr & Taylor (1999, p. 1808).

We can now determine the number of dissolved salt particles per practical salinity unit and per kg of seawater, as,

$$N_s = \frac{N_A \cdot c}{\langle A \rangle \cdot S} = 1.926845 \cdot 10^{22} / \text{kg} \quad (54)$$

Having determined the two constants $\langle Z^2 \rangle$ and N_s , we can return to the remaining unknowns of Eqs. (47) and (48). Both the relative dielectric constant $\epsilon(t, p)$ of water at 0 °C and atmospheric pressure and its temperature derivative are obtained from the IAPWS (1997) release to be $\epsilon(0,0) = 87.9034$, and $(\partial\epsilon/\partial t)_p = -0.402570/\text{K}$. The specific volume $v(t, p)$ of pure water at 0 °C and atmospheric pressure, $v(0,0) = 1.000157 \text{ dm}^3/\text{kg}$, and its thermal expansion coefficient, $\alpha(0,0) = -67.7594 \text{ ppm/K}$, are provided by the IAPWS95 equation of state.

Using these values in Eq. (47) after series expansion into powers of temperature around 0 °C up to linear terms, further 4 coefficients have been computed as given in the appendix.

13. Freezing point of seawater

The freezing temperature $t_f(S, p)$ of seawater with salinity S exposed to an applied pressure p can be calculated from the condition of thermodynamic equilibrium between seawater and ice,

$$\mu^w(S, t_f, p) = \mu^{ice}(t_f, p) \quad (55)$$

which states that the chemical potentials of water must be the same in both phases. The chemical potential of water in seawater is (Feistel and Hagen, 1995, 1998),

$$\mu^w(S, t, p) = g(S, t, p) - S \cdot \left(\frac{\partial g}{\partial S} \right)_{t, p} \quad (56)$$

The chemical potential of ice is its specific free enthalpy,

$$\mu^{ice}(t, p) = g^{ice}(t, p) \quad (57)$$

A thermodynamic potential of pure water ice, $g^{ice}(t, p)$, has been proposed by Feistel and Hagen (1995, 1998) for the vicinity of the freezing point, derived from various properties of ice. It has the simple polynomial form

Table 6
Recent values of fundamental physical constants after Mohr and Taylor (1999)

| Name | Symbol | Value | Unit |
|----------------------|--------------|-----------------------|-----------|
| Avogadro's constant | N_A | 6.022 141 994 7 E+23 | 1/mol |
| molar gas constant | R | 8.314 472 15 | J/(mol K) |
| Boltzmann's constant | $k = R/N_A$ | 1.380 650 324 E-23 | J/K |
| vacuum permittivity | ϵ_0 | 8.854 187 817 E-12 | As/(Vm) |
| electron charge | e | 1.602 176 462 63 E-19 | As |

$$g^{Ice}(t,p) = 1 \text{ J/kg} \cdot \sum_{ij} g_{ij}^{Ice} \cdot y^i \cdot z^j \quad (58)$$

with the variables $y = t/40^\circ\text{C}$ and $z = p/100 \text{ MPa}$, and coefficients as given in Table 7. The coefficients g_{00}^{Ice} and g_{10}^{Ice} have been differently determined for F03 in comparison to FH95 by adopting the IAPWS95 reference state, i.e. the condition that the chemical potentials of air-free liquid water and ice have to coincide at the triple point ($T_t = 273.16 \text{ K}$, $P_t = 611.657 \text{ Pa}$, Wagner and Pruß, 2002),

$$g^{IAPWS95}(T_t, P_t) = g^{Ice}(t_t, p_t) \quad (59)$$

and that enthalpies of liquid water and ice differ by melting heat $h^{melt} = 333.5 \text{ kJ/kg}$ (Rossini, Wagman, Evans, Levine, & Jaffe 1952) at freezing temperature $t_f = 0.0026^\circ\text{C}$ under atmospheric pressure $p_f = 0 \text{ MPa}$.

$$h^{IAPWS95}(T_f, P_f) = h^{Ice}(t_f, p_f) + h^{melt} \quad (60)$$

Introducing now temporarily a 2nd order relative free enthalpy of ice, η , by,

$$\eta(t,p) = g^{Ice}(t,p) - (g_{00}^{Ice} + g_{10}^{Ice} \cdot t/40^\circ\text{C}) \cdot 1 \text{ J/kg} \quad (61)$$

we can formally solve Eqs. (59) and (60) for the unknown coefficients, as,

$$g_{00}^{Ice} = \frac{T_0 \cdot \Delta g_t + t_t \cdot \Delta h_f}{T_t} \quad (62)$$

$$g_{10}^{Ice} = \frac{40^\circ\text{C} \cdot (\Delta g_t - \Delta h_f)}{T_t} \quad (63)$$

Here, the difference terms are abbreviations,

$$\Delta g_t \cdot 1 \text{ J/kg} = g^{IAPWS95}(T_t, P_t) - \eta(t_t, p_t) \quad (64)$$

$$\Delta h_f \cdot 1 \text{ J/kg} = h^{IAPWS95}(T_f, P_f) - h^{melt} - \eta(t_f, p_f) + T_f \cdot \frac{\partial \eta(t_f, p_f)}{\partial t} \quad (65)$$

The results are given in Table 7. A cubic high-pressure correction g_{03}^{Ice} additional to FH95 has been obtained by fitting Eq. (55) to IAPWS95 melting pressures up to 50 MPa, which are based on high-pressure HENDERSON & SPEEDY (1987) data with accuracy 100 mK.

The freezing temperature resulting from Eq. (55) of pure water at atmospheric pressure is $t_f = 0.0025^\circ\text{C}$, which is in good agreement with $t_f = 0.00260^\circ\text{C}$ of IAPWS95, and with the freezing point depression of 2.4 mK to 0°C due to saturation with air (DOHERTY & KESTER, 1974). The lowering is slightly less (1.9 mK) for seawater, such that a corresponding small correction to the freezing point measurements of DOHERTY and KESTER (1974) can be estimated as,

Table 7
Coefficients of free enthalpy of ice, Eq. (58)

| g_{ij}^{Ice} | y^0 | y^1 | y^2 | y^3 |
|----------------|------------|------------|------------|-----------|
| z^0 | 98.266 90 | 48 842.28 | −6 139.045 | 21.782 64 |
| z^1 | 109 085.8 | 690.076 5 | 60.652 68 | |
| z^2 | −1 266.486 | −99.207 47 | | |
| z^3 | 363.422 5 | | | |

$$t_f^{air-free} = t_f^{DK74} + 2.4 \text{ mK} - \frac{S}{35} \cdot 0.5 \text{ mK} \quad (66)$$

for air-free water conditions assumed in the current paper.

Wagner, Saul & Pruß (1994) provide freezing temperatures of pure water for a wide range of pressures (see also Wagner and Pruß, 2002). Fig. 27 shows several freezing point formulas in comparison to them. The low-pressure range is probably less precisely described by Wagner et al. (1994) (about 6 mK, see Fig. 27) than by Millero (1978) or Feistel and Hagen (1995, 1998), due to the use of more recent ice density data by the latter two. Both were derived for air-saturated water, causing the intercept of 2.6 mK at atmospheric pressure in the drawing. The seawater formulas of Doherty and Kester (1974) and Fujino, Lewis & Perkin (1974) are shown for $S = 0$ but are not claimed valid for pure water by their authors. The formula of Millero (1978) is assumed to hold within an error of 3 mK up to 5 MPa. If we accept a tolerance of about 10 mK, Fig. 27 shows that FH95 freezing points are likely to be valid even beyond 30 MPa (or 3000 meters of water depth), and the current improved ice potential function (Table 7) extends this range to about 50 MPa (5000 dbar), thus becoming applicable to cases like Antarctic subglacial lakes (Siebert et al., 2001). As an alternative to the Gibbs potential of ice proposed here (Eq. (58)), the one derived by Tillner-Roth (1998) can be used for very high pressures. It is derived from ice properties as well as from the melting pressure curve of Wagner et al. (1994), is valid even beyond 100 MPa, and reproduces the freezing point measurements of Henderson and Speedy (1987) within 100 mK. With only 2 mK deviation up to $p = 5$ MPa, it is in excellent agreement with F03 at low pressures (Fig. 27). Its error in case of application to seawater can be assumed to be of the same magnitude.

As follows from Eq. (46), only measurements at atmospheric pressure are required to determine the unknown parts of the thermodynamic potential function. High-pressure freezing points can be derived then

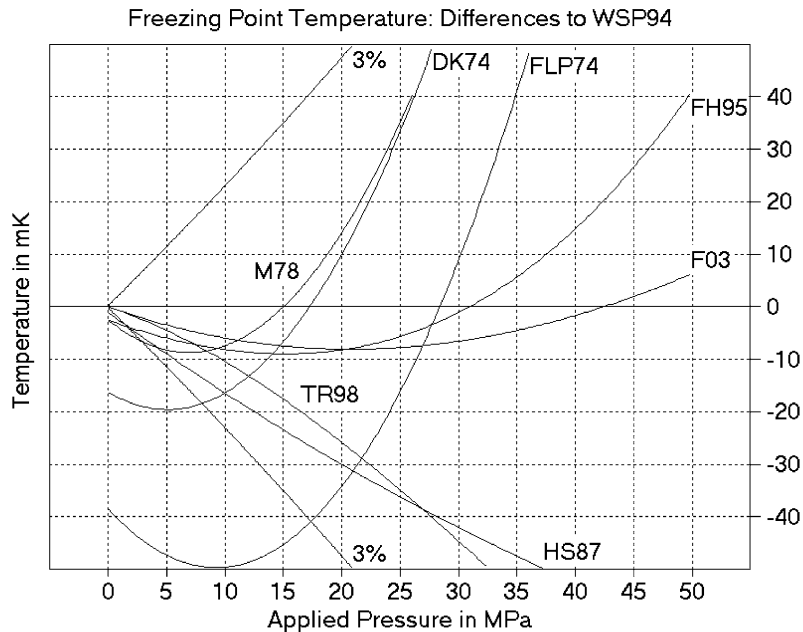


Fig. 27. Comparison of freezing point temperature formulas for pure water, $t_f(0,p)$, with WSP94 (Wagner et al., 1994). DK74: Doherty and Kester (1974), FLP74: Fujino et al. (1974), M78: Millero (1978), HS87: Henderson and Speedy (1987), TR98: Tillner-Roth (1998), FH95: Feistel and Hagen (1995, 1998), F03: this paper. The 3% cone indicates the uncertainty of the WSP94 melting pressure function, corresponding to 3% of the melting pressure.

immediately from Eqs. (46) and (55), limited in pressure mainly by the validity of the chemical potential function of water in ice, Eq. (66).

Freezing point measurements (S_f, t_f) at ambient pressure of [Doherty and Kester \(1974\)](#) were used for a joint regression together with mixing heats, as described in section 14. The expression

$$\sum \left\{ g(S_f, t_f, 0) - S_f \left(\frac{\partial g}{\partial S} \right)_{t,p=0} - g^{Ice}(t_f, 0) \right\}^2 = \text{Min} \quad (67)$$

was minimized at 32 data points after correcting temperatures due to Eq. (66), with a required tolerance of 2 J/kg in free enthalpy. 8 coefficients g_{ij0} , $i = 4 \dots 7$, $j = 0, 1$ have been calculated as given in the appendix. The resulting r.m.s. of the fit was 1.8 J/kg, corresponding to 1.5 mK mean deviation in freezing temperatures. The scatter of the data is shown in [Fig. 28](#), together with the one-atmosphere measurements of [Fujino et al. \(1974\)](#). The latter ones were not corrected for dissolved air, a tentative application of Eq. (66) to these data increases the mean error from 2.6 to 4.3 mK.

14. Mixing heat of seawater

[Bromley \(1968\)](#) reported seawater mixing experiments at $t = 25^\circ\text{C}$ (IPTS-48 scale assumed) with accuracy estimated by the author to 1 cal. Out of these, 24 samples with initial masses m_1, m_2 and salinities $S_1, S_2 < 34$ were used with their heat effect Q after mixing, converted by 4.1840 J/cal. We have minimized the sum ([Feistel and Hagen, 1995](#)),

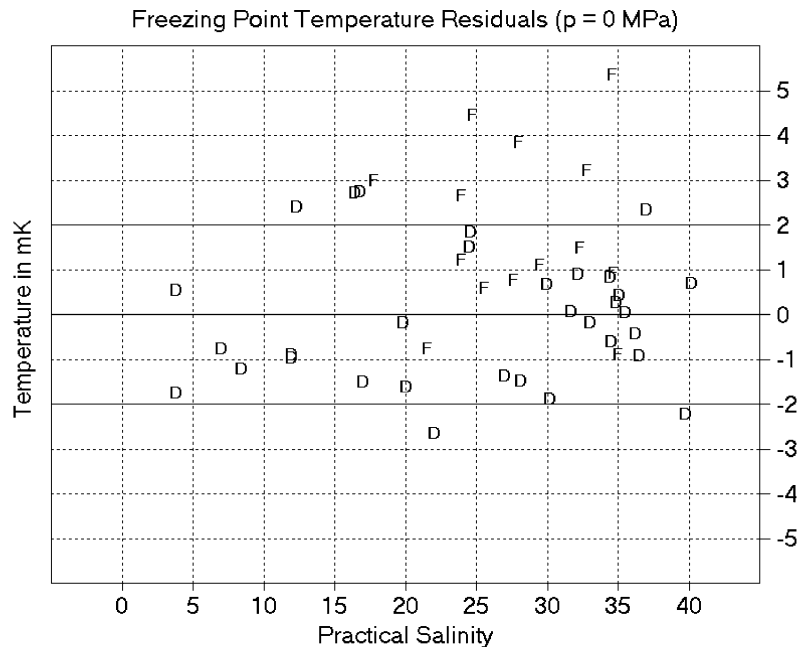


Fig. 28. Deviation of measured freezing points of seawater, $t_f(S, 0)$, at atmospheric pressure ($P = 0.101325$ MPa) from temperatures computed by Eq. (55). D: [Doherty and Kester \(1974\)](#) with air correction (56), F: [Fujino et al. \(1974\)](#) without air correction. Horizontal lines mark the experimental uncertainty.

$$\sum \left\{ (m_1 + m_2) h \left(\frac{m_1 S_1 + m_2 S_2}{m_1 + m_2}, t, 0 \right) - m_1 h(S_1, t, 0) - m_2 h(S_2, t, 0) + Q \right\}^2 = \text{Min} \quad (68)$$

over these measurements with required r.m.s. of 4 J, in conjunction with freezing point measurements (section 13) and dilution heats (below). Enthalpies h are expressed by the potential function $g(S, t, p)$ as,

$$h(S, t, p) = g(S, t, p) - (T_0 + t) \cdot \left(\frac{\partial g}{\partial t} \right)_{S, p} \quad (69)$$

The regression resulted in an r.m.s. deviation of 2.4 J, as shown in Fig. 29(a).

Millero et al. (1973b) performed experiments diluting seawater from salinities S_1 to S_2 at various temperatures t (assumed IPTS-48 scale), reporting relative enthalpies L with accuracy of 5 cal/eq, as given in that paper. We have minimized the sum (Feistel and Hagen, 1995) over 95 of their data points $L(S_1, S_2, t)$, converted from cal/eq to J/kg multiplying by 4.184/57.754,

$$\sum \left\{ \frac{h(S_2, t, 0) - h(0, t, 0)}{S_2} - \frac{h(S_1, t, 0) - h(0, t, 0)}{S_1} + L \right\}^2 = \text{Min} \quad (70)$$

with required r.m.s. of 0.4 J/kg, together with Bromley's mixing heats and freezing points of Doherty et al. The resulting scatter of 0.5 J/kg is displayed in Fig. 29(b).

Shapes of resulting excess free enthalpies, $g(S, t, 0) - g(0, t, 0)$, entropies, $\sigma(S, t, 0) - \sigma(0, t, 0)$, and enthalpies, $h(S, t, 0) - h(0, t, 0)$, relative to pure water and at atmospheric pressure, are shown in Fig. 30.

Millero and Leung (1976b) and Millero (1983) have published formulas for relative specific entropies $\Delta\sigma^{ML76} = \sigma(S, t, 0) - \sigma(0, t, 0)$, enthalpies $\Delta h^{ML76} = h(S, t, 0) - h(0, t, 0)$ and free enthalpies $\Delta g^{ML76} = g(S, t, 0) - g(0, t, 0)$ of seawater at one atmosphere. Their salinity dependencies at $t = 0$ °C show a good agreement with the corresponding expressions derived here in sections 12–14, as shown in Fig. 30. Error estimates of those authors were 2 J/kg for free enthalpy, 0.1 J/(kg K) for entropy and 3 J/kg for enthalpy. The r.m.s. deviations visible in Fig. 30 are in the order of 10%: 21 J/kg in free enthalpy, 0.08 J/(kg K) in entropy, and 9 J/kg in enthalpy.

Before both functions could be compared they had to be aligned to a common reference state by suitably adjusting the gauge constants A , B (compare Eq. (47)),

$$g(S, t, 0) - g(0, t, 0) = \Delta g^{ML76}(S, t) + (A + B \cdot t) \cdot S \quad (71)$$

$$g(S, t, 0) - g(0, t, 0) - T \frac{\partial [g(S, t, 0) - g(0, t, 0)]}{\partial t} = \Delta h^{ML76}(S, t) + (A - B \cdot T_0) \cdot S \quad (72)$$

$$-\frac{\partial [g(S, t, 0) - g(0, t, 0)]}{\partial t} = \Delta\sigma^{ML76}(S, t) - B \cdot S \quad (73)$$

Requiring $g(35, 0, 0) = 0$ and $h(35, 0, 0) = 0$ we derive A , B from Eqs. (71), (72) to be,

$$A = -\frac{1}{35} [g(0, 0, 0) + \Delta g^{ML76}(35, 0)] = 139.9 \text{ J/kg} \quad (74)$$

$$B = -\frac{1}{35 T_0} \left[T_0 \frac{\partial g(0, 0, 0)}{\partial t} + \Delta g^{ML76}(35, 0) - \Delta h^{ML76}(35, 0) \right] = 0.4867 \text{ J/(kg K)} \quad (75)$$

Temperature dependencies of the functions given by Millero and Leung (1976b), however, do not obey the thermodynamic relations $\Delta c_p = T(\partial \Delta\sigma / \partial t) = \partial \Delta h / \partial t = -T(\partial^2 \Delta g / \partial t^2)$ with relative specific heat capacities, $\Delta c_p = c_p(S, t, 0) - c_p(0, t, 0) \leq 0$. Rather, they are related to relative partial molal heat capacities,

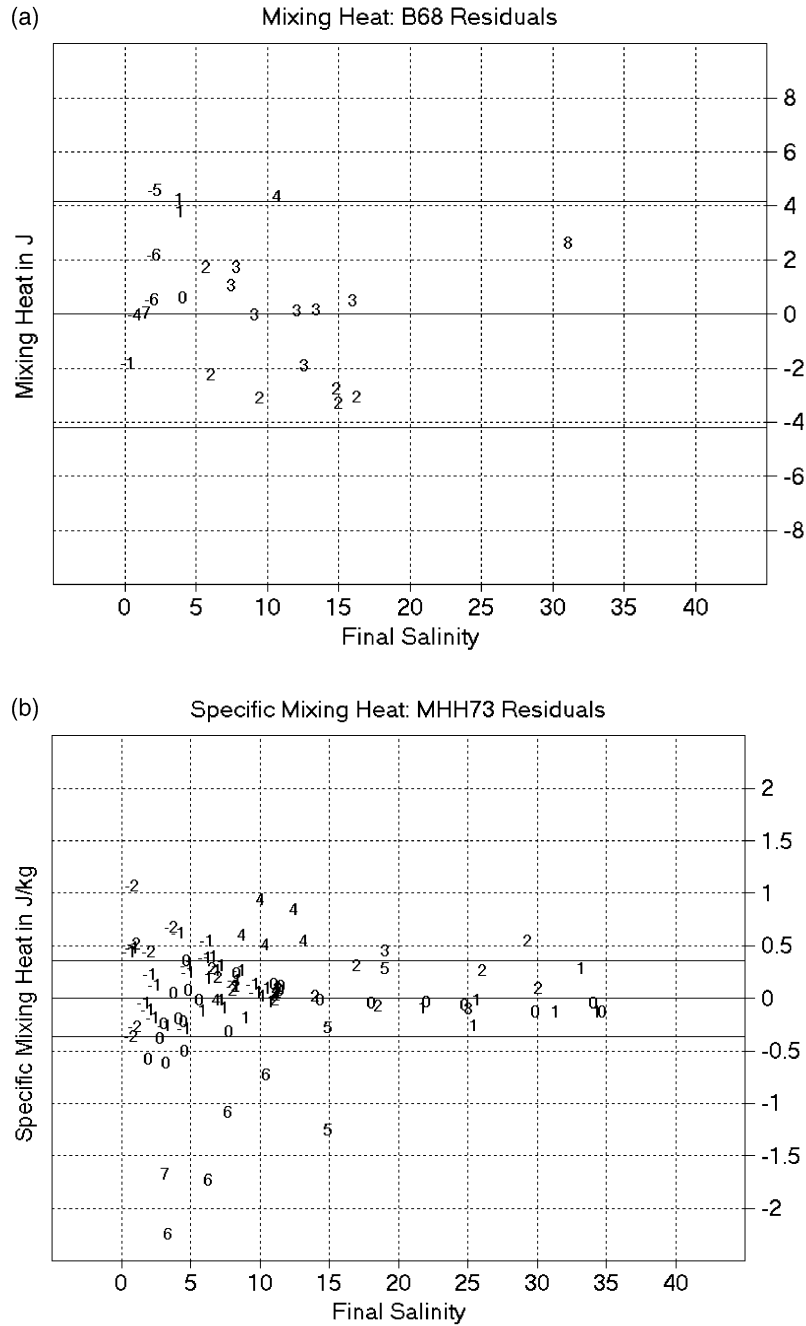


Fig. 29. Deviations of measured mixing heats, plotted vs. final salinities S of the mixtures. Experimental uncertainty is indicated by horizontal lines. (a) Bromley (1968), above, after Eq. (68). Symbols are values of Q in J, rounded to integer. (b) Millero et al. (1973b), below, after Eq. (70). Symbols are values of $L/2$ in J/kg, rounded to integer.

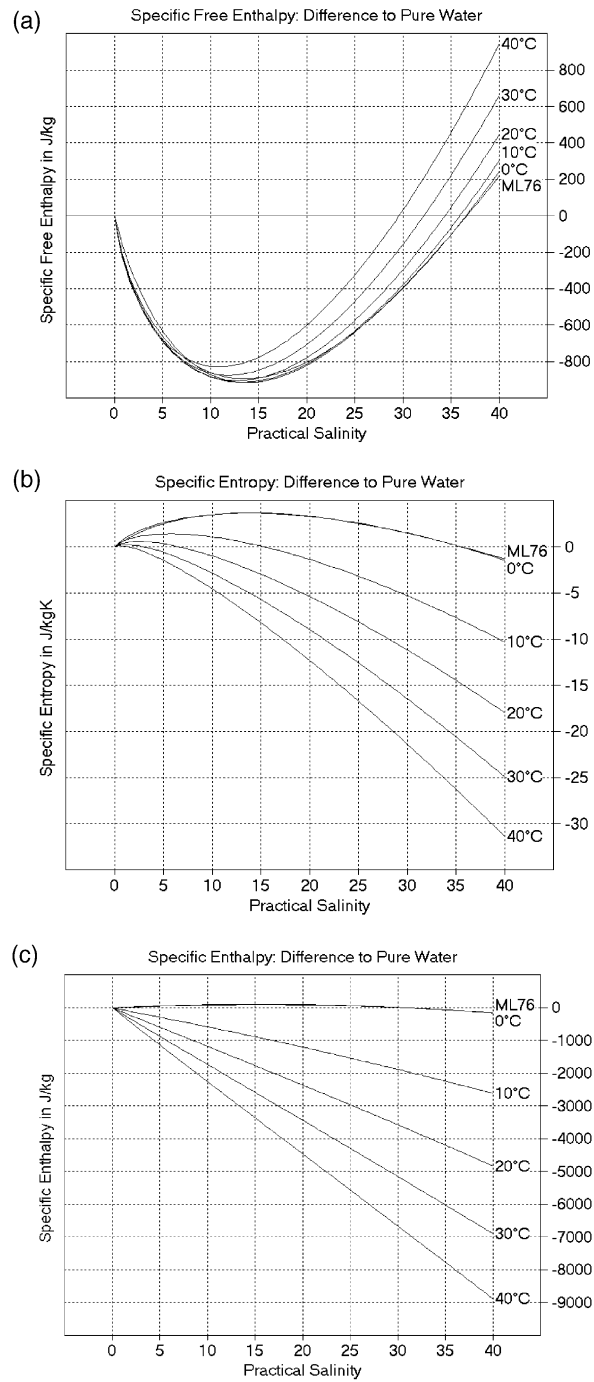


Fig. 30. (a) above, relative specific free enthalpy, $g(S,t,0) - g(0,t,0)$, (b) middle, relative specific entropy, $\sigma(S,t,0) - \sigma(0,t,0)$, and (c) below, relative specific enthalpy, $h(S,t,0) - h(0,t,0)$, as functions of salinity S and temperature t at ambient pressure $p = 0$ MPa. ML76: corresponding functions by [Millero and Leung \(1976b\)](#) at $t = 0$ °C after alignment to a common reference state due to Eqs. (71)–(73).

$\Phi_{cp} - \Phi_{cp}^0$, as defined in their paper (Millero, 2003). Hence, they cannot be compared directly with the F03 functions derived here except for $t = 0$ °C.

15. Conclusion

With the compilation of the current F03 a final state of the longer development of the Gibbs thermodynamic potential of seawater is reached, mainly marked by the now extensive involvement of experimental data together with the new pure water standard IAPWS95. It has significantly improved and extended its predecessor versions, as is summarized in Tables 8 and 9.

Modern quantitative descriptions of thermodynamic seawater properties include fresh water in the limiting case of vanishing salinity. This holds for the International Equation of State of Seawater 1980 and its accompanying equations for isobaric specific heat capacity and sound speed. EOS80 had been derived by

Table 8

Symbolic scheme of background papers used for subsequent comprehensive formulations of seawater equilibrium thermodynamics: EOS80 (Millero, Perron and Desnoyers, 1973a, Chen and Millero, 1977, Millero et al., 1980, Millero and Poisson, 1981a), F93 (Feistel, 1993), FH95 (Feistel and Hagen, 1995), F03 (this paper). This simplified list of implicit or explicit sources or links is neither unique nor complete

| Source | EOS80 | F93 | FH95 | F03 |
|---------|--------------|--------------|-----------------|-----------------|
| IAPWS95 | | | | $g(0,t,p)$ |
| PG93 | | | | $v(S,t,0)$ |
| BS86 | $v(S,t,p)$ | | | |
| EOS80 | | $v(S,t,0)$ | $v(S,t,0)$ | |
| PBB80 | $v(S,t,0)$ | | | $v(S,t,0)$ |
| C78 | | | $\alpha(S,t,p)$ | $\alpha(S,t,p)$ |
| CM77 | $U(S,t,p)$ | $v(S,t,p)$ | $v(S,t,p)$ | |
| BS76 | $v(S,t,p)$ | | | |
| CM76 | $v(S,t,p)$ | | | $v(S,t,p)$ |
| MGW76 | $v(S,t,0)$ | | | $v(S,t,0)$ |
| ML76 | | $g(S,t,0)$ | | |
| DG74 | | | $v(S,t,p)$ | $v(S,t,p)$ |
| DK74 | | | $g(S,t,0)$ | $g(S,t,0)$ |
| MPD73 | $c_p(S,t,0)$ | $c_p(S,t,0)$ | $c_p(S,t,0)$ | $c_p(S,t,0)$ |
| MHH73 | | | $h(S,t,0)$ | $h(S,t,0)$ |
| DGM72 | $U(0,t,0)$ | | | |
| DG70 | $U(S,t,0)$ | | | |
| BDSW70 | | | | $c_p(S,t,0)$ |
| BS70 | $v(S,t,p)$ | | | $v(S,t,p)$ |
| B68 | | | $h(S,t,0)$ | $h(S,t,0)$ |
| B67 | $v(0,t,0)$ | | | |
| W59 | $U(0,t,p)$ | | | |
| S55 | $c_p(0,t,0)$ | | | |

Sources are IAPWS95 (Wagner and Pruß, 2002), PG93 (Poisson and Gadhoumi, 1993), BS86 (Bradshaw and Schleicher, 1986), EOS80 (Fofonoff and Millard, 1983), PBB80 (Poisson et al., 1980), C78 (Caldwell, 1978), CM77 (Chen and Millero, 1977), BS76 (Bradshaw and Schleicher, 1976), CM76 (Chen and Millero, 1976), MGW76 (Millero et al., 1976a), ML76 (Millero and Leung, 1976b), DG74 (Del Grosso, 1974), DK74 (Doherty and Kester, 1974), MPD73 (Millero et al., 1973a), MHH73 (Millero et al., 1973b), DGM72 (Del Grosso and Mader, 1972), DG70 (Del Grosso, 1970), BDSW70 (Bromley et al., 1970), BS70 (Bradshaw and Schleicher, 1970), B68 (Bromley, 1968), B67 (Bigg, 1967), W59 (Wilson, 1959), S55 (Stimson, 1955). Quantities are S (salinity), t (temperature), p (pressure), g (specific free enthalpy), v (specific volume), α (isobaric thermal expansion coefficient), U (sound speed), c_p (specific heat at constant pressure), h (specific enthalpy).

Table 9

Summary of data used for the determination of F03 free enthalpy polynomial coefficients by regression. "Required" is the r.m.s. prescribed in the least-square condition of the particular data set, "resulting" is the returned r.m.s. of the fit. Column "s." refers to the section where further details are described. IAPWS95: Wagner and Pr   (2002), MGW76: Millero et al. (1976), PBB80: Poisson et al. (1980), PG93: Poisson and Gadhoumi (1993), BDSW70: Bromley et al. (1970), MPD73: Millero et al. (1973a), C78: Caldwell (1978), I–VI: Del Grosso (1974), CM76: Chen and Miller (1976), BS70: Bradshaw and Schleicher (1970), DK74: Doherty and Kester (1974), B68: Bromley (1968), MHH73: Millero et al. (1973b)

| Quantity | Source | S | t / $^{\circ}\text{C}$ | p /MPa | Points | Required r.m.s. | Resulting r.m.s. | s. |
|-----------------|---------|--------|--------------------------|----------|--------|-----------------|------------------|----|
| $c_p(0,t,0)$ | IAPWS95 | 0 | 0–45 | 0 | 8 | 10 J/(kg K) | 0.01 J/(kg K) | 2 |
| $\alpha(0,t,0)$ | IAPWS95 | 0 | 0–45 | 0 | 8 | 0.6 ppm/K | 0.005 ppm/K | 3 |
| $\alpha(0,t,p)$ | IAPWS95 | 0 | –7–45 | –0.1–110 | 64 | 0.6 ppm/K | 0.01 ppm/K | 3 |
| $\rho(0,t,0)$ | IAPWS95 | 0 | 0–45 | 0 | 8 | 1 ppm | 0.032 ppm | 4 |
| $\rho(0,t,p)$ | IAPWS95 | 0 | –7–45 | –0.1–110 | 64 | 30 ppm | 0.020 ppm | 4 |
| $K(0,t,p)$ | IAPWS95 | 0 | –7–45 | –0.1–110 | 64 | 0.4 ppm/MPa | 0.003 ppm/MPa | 5 |
| $\rho(S,t,0)$ | MGW76 | 0.5–40 | 0–40 | 0 | 122 | 4 ppm | 4.1 ppm | 7 |
| $\rho(S,t,0)$ | PBB80 | 5–42 | 0–30 | 0 | 345 | 4 ppm | 4.0 ppm | 7 |
| $\rho(S,t,0)$ | PG93 | 34–50 | 15–30 | 0 | 81 | 10 ppm | 11.3 ppm | 7 |
| $c_p(S,t,0)$ | BDSW70 | 10–50 | 0–40 | 0 | 25 | 2 J/(kg K) | 0.54 J/(kg K) | 8 |
| $c_p(S,t,0)$ | MPD73 | 1–40 | 5–35 | 0 | 48 | 0.5 J/(kg K) | 0.52 J/(kg K) | 8 |
| $\alpha(S,t,p)$ | C78 | 10–30 | –6–1 | 0.7–33 | 31 | 0.6 ppm/K | 0.73 ppm/K | 9 |
| $U(S,t,p)$ | I–III | 29–43 | 0–35 | 0–2 | 92 | 5 cm/s | 1.7 cm/s | 10 |
| $U(S,t,p)$ | IVa–d | 29–43 | 0–30 | 0.1–5 | 32 | 5 cm/s | 1.2 cm/s | 10 |
| $U(S,t,p)$ | V–VI | 33–37 | 0–5 | 0–100 | 128 | 5 cm/s | 3.5 cm/s | 10 |
| $v(S,t,p)$ | CM76 | 5–40 | 0–40 | 0–100 | 558 | 10 ppm | 11.0 ppm | 11 |
| $v(S,t,p)$ | BS70 | 30–40 | –2–30 | 1–100 | 221 | 4 ppm | 2.6 ppm | 11 |
| $g(S,t,0)$ | DK74 | 4–40 | –2–0 | 0 | 32 | 2 J/kg | 1.8 J/kg | 13 |
| $Q(S,t,0)$ | B68 | 0–33 | 25 | 0 | 24 | 4 J | 2.4 J | 14 |
| $L(S,t,0)$ | MHH73 | 1–41 | 0–30 | 0 | 95 | 0.4 J/kg | 0.5 J/kg | 14 |

combining various extended and precise fundamental measurements of seawater properties, many of them were calibrated with, or made relative to, or included as special case, corresponding data of pure water. The dependence of these seawater data on their pure water reference was intentionally made explicit by their authors in some cases, like for heat capacities by Millero et al. (1973a), or specific volumes by Chen et al. (1976), but in other cases it is hardly reproducible afterwards, like for heat capacities by Bromley et al. (1970).

The first Gibbs function F93 was an attempt towards a more consistent, comprehensive and extended formulation, compared to the EOS80 triple. It was a combination of EOS80 density and heat capacity at ambient pressure, as well as EOS80 sound speed for their extrapolation to higher pressures. The resulting PVT properties of the potential function were compiled to remain as numerically close as possible to the EOS80 original, and were completed with the thermochemical properties of ML76, published by Millero and Leung (1976b).

The subsequent version FH95 of the Gibbs potential was developed to allow for mainly three small but important corrections with respect to F93.

1. Sound speed of Chen and Millero (1977), CM77, had been found to exhibit systematic errors of about 0.5 m/s in deep-water travel time measurements (Dushaw et al., 1993, Millero and Li, 1994) and needed to be partially replaced by the more accurate function of Del Grosso (1974), DG74, which is valid for Neptunian waters only.
2. Temperatures of maximum density computed by EOS80 severely deviate from the measurements of Caldwell (1978) especially for brackish waters, such that these measurements needed to be involved.

3. The limiting laws of F93 included terms in the power expansion with respect to salinity which were inconsistent with electrolyte theory. The corresponding formulas used in F93 were substituted by the correct Debye-Hückel limiting law and completed with experimental data for freezing point temperatures of Doherty and Kester (1974), and mixing enthalpies of Bromley (1968) and Millero et al. (1973b), replacing the ML76 functions used for F93.

With the release of the IAPWS95 formulation (IAPWS, 1996) and its detailed description by Wagner and Pruß (2002), a comprehensive high-precision standard for equilibrium thermodynamic properties of Vienna Standard Mean Ocean Water (Gonfiantini, 1978) has become available. Like its precursor, the IAPS-84 standard (Haar, Gallagher & Kell, 1988), it is expressed by specific free energy $f(T, \rho)$ of the fluid phases as function of absolute temperature and density over a wide range of conditions, including those of oceanic and limnic waters. It has triggered the revision of the seawater potential function, involving the substitution of all explicit or implicit references to old pure water data by the new standard. It further suggested the idea that the still existing inconsistency between the sound speed formulas CM77 and DG74 could be resolved in a natural way, which is likely caused by improper pure water calibration (Millero and Li, 1994). It was therefore necessary to recalibrate the experimental data which served for the construction of EOS80, and to use them directly for a new determination of the polynomial coefficients declared by Eq. (1). As an example, old heat capacity data from 1902–1927, summarized in the paper of Stimson (1955), were used to determine seawater specific heat capacities of seawater by Millero et al. (1973a), thus became part of EOS80 and were finally passed through to F93 and FH95 this way (Table 8).

The current Gibbs potential F03 is no longer based on any of the three EOS80 functions which lead to the previous versions F93 and FH95. The background data used for EOS80 and for the new formulation are partly the same, compare Table 8, nonetheless both can be considered as independently derived analytical expressions representing the particular experimental data.

F03 is completely consistent with the most accurate and comprehensive description of pure water available. Its zero salinity part is valid from the triple point to 110 MPa applied pressure and from the freezing temperature to 45 °C. A tentative recalibration of CM77 sound speeds with respect to IAPWS95 turned out to be insufficient to explain the differences to DG74. On the other hand, specific volumes measured by Bradshaw and Schleicher (1970) and Chen and Millero (1976) after recalibration appeared fairly well consistent with DG74 sound speeds, and have been involved as preferred substitutes for CM77 in the current regression procedure. They are even slightly better reproduced now than originally by EOS80, compare Figs. 23 and 24. Densities and heat capacities at atmospheric pressure have been adjusted for the new IAPWS95 reference and extended up to salinities 50 by the data of Bromley et al. (1970) and Poisson and Gadhoumi (1993). Freezing points computed with F03 have been made compatible with IAPWS95 by correcting for dissolved air, and are extended in validity to higher pressures by an improved Gibbs potential of ice. The reference state of IAPWS95 (zero internal energy and entropy of the liquid phase at the triple point of pure water) has been adopted for the F03 Gibbs potential of ice, in distinction to FH95.

Table 9 shows a summary of all data used in four different regression computations of this paper, together with their required and achieved precisions. The new formulation F03 reproduces the measurements of Millero et al. (1976a) within 4.1 ppm, Poisson et al. (1980) within 4.0 ppm, Poisson and Gadhoumi (1993) within 11.3 ppm, Bromley et al. (1970) within 0.54 J/(kg K), Millero et al. (1973a) within 0.52 J/(kg K), Caldwell (1978) within 0.73 ppm/K, Del Grosso (1974) within 3.5 cm/s, Chen and Millero (1976) within 11.0 ppm, Bradshaw and Schleicher (1970) within 2.6 ppm, Doherty and Kester (1974) within 1.5 mK, Bromley (1968) within 2.4 J and Millero et al. (1973b) within 0.5 J/kg. 216 points from IAPWS95 functions were used for numerical integrals to fit 39 coefficients of pure water, 1834 data points were used to adjust 54 coefficients of seawater properties of the current thermodynamic potential function to various measurements. Additionally, 2 coefficients of water and 6 of seawater have been calculated from reference states and limiting laws. Compared to FH95, the number of polynomial coefficients has increased from 89

to 101. Of the additional 12 terms, 9 were required for pure water to ensure consistency with IAPWS95, and further 2 were added for an improved description of freezing points and dilution heats.

The new Gibbs thermodynamic potential function F03 is equivalent to the international pure water standard IAPWS95 in the oceanic ranges of temperatures and pressures. It represents a suitable compromise between various recalibrated seawater measurements within their corresponding experimental errors as shown in Table 9. This is of special importance for the high-pressure seawater data of Bradshaw and Schleicher (1970), Del Grosso (1974), Chen and Millero (1976) and Caldwell (1978). On one hand, the recalibration has systematically changed almost all seawater properties, some of them even significantly like sound speed at high pressure and temperature. On the other hand, changes compared to FH95 in the range of Neptunian waters are perceptible but hardly exceed the experimental tolerances. F03 can be considered more accurate and more reliable than its predecessors.

Still there are, however, carefully prepared seawater experiments which are not adequately reproduced by the actual formulation. One of them is sound speed of Chen and Millero (1977) as discussed in section 10. Further, the high-salinity extension by Poisson and Gadhoumi (1993) scatters much stronger than predicted by the authors (Section 7). Another case is lapse rates measured by Caldwell and Eide (1980) with claimed accuracy of 0.2%, which deviate from the ones computed here by up to 2%. Note that the latter value corresponds to the error estimate given by Bryden (1973), see the discussion by Fofonoff (1985).

In future versions, seawater with salinity higher than 50 at temperatures up to 500 °C and pressures up to 30 MPa will need to be covered in order to be applicable to processes like those in thermal desalination plants (Slesarenko & Shtim, 1989), or hydrothermal vents found on ocean ridges (Jupp & Schultz, 2000).

Acknowledgements

The author is grateful for various discussions about this work and help provided by C. Bonsen, E. Hagen, T. J. McDougall, F.J. Millero, A. Schröder, B. Sievert and W. Wagner. He further likes to thank the reviewers for their several helpful comments and hints.

Appendix

Tables 10–27

Table 10

Coefficients g_{ijk} of specific free enthalpy $g(S, t, p)$ with variables $S = 40 \cdot x^2$, temperature $t = 40 \cdot y$, and applied pressure $p = 100 \cdot z$:

$$g(S, t, p) = 1 \text{ J/kg} \cdot \sum_{j,k} \left\{ g_{0jk} + g_{1jk} x^2 \ln x + \sum_{i>1} g_{ijk} x^i \right\} y^j z^k$$

| i | j | k | g_{ijk} | i | j | k | g_{ijk} | i | j | k | g_{ijk} |
|---|---|---|--------------------|---|---|---|-------------------|---|---|---|-------------------|
| 0 | 0 | 0 | 101.342743139672 | 0 | 5 | 4 | 6.48190668077221 | 2 | 4 | 2 | 74.726141138756 |
| 0 | 0 | 1 | 100015.695367145 | 0 | 6 | 0 | -18.9843846514172 | 2 | 4 | 3 | -36.4872919001588 |
| 0 | 0 | 2 | -2544.5765420363 | 0 | 6 | 1 | 63.5113936641785 | 2 | 5 | 0 | -17.43743842213 |
| 0 | 0 | 3 | 284.517778446287 | 0 | 6 | 2 | -22.2897317140459 | 3 | 0 | 0 | -2432.0947227047 |
| 0 | 0 | 4 | -33.3146754253611 | 0 | 6 | 3 | 8.17060541818112 | 3 | 0 | 1 | 199.459603073901 |
| 0 | 0 | 5 | 4.20263108803084 | 0 | 7 | 0 | 3.05081646487967 | 3 | 0 | 2 | -52.2940909281335 |
| 0 | 0 | 6 | -0.546428511471039 | 0 | 7 | 1 | -9.63108119393062 | 3 | 0 | 3 | 68.0444942726459 |
| 0 | 1 | 0 | 5.90578348518236 | 1 | 0 | 0 | 5813.28667992895 | 3 | 0 | 4 | -3.41251932441282 |
| 0 | 1 | 1 | -270.983805184062 | 1 | 1 | 0 | 851.295871122672 | 3 | 1 | 0 | -493.512590658728 |
| 0 | 1 | 2 | 776.153611613101 | 2 | 0 | 0 | 1376.28030233939 | 3 | 1 | 1 | -175.292041186547 |
| 0 | 1 | 3 | -196.51255088122 | 2 | 0 | 1 | -3310.49154044839 | 3 | 1 | 2 | 83.1923927801819 |
| 0 | 1 | 4 | 28.9796526294175 | 2 | 0 | 2 | 384.794152978599 | 3 | 1 | 3 | -29.483064349429 |
| 0 | 1 | 5 | -2.13290083518327 | 2 | 0 | 3 | -96.5324320107458 | 3 | 2 | 0 | -158.720177628421 |
| 0 | 2 | 0 | -12357.785933039 | 2 | 0 | 4 | 15.8408172766824 | 3 | 2 | 1 | 383.058066002476 |
| 0 | 2 | 1 | 1455.0364540468 | 2 | 0 | 5 | -2.62480156590992 | 3 | 2 | 2 | -54.1917262517112 |
| 0 | 2 | 2 | -756.558385769359 | 2 | 1 | 0 | 140.576997717291 | 3 | 2 | 3 | 25.6398487389914 |
| 0 | 2 | 3 | 273.479662323528 | 2 | 1 | 1 | 729.116529735046 | 3 | 3 | 0 | 67.5232147262047 |
| 0 | 2 | 4 | -55.5604063817218 | 2 | 1 | 2 | -343.956902961561 | 3 | 3 | 1 | -460.319931801257 |
| 0 | 2 | 5 | 4.34420671917197 | 2 | 1 | 3 | 124.687671116248 | 3 | 4 | 0 | -16.8901274896506 |
| 0 | 3 | 0 | 736.741204151612 | 2 | 1 | 4 | -31.656964386073 | 3 | 4 | 1 | 234.565187611355 |
| 0 | 3 | 1 | -672.50778314507 | 2 | 1 | 5 | 7.04658803315449 | 4 | 0 | 0 | 2630.93863474177 |
| 0 | 3 | 2 | 499.360390819152 | 2 | 2 | 0 | 929.460016974089 | 4 | 0 | 1 | -54.7919133532887 |
| 0 | 3 | 3 | -239.545330654412 | 2 | 2 | 1 | -860.764303783977 | 4 | 0 | 2 | -4.08193978912261 |
| 0 | 3 | 4 | 48.8012518593872 | 2 | 2 | 2 | 337.409530269367 | 4 | 0 | 3 | -30.1755111971161 |
| 0 | 3 | 5 | -1.66307106208905 | 2 | 2 | 3 | -178.314556207638 | 4 | 1 | 0 | 845.15825213234 |
| 0 | 4 | 0 | -148.185936433658 | 2 | 2 | 4 | 44.2040358308 | 4 | 1 | 1 | -22.6683558512829 |
| 0 | 4 | 1 | 397.968445406972 | 2 | 2 | 5 | -7.92001547211682 | 5 | 0 | 0 | -2559.89065469719 |
| 0 | 4 | 2 | -301.815380621876 | 2 | 3 | 0 | -260.427286048143 | 5 | 0 | 1 | 36.0284195611086 |
| 0 | 4 | 3 | 152.196371733841 | 2 | 3 | 1 | 694.244814133268 | 5 | 1 | 0 | -810.552561548477 |
| 0 | 4 | 4 | -26.3748377232802 | 2 | 3 | 2 | -204.889641964903 | 6 | 0 | 0 | 1695.91780114244 |
| 0 | 5 | 0 | 58.0259125842571 | 2 | 3 | 3 | 113.561697840594 | 6 | 1 | 0 | 506.103588839417 |
| 0 | 5 | 1 | -194.618310617595 | 2 | 3 | 4 | -11.1282734326413 | 7 | 0 | 0 | -466.680815621115 |
| 0 | 5 | 2 | 120.520654902025 | 2 | 4 | 0 | 97.1562727658403 | 7 | 1 | 0 | -129.049444012372 |
| 0 | 5 | 3 | -55.2723052340152 | 2 | 4 | 1 | -297.728741987187 | | | | |

Table 11

Specific free enthalpy, $g(S, t, p)$, in kJ/kg

| MPa | °C | $S = 0$ | $S = 5$ | $S = 10$ | $S = 15$ | $S = 20$ | $S = 25$ | $S = 30$ | $S = 35$ | $S = 40$ |
|-----|----|---------|---------|----------|----------|----------|----------|----------|----------|----------|
| 0 | 0 | 0.101 | −0.560 | −0.759 | −0.786 | −0.702 | −0.533 | −0.295 | 0.000 | 0.346 |
| 0 | 5 | −0.090 | −0.762 | −0.964 | −0.991 | −0.903 | −0.729 | −0.485 | −0.181 | 0.174 |
| 0 | 10 | −0.659 | −1.339 | −1.541 | −1.564 | −1.471 | −1.289 | −1.035 | −0.721 | −0.354 |
| 0 | 15 | −1.598 | −2.284 | −2.483 | −2.500 | −2.398 | −2.206 | −1.941 | −1.613 | −1.232 |
| 0 | 20 | −2.901 | −3.590 | −3.783 | −3.792 | −3.679 | −3.474 | −3.195 | −2.852 | −2.454 |
| 0 | 25 | −4.560 | −5.250 | −5.436 | −5.433 | −5.307 | −5.087 | −4.792 | −4.431 | −4.015 |
| 0 | 30 | −6.571 | −7.259 | −7.434 | −7.418 | −7.276 | −7.040 | −6.726 | −6.346 | −5.909 |
| 0 | 35 | −8.926 | −9.610 | −9.772 | −9.741 | −9.582 | −9.327 | −8.992 | −8.591 | −8.131 |
| 0 | 40 | −11.620 | −12.297 | −12.446 | −12.397 | −12.219 | −11.942 | −11.585 | −11.160 | −10.676 |
| 10 | 0 | 10.078 | 9.377 | 9.138 | 9.071 | 9.117 | 9.248 | 9.447 | 9.704 | 10.012 |
| 10 | 5 | 9.886 | 9.175 | 8.934 | 8.869 | 8.919 | 9.055 | 9.261 | 9.528 | 9.846 |
| 10 | 10 | 9.321 | 8.601 | 8.362 | 8.301 | 8.357 | 8.501 | 8.718 | 8.995 | 9.326 |
| 10 | 15 | 8.388 | 7.663 | 7.427 | 7.373 | 7.438 | 7.593 | 7.822 | 8.113 | 8.458 |
| 10 | 20 | 7.094 | 6.367 | 6.137 | 6.092 | 6.168 | 6.336 | 6.579 | 6.886 | 7.248 |
| 10 | 25 | 5.447 | 4.719 | 4.497 | 4.463 | 4.553 | 4.736 | 4.996 | 5.320 | 5.701 |
| 10 | 30 | 3.451 | 2.726 | 2.514 | 2.493 | 2.598 | 2.799 | 3.077 | 3.421 | 3.823 |
| 10 | 35 | 1.112 | 0.391 | 0.192 | 0.187 | 0.310 | 0.529 | 0.828 | 1.194 | 1.618 |
| 10 | 40 | −1.564 | −2.278 | −2.463 | −2.451 | −2.308 | −2.068 | −1.747 | −1.357 | −0.908 |
| 20 | 0 | 20.005 | 19.265 | 18.987 | 18.882 | 18.890 | 18.983 | 19.145 | 19.365 | 19.636 |
| 20 | 5 | 19.815 | 19.065 | 18.786 | 18.683 | 18.696 | 18.795 | 18.964 | 19.194 | 19.476 |
| 20 | 10 | 19.254 | 18.496 | 18.219 | 18.121 | 18.141 | 18.248 | 18.429 | 18.670 | 18.964 |
| 20 | 15 | 18.328 | 17.566 | 17.293 | 17.202 | 17.231 | 17.350 | 17.543 | 17.798 | 18.107 |
| 20 | 20 | 17.045 | 16.281 | 16.014 | 15.932 | 15.972 | 16.105 | 16.312 | 16.583 | 16.910 |
| 20 | 25 | 15.410 | 14.646 | 14.387 | 14.317 | 14.371 | 14.519 | 14.743 | 15.032 | 15.377 |
| 20 | 30 | 13.428 | 12.667 | 12.419 | 12.362 | 12.432 | 12.597 | 12.839 | 13.148 | 13.515 |
| 20 | 35 | 11.107 | 10.349 | 10.114 | 10.073 | 10.160 | 10.344 | 10.608 | 10.938 | 11.328 |
| 20 | 40 | 8.450 | 7.699 | 7.477 | 7.454 | 7.561 | 7.766 | 8.052 | 8.407 | 8.821 |
| 40 | 0 | 39.718 | 38.901 | 38.549 | 38.370 | 38.304 | 38.323 | 38.412 | 38.560 | 38.760 |
| 40 | 5 | 39.535 | 38.710 | 38.357 | 38.181 | 38.121 | 38.148 | 38.246 | 38.404 | 38.615 |
| 40 | 10 | 38.986 | 38.155 | 37.805 | 37.635 | 37.582 | 37.619 | 37.728 | 37.899 | 38.123 |
| 40 | 15 | 38.078 | 37.243 | 36.898 | 36.736 | 36.693 | 36.742 | 36.864 | 37.049 | 37.289 |
| 40 | 20 | 36.817 | 35.981 | 35.643 | 35.490 | 35.460 | 35.522 | 35.659 | 35.861 | 36.118 |
| 40 | 25 | 35.209 | 34.373 | 34.043 | 33.903 | 33.886 | 33.964 | 34.119 | 34.339 | 34.616 |
| 40 | 30 | 33.258 | 32.425 | 32.106 | 31.979 | 31.979 | 32.074 | 32.248 | 32.488 | 32.786 |
| 40 | 35 | 30.970 | 30.142 | 29.835 | 29.725 | 29.742 | 29.857 | 30.051 | 30.313 | 30.634 |
| 40 | 40 | 28.351 | 27.528 | 27.237 | 27.143 | 27.181 | 27.317 | 27.534 | 27.820 | 28.166 |
| 100 | 0 | 97.827 | 96.798 | 96.237 | 95.851 | 95.579 | 95.393 | 95.279 | 95.224 | 95.222 |
| 100 | 5 | 97.692 | 96.657 | 96.099 | 95.718 | 95.454 | 95.279 | 95.175 | 95.133 | 95.143 |
| 100 | 10 | 97.204 | 96.165 | 95.611 | 95.238 | 94.984 | 94.820 | 94.729 | 94.700 | 94.726 |
| 100 | 15 | 96.368 | 95.327 | 94.779 | 94.415 | 94.172 | 94.021 | 93.944 | 93.932 | 93.974 |
| 100 | 20 | 95.188 | 94.147 | 93.606 | 93.253 | 93.024 | 92.887 | 92.827 | 92.831 | 92.892 |
| 100 | 25 | 93.670 | 92.630 | 92.099 | 91.759 | 91.544 | 91.424 | 91.382 | 91.405 | 91.486 |
| 100 | 30 | 91.819 | 90.782 | 90.263 | 89.937 | 89.738 | 89.636 | 89.613 | 89.657 | 89.759 |
| 100 | 35 | 89.639 | 88.607 | 88.100 | 87.790 | 87.610 | 87.528 | 87.526 | 87.592 | 87.718 |
| 100 | 40 | 87.136 | 86.109 | 85.617 | 85.325 | 85.164 | 85.104 | 85.124 | 85.215 | 85.366 |

Table 12

Specific enthalpy, $h(S, t, p)$, in kJ/kg, Eq. (13)

| MPa | °C | $S = 0$ | $S = 5$ | $S = 10$ | $S = 15$ | $S = 20$ | $S = 25$ | $S = 30$ | $S = 35$ | $S = 40$ |
|-----|----|---------|---------|----------|----------|----------|----------|----------|----------|----------|
| 0 | 0 | 0.061 | 0.119 | 0.155 | 0.168 | 0.158 | 0.127 | 0.074 | 0.000 | −0.096 |
| 0 | 5 | 21.120 | 20.999 | 20.865 | 20.714 | 20.546 | 20.359 | 20.156 | 19.934 | 19.694 |
| 0 | 10 | 42.119 | 41.831 | 41.539 | 41.235 | 40.917 | 40.586 | 40.240 | 39.879 | 39.503 |
| 0 | 15 | 63.077 | 62.633 | 62.191 | 61.742 | 61.284 | 60.814 | 60.333 | 59.839 | 59.332 |
| 0 | 20 | 84.007 | 83.415 | 82.831 | 82.243 | 81.649 | 81.047 | 80.436 | 79.814 | 79.181 |
| 0 | 25 | 104.920 | 104.185 | 103.464 | 102.743 | 102.018 | 101.287 | 100.549 | 99.803 | 99.047 |
| 0 | 30 | 125.823 | 124.950 | 124.095 | 123.244 | 122.391 | 121.534 | 120.672 | 119.803 | 118.927 |
| 0 | 35 | 146.720 | 145.712 | 144.727 | 143.748 | 142.769 | 141.789 | 140.805 | 139.817 | 138.822 |
| 0 | 40 | 167.616 | 166.476 | 165.363 | 164.258 | 163.156 | 162.055 | 160.951 | 159.844 | 158.732 |
| 10 | 0 | 10.171 | 10.134 | 10.081 | 10.009 | 9.917 | 9.806 | 9.676 | 9.527 | 9.359 |
| 10 | 5 | 31.010 | 30.807 | 30.596 | 30.370 | 30.128 | 29.870 | 29.596 | 29.306 | 29.000 |
| 10 | 10 | 51.816 | 51.457 | 51.096 | 50.725 | 50.341 | 49.945 | 49.536 | 49.113 | 48.676 |
| 10 | 15 | 72.602 | 72.094 | 71.590 | 71.081 | 70.563 | 70.035 | 69.496 | 68.946 | 68.384 |
| 10 | 20 | 93.375 | 92.725 | 92.085 | 91.442 | 90.794 | 90.139 | 89.475 | 88.801 | 88.118 |
| 10 | 25 | 114.143 | 113.356 | 112.583 | 111.812 | 111.037 | 110.257 | 109.471 | 108.677 | 107.875 |
| 10 | 30 | 134.910 | 133.990 | 133.089 | 132.191 | 131.293 | 130.391 | 129.484 | 128.571 | 127.651 |
| 10 | 35 | 155.680 | 154.631 | 153.605 | 152.584 | 151.563 | 150.541 | 149.515 | 148.484 | 147.447 |
| 10 | 40 | 176.454 | 175.282 | 174.134 | 172.992 | 171.851 | 170.710 | 169.566 | 168.417 | 167.263 |
| 20 | 0 | 20.133 | 20.008 | 19.871 | 19.719 | 19.549 | 19.363 | 19.161 | 18.941 | 18.704 |
| 20 | 5 | 40.774 | 40.494 | 40.209 | 39.912 | 39.600 | 39.275 | 38.935 | 38.580 | 38.210 |
| 20 | 10 | 61.404 | 60.977 | 60.551 | 60.115 | 59.669 | 59.212 | 58.743 | 58.260 | 57.765 |
| 20 | 15 | 82.031 | 81.463 | 80.900 | 80.333 | 79.758 | 79.174 | 78.580 | 77.976 | 77.361 |
| 20 | 20 | 102.660 | 101.955 | 101.260 | 100.565 | 99.865 | 99.158 | 98.444 | 97.721 | 96.990 |
| 20 | 25 | 123.293 | 122.456 | 121.634 | 120.814 | 119.991 | 119.164 | 118.332 | 117.493 | 116.646 |
| 20 | 30 | 143.934 | 142.969 | 142.023 | 141.081 | 140.138 | 139.192 | 138.242 | 137.287 | 136.325 |
| 20 | 35 | 164.585 | 163.497 | 162.430 | 161.368 | 160.307 | 159.243 | 158.176 | 157.104 | 156.027 |
| 20 | 40 | 185.245 | 184.041 | 182.858 | 181.680 | 180.502 | 179.321 | 178.137 | 176.948 | 175.753 |
| 40 | 0 | 39.651 | 39.363 | 39.073 | 38.773 | 38.461 | 38.138 | 37.801 | 37.452 | 37.089 |
| 40 | 5 | 59.948 | 59.528 | 59.107 | 58.678 | 58.238 | 57.787 | 57.324 | 56.849 | 56.361 |
| 40 | 10 | 80.271 | 79.720 | 79.173 | 78.619 | 78.056 | 77.484 | 76.902 | 76.309 | 75.705 |
| 40 | 15 | 100.620 | 99.939 | 99.267 | 98.591 | 97.910 | 97.222 | 96.525 | 95.820 | 95.104 |
| 40 | 20 | 120.992 | 120.184 | 119.389 | 118.594 | 117.797 | 116.994 | 116.186 | 115.370 | 114.546 |
| 40 | 25 | 141.386 | 140.453 | 139.539 | 138.627 | 137.715 | 136.799 | 135.879 | 134.954 | 134.022 |
| 40 | 30 | 161.800 | 160.749 | 159.718 | 158.691 | 157.664 | 156.636 | 155.604 | 154.568 | 153.526 |
| 40 | 35 | 182.235 | 181.071 | 179.928 | 178.788 | 177.649 | 176.507 | 175.362 | 174.211 | 173.055 |
| 40 | 40 | 202.687 | 201.423 | 200.173 | 198.924 | 197.672 | 196.417 | 195.156 | 193.888 | 192.613 |
| 100 | 0 | 95.496 | 94.811 | 94.145 | 93.483 | 92.823 | 92.162 | 91.499 | 90.832 | 90.161 |
| 100 | 5 | 115.076 | 114.312 | 113.559 | 112.805 | 112.048 | 111.287 | 110.520 | 109.746 | 108.966 |
| 100 | 10 | 134.750 | 133.893 | 133.046 | 132.197 | 131.345 | 130.487 | 129.623 | 128.752 | 127.874 |
| 100 | 15 | 154.498 | 153.539 | 152.592 | 151.646 | 150.698 | 149.746 | 148.788 | 147.825 | 146.855 |
| 100 | 20 | 174.307 | 173.241 | 172.192 | 171.146 | 170.100 | 169.052 | 168.001 | 166.946 | 165.886 |
| 100 | 25 | 194.167 | 192.994 | 191.841 | 190.694 | 189.549 | 188.403 | 187.256 | 186.105 | 184.951 |
| 100 | 30 | 214.070 | 212.796 | 211.542 | 210.293 | 209.046 | 207.799 | 206.549 | 205.297 | 204.040 |
| 100 | 35 | 234.010 | 232.647 | 231.298 | 229.949 | 228.598 | 227.244 | 225.884 | 224.519 | 223.148 |
| 100 | 40 | 253.981 | 252.551 | 251.116 | 249.672 | 248.216 | 246.748 | 245.269 | 243.778 | 242.274 |

Table 13

Specific internal energy, $e(S, t, p)$, in kJ/kg, Eq. (14)

| MPa | °C | $S = 0$ | $S = 5$ | $S = 10$ | $S = 15$ | $S = 20$ | $S = 25$ | $S = 30$ | $S = 35$ | $S = 40$ |
|-----|----|---------|---------|----------|----------|----------|----------|----------|----------|----------|
| 0 | 0 | −0.040 | 0.008 | 0.045 | 0.062 | 0.057 | 0.029 | −0.022 | −0.099 | −0.201 |
| 0 | 5 | 21.019 | 20.892 | 20.760 | 20.612 | 20.446 | 20.262 | 20.059 | 19.836 | 19.591 |
| 0 | 10 | 42.018 | 41.728 | 41.437 | 41.134 | 40.818 | 40.487 | 40.141 | 39.779 | 39.398 |
| 0 | 15 | 62.975 | 62.532 | 62.092 | 61.643 | 61.185 | 60.716 | 60.235 | 59.741 | 59.230 |
| 0 | 20 | 83.906 | 83.315 | 82.733 | 82.146 | 81.552 | 80.950 | 80.339 | 79.718 | 79.083 |
| 0 | 25 | 104.819 | 104.086 | 103.366 | 102.644 | 101.919 | 101.188 | 100.451 | 99.705 | 98.948 |
| 0 | 30 | 125.721 | 124.850 | 123.995 | 123.142 | 122.288 | 121.432 | 120.571 | 119.704 | 118.825 |
| 0 | 35 | 146.618 | 145.612 | 144.626 | 143.645 | 142.666 | 141.686 | 140.704 | 139.717 | 138.720 |
| 0 | 40 | 167.514 | 166.375 | 165.261 | 164.154 | 163.051 | 161.951 | 160.850 | 159.745 | 158.631 |
| 10 | 0 | 0.118 | 0.116 | 0.100 | 0.069 | 0.021 | −0.048 | −0.138 | −0.252 | −0.391 |
| 10 | 5 | 20.957 | 20.791 | 20.618 | 20.432 | 20.230 | 20.013 | 19.777 | 19.522 | 19.246 |
| 10 | 10 | 41.759 | 41.437 | 41.114 | 40.781 | 40.436 | 40.078 | 39.705 | 39.317 | 38.912 |
| 10 | 15 | 62.538 | 62.067 | 61.602 | 61.130 | 60.649 | 60.158 | 59.656 | 59.142 | 58.613 |
| 10 | 20 | 83.301 | 82.689 | 82.088 | 81.483 | 80.871 | 80.252 | 79.625 | 78.988 | 78.338 |
| 10 | 25 | 104.057 | 103.309 | 102.575 | 101.840 | 101.101 | 100.358 | 99.608 | 98.850 | 98.080 |
| 10 | 30 | 124.810 | 123.929 | 123.065 | 122.203 | 121.340 | 120.474 | 119.604 | 118.727 | 117.837 |
| 10 | 35 | 145.562 | 144.551 | 143.560 | 142.573 | 141.588 | 140.603 | 139.616 | 138.622 | 137.615 |
| 10 | 40 | 166.318 | 165.177 | 164.058 | 162.947 | 161.842 | 160.741 | 159.640 | 158.532 | 157.410 |
| 20 | 0 | 0.227 | 0.179 | 0.114 | 0.038 | −0.051 | −0.158 | −0.284 | −0.432 | −0.606 |
| 20 | 5 | 20.863 | 20.660 | 20.449 | 20.227 | 19.993 | 19.743 | 19.477 | 19.193 | 18.889 |
| 20 | 10 | 41.483 | 41.130 | 40.777 | 40.416 | 40.044 | 39.660 | 39.263 | 38.851 | 38.424 |
| 20 | 15 | 62.094 | 61.598 | 61.110 | 60.616 | 60.113 | 59.602 | 59.080 | 58.547 | 58.001 |
| 20 | 20 | 82.702 | 82.069 | 81.450 | 80.828 | 80.200 | 79.565 | 78.922 | 78.270 | 77.607 |
| 20 | 25 | 103.310 | 102.546 | 101.800 | 101.053 | 100.301 | 99.545 | 98.784 | 98.014 | 97.233 |
| 20 | 30 | 123.921 | 123.030 | 122.159 | 121.288 | 120.416 | 119.542 | 118.663 | 117.776 | 116.876 |
| 20 | 35 | 144.537 | 143.522 | 142.526 | 141.533 | 140.542 | 139.552 | 138.559 | 137.558 | 136.541 |
| 20 | 40 | 165.160 | 164.016 | 162.893 | 161.779 | 160.672 | 159.569 | 158.467 | 157.356 | 156.228 |
| 40 | 0 | 0.308 | 0.183 | 0.028 | −0.129 | −0.292 | −0.466 | −0.657 | −0.867 | −1.101 |
| 40 | 5 | 20.586 | 20.320 | 20.039 | 19.753 | 19.458 | 19.152 | 18.831 | 18.493 | 18.138 |
| 40 | 10 | 40.880 | 40.473 | 40.066 | 39.655 | 39.234 | 38.803 | 38.361 | 37.906 | 37.438 |
| 40 | 15 | 61.190 | 60.646 | 60.117 | 59.584 | 59.043 | 58.494 | 57.936 | 57.369 | 56.792 |
| 40 | 20 | 81.514 | 80.842 | 80.193 | 79.541 | 78.883 | 78.219 | 77.548 | 76.869 | 76.182 |
| 40 | 25 | 101.852 | 101.059 | 100.292 | 99.524 | 98.750 | 97.971 | 97.187 | 96.396 | 95.594 |
| 40 | 30 | 122.204 | 121.295 | 120.411 | 119.526 | 118.637 | 117.746 | 116.850 | 115.945 | 115.026 |
| 40 | 35 | 142.569 | 141.544 | 140.542 | 139.540 | 138.538 | 137.536 | 136.532 | 135.517 | 134.482 |
| 40 | 40 | 162.946 | 161.799 | 160.671 | 159.549 | 158.436 | 157.329 | 156.223 | 155.105 | 153.962 |
| 100 | 0 | −0.266 | −0.534 | −0.905 | −1.262 | −1.602 | −1.933 | −2.268 | −2.616 | −2.986 |
| 100 | 5 | 19.206 | 18.815 | 18.370 | 17.930 | 17.493 | 17.055 | 16.610 | 16.153 | 15.682 |
| 100 | 10 | 38.756 | 38.231 | 37.702 | 37.173 | 36.642 | 36.105 | 35.562 | 35.011 | 34.452 |
| 100 | 15 | 58.366 | 57.712 | 57.093 | 56.474 | 55.848 | 55.215 | 54.577 | 53.936 | 53.291 |
| 100 | 20 | 78.025 | 77.252 | 76.542 | 75.830 | 75.108 | 74.377 | 73.642 | 72.904 | 72.164 |
| 100 | 25 | 97.722 | 96.847 | 96.045 | 95.235 | 94.412 | 93.580 | 92.741 | 91.898 | 91.049 |
| 100 | 30 | 117.450 | 116.486 | 115.588 | 114.677 | 113.749 | 112.811 | 111.866 | 110.913 | 109.945 |
| 100 | 35 | 137.205 | 136.152 | 135.151 | 134.132 | 133.099 | 132.057 | 131.009 | 129.948 | 128.862 |
| 100 | 40 | 156.979 | 155.825 | 154.703 | 153.568 | 152.430 | 151.293 | 150.155 | 149.005 | 147.820 |

Note that this Table 14 is in J/(kg K),

Table 14

Specific entropy, $\sigma(S, t, p)$, in kJ/(kg K), Eq. (3) not kJ/(kg K).

| MPa | °C | $S = 0$ | $S = 5$ | $S = 10$ | $S = 15$ | $S = 20$ | $S = 25$ | $S = 30$ | $S = 35$ | $S = 40$ |
|-----|----|---------|---------|----------|----------|----------|----------|----------|----------|----------|
| 0 | 0 | −0.148 | 2.484 | 3.344 | 3.492 | 3.149 | 2.416 | 1.353 | 0.000 | −1.616 |
| 0 | 5 | 76.252 | 78.234 | 78.478 | 78.032 | 77.111 | 75.817 | 74.207 | 72.318 | 70.178 |
| 0 | 10 | 151.077 | 152.466 | 152.145 | 151.153 | 149.702 | 147.890 | 145.773 | 143.388 | 140.762 |
| 0 | 15 | 224.448 | 225.290 | 224.447 | 222.947 | 221.001 | 218.706 | 216.115 | 213.265 | 210.183 |
| 0 | 20 | 296.463 | 296.794 | 295.461 | 293.485 | 291.073 | 288.321 | 285.282 | 281.992 | 278.476 |
| 0 | 25 | 367.200 | 367.049 | 365.252 | 362.823 | 359.968 | 356.781 | 353.314 | 349.602 | 345.670 |
| 0 | 30 | 436.725 | 436.116 | 433.875 | 431.013 | 427.732 | 424.126 | 420.247 | 416.129 | 411.796 |
| 0 | 35 | 505.097 | 504.046 | 501.378 | 498.098 | 494.407 | 490.397 | 486.119 | 481.608 | 476.886 |
| 0 | 40 | 572.365 | 570.888 | 567.808 | 564.124 | 560.036 | 555.634 | 550.971 | 546.078 | 540.981 |
| 10 | 0 | 0.341 | 2.774 | 3.453 | 3.432 | 2.929 | 2.046 | 0.840 | −0.648 | −2.392 |
| 10 | 5 | 75.943 | 77.774 | 77.878 | 77.298 | 76.251 | 74.835 | 73.108 | 71.108 | 68.862 |
| 10 | 10 | 150.081 | 151.354 | 150.925 | 149.828 | 148.277 | 146.368 | 144.159 | 141.685 | 138.973 |
| 10 | 15 | 222.848 | 223.601 | 222.673 | 221.093 | 219.069 | 216.698 | 214.035 | 211.116 | 207.967 |
| 10 | 20 | 294.323 | 294.585 | 293.187 | 291.149 | 288.678 | 285.868 | 282.775 | 279.432 | 275.866 |
| 10 | 25 | 364.570 | 364.368 | 362.523 | 360.048 | 357.149 | 353.919 | 350.411 | 346.661 | 342.693 |
| 10 | 30 | 433.645 | 433.003 | 430.729 | 427.835 | 424.523 | 420.887 | 416.979 | 412.833 | 408.473 |
| 10 | 35 | 501.598 | 500.536 | 497.852 | 494.554 | 490.844 | 486.813 | 482.515 | 477.982 | 473.239 |
| 10 | 40 | 568.474 | 567.013 | 563.937 | 560.250 | 556.154 | 551.741 | 547.061 | 542.150 | 537.031 |
| 20 | 0 | 0.469 | 2.722 | 3.237 | 3.062 | 2.414 | 1.394 | 0.059 | −1.552 | −3.412 |
| 20 | 5 | 75.350 | 77.044 | 77.020 | 76.319 | 75.156 | 73.630 | 71.797 | 69.696 | 67.353 |
| 20 | 10 | 148.862 | 150.030 | 149.502 | 148.311 | 146.668 | 144.671 | 142.377 | 139.822 | 137.031 |
| 20 | 15 | 221.075 | 221.747 | 220.743 | 219.088 | 216.994 | 214.554 | 211.826 | 208.844 | 205.634 |
| 20 | 20 | 292.051 | 292.252 | 290.795 | 288.701 | 286.175 | 283.314 | 280.171 | 276.781 | 273.170 |
| 20 | 25 | 361.844 | 361.597 | 359.708 | 357.191 | 354.252 | 350.984 | 347.440 | 343.656 | 339.655 |
| 20 | 30 | 430.500 | 429.828 | 427.525 | 424.603 | 421.263 | 417.600 | 413.666 | 409.496 | 405.113 |
| 20 | 35 | 498.062 | 496.990 | 494.293 | 490.979 | 487.252 | 483.203 | 478.886 | 474.334 | 469.572 |
| 20 | 40 | 564.570 | 563.125 | 560.054 | 556.365 | 552.262 | 547.837 | 543.143 | 538.214 | 533.074 |
| 40 | 0 | −0.246 | 1.692 | 1.919 | 1.477 | 0.578 | −0.679 | −2.237 | −4.058 | −6.116 |
| 40 | 5 | 73.389 | 74.846 | 74.600 | 73.688 | 72.325 | 70.606 | 68.590 | 66.313 | 63.801 |
| 40 | 10 | 145.807 | 146.797 | 146.097 | 144.742 | 142.941 | 140.792 | 138.351 | 135.654 | 132.728 |
| 40 | 15 | 217.045 | 217.580 | 216.445 | 214.664 | 212.447 | 209.890 | 207.048 | 203.957 | 200.642 |
| 40 | 20 | 287.137 | 287.234 | 285.677 | 283.487 | 280.870 | 277.921 | 274.693 | 271.223 | 267.535 |
| 40 | 25 | 356.118 | 355.796 | 353.833 | 351.247 | 348.241 | 344.910 | 341.306 | 337.465 | 333.411 |
| 40 | 30 | 424.022 | 423.303 | 420.952 | 417.983 | 414.598 | 410.891 | 406.915 | 402.705 | 398.284 |
| 40 | 35 | 490.878 | 489.793 | 487.075 | 483.737 | 479.982 | 475.905 | 471.557 | 466.974 | 462.181 |
| 40 | 40 | 556.718 | 555.307 | 552.246 | 548.556 | 544.441 | 539.997 | 535.276 | 530.315 | 525.138 |
| 100 | 0 | −8.535 | −7.277 | −7.661 | −8.667 | −10.088 | −11.830 | −13.839 | −16.080 | −18.528 |
| 100 | 5 | 62.499 | 63.470 | 62.771 | 61.430 | 59.658 | 57.551 | 55.166 | 52.538 | 49.694 |
| 100 | 10 | 132.600 | 133.242 | 132.208 | 130.529 | 128.417 | 125.967 | 123.237 | 120.262 | 117.069 |
| 100 | 15 | 201.735 | 202.020 | 200.638 | 198.618 | 196.170 | 193.389 | 190.331 | 187.033 | 183.519 |
| 100 | 20 | 269.891 | 269.807 | 268.072 | 265.708 | 262.925 | 259.816 | 256.437 | 252.822 | 248.998 |
| 100 | 25 | 337.067 | 336.620 | 334.535 | 331.829 | 328.709 | 325.269 | 321.563 | 317.627 | 313.485 |
| 100 | 30 | 403.269 | 402.487 | 400.064 | 397.020 | 393.561 | 389.782 | 385.737 | 381.461 | 376.979 |
| 100 | 35 | 468.508 | 467.436 | 464.701 | 461.330 | 457.532 | 453.402 | 448.998 | 444.353 | 439.494 |
| 100 | 40 | 532.797 | 531.507 | 528.499 | 524.818 | 520.682 | 516.189 | 511.399 | 506.348 | 501.065 |

Table 15

Chemical potential of water in seawater, $\mu^w(S, t, p)$, in kJ/kg, Eq. (15)

| MPa | °C | $S = 0$ | $S = 5$ | $S = 10$ | $S = 15$ | $S = 20$ | $S = 25$ | $S = 30$ | $S = 35$ | $S = 40$ |
|-----|----|---------|---------|----------|----------|----------|----------|----------|----------|----------|
| 0 | 0 | 0.101 | −0.234 | −0.562 | −0.890 | −1.222 | −1.559 | −1.903 | −2.252 | −2.605 |
| 0 | 5 | −0.090 | −0.431 | −0.765 | −1.101 | −1.440 | −1.785 | −2.137 | −2.495 | −2.857 |
| 0 | 10 | −0.659 | −1.006 | −1.347 | −1.689 | −2.035 | −2.388 | −2.748 | −3.114 | −3.485 |
| 0 | 15 | −1.598 | −1.952 | −2.299 | −2.647 | −3.000 | −3.360 | −3.728 | −4.102 | −4.482 |
| 0 | 20 | −2.901 | −3.261 | −3.614 | −3.968 | −4.328 | −4.695 | −5.070 | −5.452 | −5.840 |
| 0 | 25 | −4.560 | −4.926 | −5.285 | −5.646 | −6.013 | −6.386 | −6.769 | −7.158 | −7.554 |
| 0 | 30 | −6.571 | −6.943 | −7.307 | −7.674 | −8.047 | −8.428 | −8.817 | −9.214 | −9.618 |
| 0 | 35 | −8.926 | −9.303 | −9.674 | −10.047 | −10.426 | −10.813 | −11.209 | −11.614 | −12.025 |
| 0 | 40 | −11.620 | −12.003 | −12.380 | −12.759 | −13.144 | −13.537 | −13.940 | −14.352 | −14.770 |
| 10 | 0 | 10.078 | 9.742 | 9.414 | 9.085 | 8.752 | 8.413 | 8.068 | 7.717 | 7.361 |
| 10 | 5 | 9.886 | 9.545 | 9.210 | 8.874 | 8.533 | 8.187 | 7.834 | 7.474 | 7.110 |
| 10 | 10 | 9.321 | 8.973 | 8.632 | 8.289 | 7.942 | 7.588 | 7.227 | 6.859 | 6.486 |
| 10 | 15 | 8.388 | 8.034 | 7.686 | 7.337 | 6.983 | 6.622 | 6.254 | 5.878 | 5.497 |
| 10 | 20 | 7.094 | 6.734 | 6.381 | 6.025 | 5.665 | 5.297 | 4.921 | 4.537 | 4.148 |
| 10 | 25 | 5.447 | 5.081 | 4.721 | 4.360 | 3.992 | 3.618 | 3.235 | 2.844 | 2.446 |
| 10 | 30 | 3.451 | 3.079 | 2.713 | 2.346 | 1.972 | 1.591 | 1.201 | 0.802 | 0.397 |
| 10 | 35 | 1.112 | 0.734 | 0.363 | −0.011 | −0.390 | −0.778 | −1.175 | −1.581 | −1.993 |
| 10 | 40 | −1.564 | −1.947 | −2.324 | −2.704 | −3.090 | −3.484 | −3.888 | −4.301 | −4.721 |
| 20 | 0 | 20.005 | 19.669 | 19.340 | 19.010 | 18.676 | 18.336 | 17.989 | 17.637 | 17.279 |
| 20 | 5 | 19.815 | 19.473 | 19.137 | 18.801 | 18.459 | 18.112 | 17.757 | 17.396 | 17.030 |
| 20 | 10 | 19.254 | 18.905 | 18.564 | 18.220 | 17.872 | 17.518 | 17.155 | 16.786 | 16.412 |
| 20 | 15 | 18.328 | 17.974 | 17.626 | 17.276 | 16.922 | 16.560 | 16.190 | 15.813 | 15.430 |
| 20 | 20 | 17.045 | 16.685 | 16.331 | 15.975 | 15.613 | 15.245 | 14.868 | 14.483 | 14.092 |
| 20 | 25 | 15.410 | 15.043 | 14.684 | 14.321 | 13.954 | 13.578 | 13.194 | 12.802 | 12.403 |
| 20 | 30 | 13.428 | 13.056 | 12.690 | 12.322 | 11.948 | 11.566 | 11.175 | 10.775 | 10.369 |
| 20 | 35 | 11.107 | 10.728 | 10.357 | 9.983 | 9.602 | 9.214 | 8.816 | 8.409 | 7.995 |
| 20 | 40 | 8.450 | 8.066 | 7.688 | 7.308 | 6.921 | 6.526 | 6.121 | 5.707 | 5.286 |
| 40 | 0 | 39.718 | 39.381 | 39.051 | 38.720 | 38.384 | 38.041 | 37.692 | 37.337 | 36.976 |
| 40 | 5 | 39.535 | 39.192 | 38.855 | 38.517 | 38.174 | 37.825 | 37.468 | 37.105 | 36.736 |
| 40 | 10 | 38.986 | 38.637 | 38.294 | 37.950 | 37.600 | 37.244 | 36.880 | 36.508 | 36.131 |
| 40 | 15 | 38.078 | 37.723 | 37.375 | 37.024 | 36.668 | 36.304 | 35.932 | 35.553 | 35.168 |
| 40 | 20 | 36.817 | 36.457 | 36.102 | 35.745 | 35.382 | 35.011 | 34.633 | 34.246 | 33.852 |
| 40 | 25 | 35.209 | 34.842 | 34.481 | 34.118 | 33.749 | 33.372 | 32.986 | 32.592 | 32.191 |
| 40 | 30 | 33.258 | 32.885 | 32.519 | 32.149 | 31.774 | 31.390 | 30.998 | 30.596 | 30.188 |
| 40 | 35 | 30.970 | 30.592 | 30.219 | 29.844 | 29.462 | 29.072 | 28.673 | 28.264 | 27.848 |
| 40 | 40 | 28.351 | 27.966 | 27.588 | 27.207 | 26.819 | 26.422 | 26.015 | 25.599 | 25.176 |
| 100 | 0 | 97.827 | 97.488 | 97.155 | 96.820 | 96.479 | 96.132 | 95.778 | 95.417 | 95.050 |
| 100 | 5 | 97.692 | 97.347 | 97.008 | 96.666 | 96.320 | 95.966 | 95.605 | 95.236 | 94.861 |
| 100 | 10 | 97.204 | 96.853 | 96.507 | 96.160 | 95.807 | 95.446 | 95.078 | 94.701 | 94.319 |
| 100 | 15 | 96.368 | 96.011 | 95.659 | 95.305 | 94.945 | 94.578 | 94.203 | 93.819 | 93.429 |
| 100 | 20 | 95.188 | 94.825 | 94.468 | 94.107 | 93.741 | 93.368 | 92.985 | 92.594 | 92.197 |
| 100 | 25 | 93.670 | 93.301 | 92.938 | 92.572 | 92.200 | 91.819 | 91.430 | 91.032 | 90.627 |
| 100 | 30 | 91.819 | 91.444 | 91.075 | 90.703 | 90.324 | 89.937 | 89.541 | 89.136 | 88.724 |
| 100 | 35 | 89.639 | 89.259 | 88.883 | 88.505 | 88.120 | 87.727 | 87.324 | 86.912 | 86.492 |
| 100 | 40 | 87.136 | 86.749 | 86.367 | 85.983 | 85.591 | 85.191 | 84.781 | 84.361 | 83.933 |

Table 16

Density anomaly, $\chi(S, t, p)$, in kg/m³, Eq. (2)

| MPa | °C | $S = 0$ | $S = 5$ | $S = 10$ | $S = 15$ | $S = 20$ | $S = 25$ | $S = 30$ | $S = 35$ | $S = 40$ |
|-----|----|---------|---------|----------|----------|----------|----------|----------|----------|----------|
| 0 | 0 | −0.1569 | 3.9148 | 7.9557 | 11.9874 | 16.0161 | 20.0447 | 24.0749 | 28.1072 | 32.1419 |
| 0 | 5 | −0.0334 | 3.9478 | 7.9038 | 11.8542 | 15.8046 | 19.7576 | 23.7144 | 27.6756 | 31.6414 |
| 0 | 10 | −0.2975 | 3.6117 | 7.4989 | 11.3827 | 15.2684 | 19.1582 | 23.0533 | 26.9541 | 30.8608 |
| 0 | 15 | −0.8974 | 2.9534 | 6.7844 | 10.6133 | 14.4452 | 18.2824 | 22.1258 | 25.9760 | 29.8331 |
| 0 | 20 | −1.7929 | 2.0097 | 5.7939 | 9.5771 | 13.3643 | 17.1575 | 20.9580 | 24.7660 | 28.5816 |
| 0 | 25 | −2.9524 | 0.8100 | 4.5551 | 8.3001 | 12.0498 | 15.8064 | 19.5709 | 23.3436 | 27.1248 |
| 0 | 30 | −4.3505 | −0.6207 | 3.0921 | 6.8053 | 10.5236 | 14.2493 | 17.9833 | 21.7261 | 25.4778 |
| 0 | 35 | −5.9667 | −2.2610 | 1.4267 | 5.1142 | 8.8064 | 12.5058 | 16.2134 | 19.9298 | 23.6550 |
| 0 | 40 | −7.7836 | −4.0910 | −0.4202 | 3.2481 | 6.9193 | 10.5962 | 14.2800 | 17.9715 | 21.6708 |
| 10 | 0 | 4.8718 | 8.8944 | 12.8883 | 16.8743 | 20.8584 | 24.8433 | 28.8304 | 32.8204 | 36.8135 |
| 10 | 5 | 4.8289 | 8.7671 | 12.6818 | 16.5919 | 20.5029 | 24.4172 | 28.3359 | 32.2596 | 36.1883 |
| 10 | 10 | 4.4305 | 8.3016 | 12.1520 | 15.9998 | 19.8501 | 23.7051 | 27.5658 | 31.4328 | 35.3060 |
| 10 | 15 | 3.7224 | 7.5390 | 11.3366 | 15.1329 | 18.9326 | 22.7380 | 26.5500 | 30.3692 | 34.1955 |
| 10 | 20 | 2.7401 | 6.5115 | 10.2652 | 14.0184 | 17.7759 | 21.5399 | 25.3113 | 29.0906 | 32.8778 |
| 10 | 25 | 1.5117 | 5.2454 | 8.9622 | 12.6793 | 16.4015 | 20.1308 | 23.8682 | 27.6143 | 31.3689 |
| 10 | 30 | 0.0601 | 3.7629 | 7.4492 | 11.1362 | 14.8287 | 18.5288 | 22.2374 | 25.9552 | 29.6821 |
| 10 | 35 | −1.5961 | 2.0838 | 5.7461 | 9.4086 | 13.0763 | 16.7513 | 20.4349 | 24.1276 | 27.8294 |
| 10 | 40 | −3.4413 | 0.2259 | 3.8719 | 7.5158 | 11.1631 | 14.8164 | 18.4770 | 22.1456 | 25.8224 |
| 20 | 0 | 9.7851 | 13.7616 | 17.7107 | 21.6529 | 25.5940 | 29.5369 | 33.4828 | 37.4324 | 41.3859 |
| 20 | 5 | 9.5844 | 13.4821 | 17.3572 | 21.2285 | 25.1014 | 28.9783 | 32.8603 | 36.7480 | 40.6414 |
| 20 | 10 | 9.0578 | 12.8930 | 16.7080 | 20.5209 | 24.3369 | 28.1581 | 31.9856 | 35.8200 | 39.6612 |
| 20 | 15 | 8.2457 | 12.0300 | 15.7956 | 19.5601 | 23.3286 | 27.1031 | 30.8848 | 34.6741 | 38.4710 |
| 20 | 20 | 7.1793 | 10.9214 | 14.6458 | 18.3699 | 22.0986 | 25.8342 | 29.5776 | 33.3293 | 37.0893 |
| 20 | 25 | 5.8839 | 9.5905 | 13.2803 | 16.9704 | 20.6659 | 24.3688 | 28.0803 | 31.8006 | 35.5300 |
| 20 | 30 | 4.3797 | 8.0574 | 11.7184 | 15.3801 | 19.0476 | 22.7229 | 26.4073 | 30.1010 | 33.8043 |
| 20 | 35 | 2.6837 | 6.3397 | 9.9779 | 13.6164 | 17.2603 | 20.9120 | 24.5726 | 28.2426 | 31.9221 |
| 20 | 40 | 0.8099 | 4.4538 | 8.0763 | 11.6969 | 15.3212 | 18.9519 | 22.5903 | 26.2371 | 29.8926 |
| 40 | 0 | 19.2789 | 23.1712 | 27.0364 | 30.8960 | 34.7560 | 38.6194 | 42.4877 | 46.3616 | 50.2414 |
| 40 | 5 | 18.7879 | 22.6113 | 26.4117 | 30.2092 | 34.0094 | 37.8150 | 41.6274 | 45.4472 | 49.2746 |
| 40 | 10 | 18.0229 | 21.7919 | 25.5398 | 29.2861 | 33.0363 | 36.7929 | 40.5573 | 44.3301 | 48.1115 |
| 40 | 15 | 17.0151 | 20.7401 | 24.4449 | 28.1488 | 31.8572 | 35.5727 | 39.2967 | 43.0296 | 46.7718 |
| 40 | 20 | 15.7892 | 19.4777 | 23.1465 | 26.8150 | 30.4885 | 34.1697 | 37.8598 | 41.5596 | 45.2691 |
| 40 | 25 | 14.3652 | 18.0229 | 21.6615 | 25.3001 | 28.9443 | 32.5968 | 36.2588 | 39.9309 | 43.6135 |
| 40 | 30 | 12.7594 | 16.3917 | 20.0049 | 23.6184 | 27.2380 | 30.8661 | 34.5041 | 38.1528 | 41.8124 |
| 40 | 35 | 10.9852 | 14.5984 | 18.1913 | 21.7841 | 25.3825 | 28.9893 | 32.6060 | 36.2333 | 39.8716 |
| 40 | 40 | 9.0540 | 12.6565 | 16.2351 | 19.8113 | 23.3915 | 26.9788 | 30.5747 | 34.1803 | 37.7960 |
| 100 | 0 | 45.3191 | 49.0158 | 52.6680 | 56.3118 | 59.9584 | 63.6139 | 67.2821 | 70.9654 | 74.6655 |
| 100 | 5 | 44.1398 | 47.7878 | 51.3949 | 54.9959 | 58.6019 | 62.2188 | 65.8501 | 69.4982 | 73.1648 |
| 100 | 10 | 42.7940 | 46.4060 | 49.9783 | 53.5454 | 57.1184 | 60.7031 | 64.3030 | 67.9206 | 71.5575 |
| 100 | 15 | 41.2987 | 44.8831 | 48.4277 | 51.9674 | 55.5133 | 59.0712 | 62.6448 | 66.2363 | 69.8476 |
| 100 | 20 | 39.6671 | 43.2290 | 46.7508 | 50.2676 | 53.7907 | 57.3260 | 60.8773 | 64.4468 | 68.0364 |
| 100 | 25 | 37.9095 | 41.4521 | 44.9542 | 48.4513 | 51.9547 | 55.4705 | 59.0024 | 62.5529 | 66.1237 |
| 100 | 30 | 36.0337 | 39.5601 | 43.0452 | 46.5247 | 50.0105 | 53.5085 | 57.0226 | 60.5554 | 64.1087 |
| 100 | 35 | 34.0463 | 37.5605 | 41.0311 | 44.4950 | 47.9641 | 51.4449 | 54.9412 | 58.4558 | 61.9904 |
| 100 | 40 | 31.9524 | 35.4608 | 38.9206 | 42.3708 | 45.8238 | 49.2866 | 52.7632 | 56.2564 | 59.7684 |

Table 17

Isobaric specific heat capacity, $c_p(S, t, p)$, in J/kgK, Eq. (7)

| MPa | °C | $S = 0$ | $S = 5$ | $S = 10$ | $S = 15$ | $S = 20$ | $S = 25$ | $S = 30$ | $S = 35$ | $S = 40$ |
|-----|----|---------|---------|----------|----------|----------|----------|----------|----------|----------|
| 0 | 0 | 4219.41 | 4182.14 | 4146.85 | 4112.85 | 4079.90 | 4047.84 | 4016.60 | 3986.08 | 3956.25 |
| 0 | 5 | 4205.05 | 4170.59 | 4137.85 | 4106.23 | 4075.51 | 4045.58 | 4016.34 | 3987.74 | 3959.73 |
| 0 | 10 | 4195.14 | 4162.96 | 4132.26 | 4102.53 | 4073.58 | 4045.30 | 4017.62 | 3990.49 | 3963.87 |
| 0 | 15 | 4188.45 | 4158.07 | 4128.96 | 4100.68 | 4073.08 | 4046.05 | 4019.55 | 3993.52 | 3967.93 |
| 0 | 20 | 4184.06 | 4155.05 | 4127.14 | 4099.96 | 4073.36 | 4047.26 | 4021.62 | 3996.39 | 3971.53 |
| 0 | 25 | 4181.32 | 4153.33 | 4126.31 | 4099.93 | 4074.07 | 4048.64 | 4023.62 | 3998.96 | 3974.63 |
| 0 | 30 | 4179.81 | 4152.56 | 4126.20 | 4100.41 | 4075.09 | 4050.17 | 4025.61 | 4001.37 | 3977.44 |
| 0 | 35 | 4179.25 | 4152.55 | 4126.69 | 4101.37 | 4076.49 | 4051.98 | 4027.82 | 4003.96 | 3980.39 |
| 0 | 40 | 4179.42 | 4153.18 | 4127.75 | 4102.87 | 4078.42 | 4054.34 | 4030.59 | 4007.16 | 3984.00 |
| 10 | 0 | 4172.22 | 4137.92 | 4105.12 | 4073.31 | 4042.29 | 4011.96 | 3982.25 | 3953.09 | 3924.46 |
| 10 | 5 | 4164.06 | 4131.87 | 4101.11 | 4071.29 | 4042.21 | 4013.78 | 3985.94 | 3958.62 | 3931.80 |
| 10 | 10 | 4158.81 | 4128.35 | 4099.21 | 4070.94 | 4043.37 | 4016.40 | 3989.97 | 3964.02 | 3938.54 |
| 10 | 15 | 4155.65 | 4126.59 | 4098.73 | 4071.65 | 4045.20 | 4019.30 | 3993.89 | 3968.93 | 3944.37 |
| 10 | 20 | 4153.98 | 4126.06 | 4099.19 | 4073.01 | 4047.39 | 4022.25 | 3997.54 | 3973.22 | 3949.26 |
| 10 | 25 | 4153.37 | 4126.41 | 4100.34 | 4074.85 | 4049.82 | 4025.20 | 4000.94 | 3977.01 | 3953.39 |
| 10 | 30 | 4153.55 | 4127.45 | 4102.06 | 4077.12 | 4052.55 | 4028.29 | 4004.32 | 3980.61 | 3957.14 |
| 10 | 35 | 4154.32 | 4129.09 | 4104.35 | 4079.92 | 4055.75 | 4031.79 | 4008.04 | 3984.46 | 3961.05 |
| 10 | 40 | 4155.54 | 4131.28 | 4107.26 | 4083.39 | 4059.66 | 4036.04 | 4012.52 | 3989.08 | 3965.74 |
| 20 | 0 | 4129.67 | 4098.10 | 4067.58 | 4037.74 | 4008.46 | 3979.65 | 3951.27 | 3923.28 | 3895.65 |
| 20 | 5 | 4126.81 | 4096.71 | 4067.77 | 4039.57 | 4011.97 | 3984.91 | 3958.30 | 3932.13 | 3906.35 |
| 20 | 10 | 4125.56 | 4096.68 | 4068.97 | 4042.04 | 4015.72 | 3989.95 | 3964.65 | 3939.79 | 3915.34 |
| 20 | 15 | 4125.46 | 4097.60 | 4070.88 | 4044.90 | 4019.52 | 3994.66 | 3970.26 | 3946.29 | 3922.70 |
| 20 | 20 | 4126.15 | 4099.22 | 4073.30 | 4048.05 | 4023.34 | 3999.08 | 3975.24 | 3951.78 | 3928.66 |
| 20 | 25 | 4127.40 | 4101.38 | 4076.18 | 4051.50 | 4027.25 | 4003.37 | 3979.83 | 3956.58 | 3933.62 |
| 20 | 30 | 4129.06 | 4104.02 | 4079.51 | 4055.35 | 4031.46 | 4007.81 | 3984.38 | 3961.14 | 3938.08 |
| 20 | 35 | 4130.99 | 4107.12 | 4083.40 | 4059.78 | 4036.24 | 4012.76 | 3989.34 | 3965.98 | 3942.67 |
| 20 | 40 | 4133.13 | 4110.71 | 4087.97 | 4065.02 | 4041.90 | 4018.63 | 3995.23 | 3971.72 | 3948.09 |
| 40 | 0 | 4056.52 | 4029.87 | 4003.38 | 3976.99 | 3950.68 | 3924.45 | 3898.28 | 3872.16 | 3846.10 |
| 40 | 5 | 4062.15 | 4035.78 | 4010.03 | 3984.69 | 3959.68 | 3934.96 | 3910.48 | 3886.24 | 3862.21 |
| 40 | 10 | 4067.29 | 4041.19 | 4016.02 | 3991.44 | 3967.35 | 3943.68 | 3920.38 | 3897.42 | 3874.78 |
| 40 | 15 | 4072.09 | 4046.35 | 4021.64 | 3997.62 | 3974.14 | 3951.13 | 3928.54 | 3906.34 | 3884.50 |
| 40 | 20 | 4076.61 | 4051.40 | 4027.17 | 4003.56 | 3980.46 | 3957.80 | 3935.53 | 3913.62 | 3892.04 |
| 40 | 25 | 4080.89 | 4056.50 | 4032.81 | 4009.58 | 3986.71 | 3964.15 | 3941.88 | 3919.86 | 3898.08 |
| 40 | 30 | 4084.93 | 4061.76 | 4038.81 | 4015.99 | 3993.28 | 3970.67 | 3948.15 | 3925.70 | 3903.33 |
| 40 | 35 | 4088.75 | 4067.30 | 4045.37 | 4023.12 | 4000.61 | 3977.88 | 3954.95 | 3931.83 | 3908.55 |
| 40 | 40 | 4092.36 | 4073.28 | 4052.77 | 4031.34 | 4009.16 | 3986.33 | 3962.92 | 3938.99 | 3914.57 |
| 100 | 0 | 3905.04 | 3890.81 | 3874.14 | 3855.87 | 3836.32 | 3815.65 | 3793.99 | 3771.43 | 3748.02 |
| 100 | 5 | 3926.12 | 3908.86 | 3890.72 | 3872.01 | 3852.85 | 3833.28 | 3813.35 | 3793.10 | 3772.56 |
| 100 | 10 | 3942.68 | 3923.08 | 3903.71 | 3884.48 | 3865.37 | 3846.36 | 3827.44 | 3808.60 | 3789.84 |
| 100 | 15 | 3956.09 | 3934.99 | 3914.71 | 3894.97 | 3875.67 | 3856.74 | 3838.14 | 3819.85 | 3801.84 |
| 100 | 20 | 3967.22 | 3945.60 | 3924.87 | 3904.72 | 3885.05 | 3865.78 | 3846.88 | 3828.31 | 3810.05 |
| 100 | 25 | 3976.60 | 3955.56 | 3934.94 | 3914.60 | 3894.47 | 3874.53 | 3854.76 | 3835.14 | 3815.67 |
| 100 | 30 | 3984.51 | 3965.34 | 3945.52 | 3925.29 | 3904.71 | 3883.84 | 3862.70 | 3841.33 | 3819.73 |
| 100 | 35 | 3991.22 | 3975.35 | 3957.16 | 3937.46 | 3916.53 | 3894.55 | 3871.63 | 3847.85 | 3823.27 |
| 100 | 40 | 3997.14 | 3986.17 | 3970.57 | 3951.95 | 3930.89 | 3907.72 | 3882.68 | 3855.91 | 3827.56 |

Table 18

Sound speed, $U(S, t, p)$, in m/s, Eq. (9)

| MPa | °C | $S = 0$ | $S = 5$ | $S = 10$ | $S = 15$ | $S = 20$ | $S = 25$ | $S = 30$ | $S = 35$ | $S = 40$ |
|-----|----|---------|---------|----------|----------|----------|----------|----------|----------|----------|
| 0 | 0 | 1402.40 | 1409.23 | 1415.88 | 1422.48 | 1429.08 | 1435.70 | 1442.34 | 1449.02 | 1455.76 |
| 0 | 5 | 1426.18 | 1432.71 | 1439.07 | 1445.38 | 1451.67 | 1457.97 | 1464.29 | 1470.65 | 1477.04 |
| 0 | 10 | 1447.28 | 1453.50 | 1459.58 | 1465.61 | 1471.63 | 1477.66 | 1483.71 | 1489.79 | 1495.91 |
| 0 | 15 | 1465.94 | 1471.87 | 1477.69 | 1483.47 | 1489.24 | 1495.03 | 1500.83 | 1506.67 | 1512.55 |
| 0 | 20 | 1482.35 | 1488.03 | 1493.61 | 1499.17 | 1504.72 | 1510.28 | 1515.87 | 1521.48 | 1527.13 |
| 0 | 25 | 1496.71 | 1502.17 | 1507.54 | 1512.89 | 1518.24 | 1523.59 | 1528.96 | 1534.36 | 1539.78 |
| 0 | 30 | 1509.16 | 1514.43 | 1519.61 | 1524.78 | 1529.94 | 1535.10 | 1540.28 | 1545.47 | 1550.70 |
| 0 | 35 | 1519.85 | 1524.93 | 1529.95 | 1534.95 | 1539.96 | 1544.97 | 1550.00 | 1555.05 | 1560.12 |
| 0 | 40 | 1528.91 | 1533.80 | 1538.67 | 1543.56 | 1548.46 | 1553.39 | 1558.36 | 1563.37 | 1568.42 |
| 10 | 0 | 1418.50 | 1425.27 | 1431.94 | 1438.60 | 1445.25 | 1451.90 | 1458.57 | 1465.24 | 1471.93 |
| 10 | 5 | 1442.33 | 1448.79 | 1455.17 | 1461.53 | 1467.88 | 1474.23 | 1480.58 | 1486.94 | 1493.30 |
| 10 | 10 | 1463.53 | 1469.67 | 1475.76 | 1481.83 | 1487.91 | 1493.98 | 1500.06 | 1506.14 | 1512.22 |
| 10 | 15 | 1482.32 | 1488.15 | 1493.97 | 1499.78 | 1505.59 | 1511.41 | 1517.24 | 1523.06 | 1528.89 |
| 10 | 20 | 1498.90 | 1504.45 | 1510.02 | 1515.58 | 1521.16 | 1526.73 | 1532.31 | 1537.89 | 1543.47 |
| 10 | 25 | 1513.44 | 1518.75 | 1524.08 | 1529.42 | 1534.76 | 1540.11 | 1545.46 | 1550.80 | 1556.13 |
| 10 | 30 | 1526.09 | 1531.17 | 1536.29 | 1541.42 | 1546.56 | 1551.70 | 1556.83 | 1561.96 | 1567.07 |
| 10 | 35 | 1536.99 | 1541.85 | 1546.77 | 1551.72 | 1556.69 | 1561.66 | 1566.63 | 1571.60 | 1576.56 |
| 10 | 40 | 1546.27 | 1550.90 | 1555.65 | 1560.46 | 1565.31 | 1570.19 | 1575.10 | 1580.03 | 1584.97 |
| 20 | 0 | 1434.92 | 1441.62 | 1448.33 | 1455.03 | 1461.74 | 1468.45 | 1475.14 | 1481.81 | 1488.45 |
| 20 | 5 | 1458.71 | 1465.09 | 1471.50 | 1477.91 | 1484.32 | 1490.72 | 1497.10 | 1503.46 | 1509.79 |
| 20 | 10 | 1479.93 | 1485.98 | 1492.08 | 1498.20 | 1504.33 | 1510.45 | 1516.55 | 1522.63 | 1528.67 |
| 20 | 15 | 1498.79 | 1504.51 | 1510.33 | 1516.17 | 1522.03 | 1527.88 | 1533.72 | 1539.52 | 1545.29 |
| 20 | 20 | 1515.47 | 1520.90 | 1526.44 | 1532.03 | 1537.63 | 1543.22 | 1548.80 | 1554.34 | 1559.84 |
| 20 | 25 | 1530.14 | 1535.30 | 1540.60 | 1545.94 | 1551.29 | 1556.64 | 1561.97 | 1567.26 | 1572.50 |
| 20 | 30 | 1542.95 | 1547.85 | 1552.92 | 1558.04 | 1563.17 | 1568.30 | 1573.40 | 1578.47 | 1583.48 |
| 20 | 35 | 1554.02 | 1558.68 | 1563.53 | 1568.45 | 1573.41 | 1578.36 | 1583.31 | 1588.22 | 1593.09 |
| 20 | 40 | 1563.49 | 1567.88 | 1572.54 | 1577.32 | 1582.16 | 1587.03 | 1591.92 | 1596.81 | 1601.67 |
| 40 | 0 | 1468.66 | 1475.21 | 1481.97 | 1488.80 | 1495.64 | 1502.46 | 1509.21 | 1515.88 | 1522.44 |
| 40 | 5 | 1492.11 | 1498.32 | 1504.77 | 1511.30 | 1517.85 | 1524.35 | 1530.80 | 1537.15 | 1543.39 |
| 40 | 10 | 1513.17 | 1519.01 | 1525.15 | 1531.37 | 1537.61 | 1543.82 | 1549.96 | 1556.00 | 1561.92 |
| 40 | 15 | 1531.99 | 1537.48 | 1543.30 | 1549.22 | 1555.17 | 1561.08 | 1566.92 | 1572.66 | 1578.27 |
| 40 | 20 | 1548.72 | 1553.89 | 1559.41 | 1565.05 | 1570.71 | 1576.34 | 1581.89 | 1587.34 | 1592.65 |
| 40 | 25 | 1563.51 | 1568.37 | 1573.62 | 1579.00 | 1584.40 | 1589.78 | 1595.07 | 1600.25 | 1605.29 |
| 40 | 30 | 1576.48 | 1581.06 | 1586.07 | 1591.21 | 1596.40 | 1601.56 | 1606.64 | 1611.61 | 1616.44 |
| 40 | 35 | 1587.77 | 1592.07 | 1596.85 | 1601.81 | 1606.83 | 1611.85 | 1616.81 | 1621.67 | 1626.41 |
| 40 | 40 | 1597.50 | 1601.49 | 1606.08 | 1610.91 | 1615.85 | 1620.82 | 1625.79 | 1630.70 | 1635.52 |
| 100 | 0 | 1575.62 | 1581.32 | 1588.09 | 1595.16 | 1602.26 | 1609.22 | 1615.89 | 1622.18 | 1627.98 |
| 100 | 5 | 1596.65 | 1602.03 | 1608.50 | 1615.26 | 1622.04 | 1628.65 | 1634.96 | 1640.84 | 1646.22 |
| 100 | 10 | 1615.89 | 1620.90 | 1627.03 | 1633.46 | 1639.89 | 1646.13 | 1652.04 | 1657.51 | 1662.43 |
| 100 | 15 | 1633.37 | 1638.01 | 1643.81 | 1649.92 | 1656.03 | 1661.93 | 1667.48 | 1672.57 | 1677.10 |
| 100 | 20 | 1649.12 | 1653.44 | 1658.97 | 1664.82 | 1670.66 | 1676.30 | 1681.58 | 1686.39 | 1690.62 |
| 100 | 25 | 1663.24 | 1667.27 | 1672.58 | 1678.24 | 1683.92 | 1689.40 | 1694.52 | 1699.18 | 1703.26 |
| 100 | 30 | 1675.80 | 1679.55 | 1684.69 | 1690.24 | 1695.84 | 1701.28 | 1706.40 | 1711.07 | 1715.18 |
| 100 | 35 | 1686.89 | 1690.33 | 1695.30 | 1700.78 | 1706.39 | 1711.91 | 1717.17 | 1722.03 | 1726.39 |
| 100 | 40 | 1696.61 | 1699.58 | 1704.33 | 1709.74 | 1715.42 | 1721.10 | 1726.64 | 1731.88 | 1736.72 |

Table 19

Potential temperature, $\theta(S, t, p, 0)$, in °C, Eq. (16)

| MPa | °C | $S = 0$ | $S = 5$ | $S = 10$ | $S = 15$ | $S = 20$ | $S = 25$ | $S = 30$ | $S = 35$ | $S = 40$ |
|-----|----|---------|---------|----------|----------|----------|----------|----------|----------|----------|
| 0 | 0 | 0.0000 | 0.0000 | 0.0000 | 0.0000 | 0.0000 | 0.0000 | 0.0000 | 0.0000 | 0.0000 |
| 0 | 5 | 5.0000 | 5.0000 | 5.0000 | 5.0000 | 5.0000 | 5.0000 | 5.0000 | 5.0000 | 5.0000 |
| 0 | 10 | 10.0000 | 10.0000 | 10.0000 | 10.0000 | 10.0000 | 10.0000 | 10.0000 | 10.0000 | 10.0000 |
| 0 | 15 | 15.0000 | 15.0000 | 15.0000 | 15.0000 | 15.0000 | 15.0000 | 15.0000 | 15.0000 | 15.0000 |
| 0 | 20 | 20.0000 | 20.0000 | 20.0000 | 20.0000 | 20.0000 | 20.0000 | 20.0000 | 20.0000 | 20.0000 |
| 0 | 25 | 25.0000 | 25.0000 | 25.0000 | 25.0000 | 25.0000 | 25.0000 | 25.0000 | 25.0000 | 25.0000 |
| 0 | 30 | 30.0000 | 30.0000 | 30.0000 | 30.0000 | 30.0000 | 30.0000 | 30.0000 | 30.0000 | 30.0000 |
| 0 | 35 | 35.0000 | 35.0000 | 35.0000 | 35.0000 | 35.0000 | 35.0000 | 35.0000 | 35.0000 | 35.0000 |
| 0 | 40 | 40.0000 | 40.0000 | 40.0000 | 40.0000 | 40.0000 | 40.0000 | 40.0000 | 40.0000 | 40.0000 |
| 10 | 0 | 0.0316 | 0.0190 | 0.0072 | −0.0040 | −0.0147 | −0.0250 | −0.0349 | −0.0444 | −0.0536 |
| 10 | 5 | 4.9796 | 4.9693 | 4.9596 | 4.9503 | 4.9413 | 4.9325 | 4.9239 | 4.9156 | 4.9076 |
| 10 | 10 | 9.9328 | 9.9244 | 9.9164 | 9.9086 | 9.9010 | 9.8935 | 9.8863 | 9.8792 | 9.8722 |
| 10 | 15 | 14.8900 | 14.8830 | 14.8763 | 14.8697 | 14.8633 | 14.8571 | 14.8509 | 14.8450 | 14.8391 |
| 10 | 20 | 19.8501 | 19.8442 | 19.8386 | 19.8330 | 19.8277 | 19.8224 | 19.8173 | 19.8123 | 19.8074 |
| 10 | 25 | 24.8125 | 24.8076 | 24.8029 | 24.7982 | 24.7937 | 24.7893 | 24.7850 | 24.7808 | 24.7767 |
| 10 | 30 | 29.7767 | 29.7728 | 29.7690 | 29.7651 | 29.7614 | 29.7576 | 29.7540 | 29.7504 | 29.7468 |
| 10 | 35 | 34.7422 | 34.7396 | 34.7368 | 34.7338 | 34.7308 | 34.7276 | 34.7244 | 34.7211 | 34.7177 |
| 10 | 40 | 39.7086 | 39.7079 | 39.7065 | 39.7045 | 39.7021 | 39.6994 | 39.6964 | 39.6931 | 39.6896 |
| 20 | 0 | 0.0399 | 0.0156 | −0.0071 | −0.0286 | −0.0492 | −0.0690 | −0.0880 | −0.1063 | −0.1240 |
| 20 | 5 | 4.9403 | 4.9207 | 4.9020 | 4.8840 | 4.8666 | 4.8497 | 4.8332 | 4.8172 | 4.8016 |
| 20 | 10 | 9.8505 | 9.8344 | 9.8189 | 9.8039 | 9.7892 | 9.7748 | 9.7608 | 9.7471 | 9.7336 |
| 20 | 15 | 14.7680 | 14.7546 | 14.7416 | 14.7290 | 14.7166 | 14.7045 | 14.6927 | 14.6811 | 14.6698 |
| 20 | 20 | 19.6911 | 19.6797 | 19.6688 | 19.6581 | 19.6477 | 19.6376 | 19.6277 | 19.6180 | 19.6086 |
| 20 | 25 | 24.6183 | 24.6089 | 24.5997 | 24.5907 | 24.5819 | 24.5734 | 24.5651 | 24.5570 | 24.5491 |
| 20 | 30 | 29.5488 | 29.5413 | 29.5339 | 29.5265 | 29.5191 | 29.5119 | 29.5048 | 29.4978 | 29.4910 |
| 20 | 35 | 34.4817 | 34.4768 | 34.4714 | 34.4656 | 34.4596 | 34.4534 | 34.4471 | 34.4407 | 34.4342 |
| 20 | 40 | 39.4165 | 39.4152 | 39.4123 | 39.4083 | 39.4036 | 39.3983 | 39.3924 | 39.3860 | 39.3791 |
| 40 | 0 | −0.0064 | −0.0517 | −0.0938 | −0.1338 | −0.1721 | −0.2088 | −0.2440 | −0.2779 | −0.3106 |
| 40 | 5 | 4.8107 | 4.7741 | 4.7394 | 4.7059 | 4.6735 | 4.6420 | 4.6113 | 4.5815 | 4.5524 |
| 40 | 10 | 9.6446 | 9.6147 | 9.5859 | 9.5579 | 9.5305 | 9.5037 | 9.4774 | 9.4518 | 9.4266 |
| 40 | 15 | 14.4912 | 14.4663 | 14.4421 | 14.4185 | 14.3955 | 14.3729 | 14.3508 | 14.3291 | 14.3079 |
| 40 | 20 | 19.3474 | 19.3263 | 19.3059 | 19.2860 | 19.2666 | 19.2476 | 19.2291 | 19.2111 | 19.1935 |
| 40 | 25 | 24.2109 | 24.1933 | 24.1761 | 24.1593 | 24.1430 | 24.1270 | 24.1115 | 24.0964 | 24.0817 |
| 40 | 30 | 29.0800 | 29.0661 | 29.0521 | 29.0382 | 29.0245 | 29.0109 | 28.9977 | 28.9846 | 28.9718 |
| 40 | 35 | 33.9534 | 33.9441 | 33.9338 | 33.9228 | 33.9115 | 33.8998 | 33.8879 | 33.8758 | 33.8635 |
| 40 | 40 | 38.8298 | 38.8273 | 38.8216 | 38.8140 | 38.8048 | 38.7944 | 38.7829 | 38.7704 | 38.7570 |
| 100 | 0 | −0.5423 | −0.6366 | −0.7238 | −0.8062 | −0.8846 | −0.9596 | −1.0312 | −1.0997 | −1.1653 |
| 100 | 5 | 4.0920 | 4.0173 | 3.9463 | 3.8778 | 3.8115 | 3.7470 | 3.6845 | 3.6237 | 3.5646 |
| 100 | 10 | 8.7560 | 8.6958 | 8.6374 | 8.5803 | 8.5244 | 8.4697 | 8.4161 | 8.3636 | 8.3123 |
| 100 | 15 | 13.4420 | 13.3922 | 13.3434 | 13.2956 | 13.2486 | 13.2026 | 13.1574 | 13.1131 | 13.0698 |
| 100 | 20 | 18.1445 | 18.1024 | 18.0611 | 18.0207 | 17.9812 | 17.9425 | 17.9047 | 17.8678 | 17.8318 |
| 100 | 25 | 22.8594 | 22.8238 | 22.7888 | 22.7545 | 22.7210 | 22.6882 | 22.6563 | 22.6252 | 22.5950 |
| 100 | 30 | 27.5834 | 27.5550 | 27.5260 | 27.4971 | 27.4684 | 27.4400 | 27.4120 | 27.3844 | 27.3574 |
| 100 | 35 | 32.3140 | 32.2952 | 32.2732 | 32.2496 | 32.2248 | 32.1990 | 32.1726 | 32.1456 | 32.1181 |
| 100 | 40 | 37.0492 | 37.0445 | 37.0317 | 37.0140 | 36.9924 | 36.9675 | 36.9399 | 36.9097 | 36.8772 |

Table 20

Potential density anomaly, $\gamma_{\theta}(S, t, p, 0)$, in kg/m³, Eq. (17)

| MPa | °C | $S = 0$ | $S = 5$ | $S = 10$ | $S = 15$ | $S = 20$ | $S = 25$ | $S = 30$ | $S = 35$ | $S = 40$ |
|-----|----|---------|---------|----------|----------|----------|----------|----------|----------|----------|
| 0 | 0 | −0.1569 | 3.9148 | 7.9557 | 11.9874 | 16.0161 | 20.0447 | 24.0749 | 28.1072 | 32.1419 |
| 0 | 5 | −0.0334 | 3.9478 | 7.9038 | 11.8542 | 15.8046 | 19.7576 | 23.7144 | 27.6756 | 31.6414 |
| 0 | 10 | −0.2975 | 3.6117 | 7.4989 | 11.3827 | 15.2684 | 19.1582 | 23.0533 | 26.9541 | 30.8608 |
| 0 | 15 | −0.8974 | 2.9534 | 6.7844 | 10.6133 | 14.4452 | 18.2824 | 22.1258 | 25.9760 | 29.8331 |
| 0 | 20 | −1.7929 | 2.0097 | 5.7939 | 9.5771 | 13.3643 | 17.1575 | 20.9580 | 24.7660 | 28.5816 |
| 0 | 25 | −2.9524 | 0.8100 | 4.5551 | 8.3001 | 12.0498 | 15.8064 | 19.5709 | 23.3436 | 27.1248 |
| 0 | 30 | −4.3505 | −0.6207 | 3.0921 | 6.8053 | 10.5236 | 14.2493 | 17.9833 | 21.7261 | 25.4778 |
| 0 | 35 | −5.9667 | −2.2610 | 1.4267 | 5.1142 | 8.8064 | 12.5058 | 16.2134 | 19.9298 | 23.6550 |
| 0 | 40 | −7.7836 | −4.0910 | −0.4202 | 3.2481 | 6.9193 | 10.5962 | 14.2800 | 17.9715 | 21.6708 |
| 10 | 0 | −0.1548 | 3.9157 | 7.9559 | 11.9873 | 16.0162 | 20.0453 | 24.0762 | 28.1096 | 32.1456 |
| 10 | 5 | −0.0330 | 3.9488 | 7.9057 | 11.8573 | 15.8091 | 19.7636 | 23.7222 | 27.6854 | 31.6533 |
| 10 | 10 | −0.2916 | 3.6192 | 7.5083 | 11.3942 | 15.2819 | 19.1739 | 23.0714 | 26.9747 | 30.8840 |
| 10 | 15 | −0.8809 | 2.9722 | 6.8055 | 10.6368 | 14.4712 | 18.3110 | 22.1571 | 26.0100 | 29.8697 |
| 10 | 20 | −1.7620 | 2.0431 | 5.8299 | 9.6157 | 13.4055 | 17.2015 | 21.0046 | 24.8154 | 28.6338 |
| 10 | 25 | −2.9044 | 0.8606 | 4.6084 | 8.3560 | 12.1084 | 15.8676 | 19.6348 | 23.4102 | 27.1940 |
| 10 | 30 | −4.2833 | −0.5510 | 3.1643 | 6.8801 | 10.6009 | 14.3292 | 18.0658 | 21.8112 | 25.5655 |
| 10 | 35 | −5.8783 | −2.1707 | 1.5191 | 5.2088 | 8.9034 | 12.6053 | 16.3154 | 20.0344 | 23.7624 |
| 10 | 40 | −7.6725 | −3.9792 | −0.3071 | 3.3628 | 7.0361 | 10.7153 | 14.4017 | 18.0960 | 21.7984 |
| 20 | 0 | −0.1542 | 3.9156 | 7.9555 | 11.9871 | 16.0164 | 20.0463 | 24.0783 | 28.1129 | 32.1504 |
| 20 | 5 | −0.0324 | 3.9503 | 7.9084 | 11.8613 | 15.8147 | 19.7710 | 23.7315 | 27.6967 | 31.6668 |
| 20 | 10 | −0.2845 | 3.6282 | 7.5192 | 11.4071 | 15.2970 | 19.1913 | 23.0912 | 26.9970 | 30.9089 |
| 20 | 15 | −0.8628 | 2.9926 | 6.8283 | 10.6621 | 14.4990 | 18.3413 | 22.1900 | 26.0456 | 29.9080 |
| 20 | 20 | −1.7296 | 2.0781 | 5.8674 | 9.6559 | 13.4483 | 17.2469 | 21.0528 | 24.8662 | 28.6872 |
| 20 | 25 | −2.8551 | 0.9125 | 4.6629 | 8.4131 | 12.1681 | 15.9300 | 19.6997 | 23.4778 | 27.2642 |
| 20 | 30 | −4.2151 | −0.4805 | 3.2374 | 6.9556 | 10.6790 | 14.4098 | 18.1489 | 21.8969 | 25.6537 |
| 20 | 35 | −5.7896 | −2.0801 | 1.6118 | 5.3037 | 9.0006 | 12.7049 | 16.4175 | 20.1391 | 23.8697 |
| 20 | 40 | −7.5617 | −3.8677 | −0.1943 | 3.4773 | 7.1526 | 10.8341 | 14.5231 | 18.2201 | 21.9255 |
| 40 | 0 | −0.1574 | 3.9124 | 7.9530 | 11.9858 | 16.0170 | 20.0493 | 24.0840 | 28.1218 | 32.1628 |
| 40 | 5 | −0.0306 | 3.9547 | 7.9157 | 11.8718 | 15.8288 | 19.7890 | 23.7537 | 27.7234 | 31.6981 |
| 40 | 10 | −0.2671 | 3.6496 | 7.5447 | 11.4370 | 15.3315 | 19.2305 | 23.1353 | 27.0463 | 30.9634 |
| 40 | 15 | −0.8222 | 3.0379 | 6.8783 | 10.7170 | 14.5589 | 18.4064 | 22.2603 | 26.1212 | 29.9891 |
| 40 | 20 | −1.6604 | 2.1524 | 5.9468 | 9.7404 | 13.5380 | 17.3418 | 21.1528 | 24.9715 | 28.7978 |
| 40 | 25 | −2.7529 | 1.0198 | 4.7753 | 8.5307 | 12.2907 | 16.0577 | 19.8325 | 23.6156 | 27.4070 |
| 40 | 30 | −4.0764 | −0.3370 | 3.3857 | 7.1087 | 10.8370 | 14.5727 | 18.3167 | 22.0696 | 25.8313 |
| 40 | 35 | −5.6113 | −1.8982 | 1.7978 | 5.4940 | 9.1955 | 12.9044 | 16.6219 | 20.3484 | 24.0840 |
| 40 | 40 | −7.3412 | −3.6457 | 0.0304 | 3.7054 | 7.3847 | 11.0707 | 14.7647 | 18.4671 | 22.1784 |
| 100 | 0 | −0.1963 | 3.8812 | 7.9308 | 11.9738 | 16.0161 | 20.0603 | 24.1078 | 28.1589 | 32.2137 |
| 100 | 5 | −0.0252 | 3.9722 | 7.9458 | 11.9152 | 15.8859 | 19.8605 | 23.8401 | 27.8250 | 31.8155 |
| 100 | 10 | −0.1986 | 3.7321 | 7.6416 | 11.5485 | 15.4580 | 19.3724 | 23.2929 | 27.2199 | 31.1533 |
| 100 | 15 | −0.6771 | 3.1978 | 7.0532 | 10.9070 | 14.7642 | 18.6272 | 22.4968 | 26.3736 | 30.2575 |
| 100 | 20 | −1.4282 | 2.3995 | 6.2088 | 10.0174 | 13.8301 | 17.6490 | 21.4752 | 25.3090 | 29.1505 |
| 100 | 25 | −2.4254 | 1.3620 | 5.1320 | 8.9019 | 12.6765 | 16.4579 | 20.2471 | 24.0446 | 27.8502 |
| 100 | 30 | −3.6464 | 0.1064 | 3.8426 | 7.5794 | 11.3215 | 15.0710 | 18.8289 | 22.5956 | 26.3711 |
| 100 | 35 | −5.0725 | −1.3489 | 2.3588 | 6.0674 | 9.7819 | 13.5043 | 17.2356 | 20.9762 | 24.7263 |
| 100 | 40 | −6.6879 | −2.9874 | 0.6970 | 4.3824 | 8.0736 | 11.7730 | 15.4817 | 19.2000 | 22.9282 |

Table 21

Potential enthalpy, $h_\theta(S, t, p, 0)$, in kJ/kg, Eq. (18)

| MPa | °C | $S = 0$ | $S = 5$ | $S = 10$ | $S = 15$ | $S = 20$ | $S = 25$ | $S = 30$ | $S = 35$ | $S = 40$ |
|-----|----|---------|---------|----------|----------|----------|----------|----------|----------|----------|
| 0 | 0 | 0.061 | 0.119 | 0.155 | 0.168 | 0.158 | 0.127 | 0.074 | 0.000 | −0.096 |
| 0 | 5 | 21.120 | 20.999 | 20.865 | 20.714 | 20.546 | 20.359 | 20.156 | 19.934 | 19.694 |
| 0 | 10 | 42.119 | 41.831 | 41.539 | 41.235 | 40.917 | 40.586 | 40.240 | 39.879 | 39.503 |
| 0 | 15 | 63.077 | 62.633 | 62.191 | 61.742 | 61.284 | 60.814 | 60.333 | 59.839 | 59.332 |
| 0 | 20 | 84.007 | 83.415 | 82.831 | 82.243 | 81.649 | 81.047 | 80.436 | 79.814 | 79.181 |
| 0 | 25 | 104.920 | 104.185 | 103.464 | 102.743 | 102.018 | 101.287 | 100.549 | 99.803 | 99.047 |
| 0 | 30 | 125.823 | 124.950 | 124.095 | 123.244 | 122.391 | 121.534 | 120.672 | 119.803 | 118.927 |
| 0 | 35 | 146.720 | 145.712 | 144.727 | 143.748 | 142.769 | 141.789 | 140.805 | 139.817 | 138.822 |
| 0 | 40 | 167.616 | 166.476 | 165.363 | 164.258 | 163.156 | 162.055 | 160.951 | 159.844 | 158.732 |
| 10 | 0 | 0.194 | 0.198 | 0.185 | 0.151 | 0.098 | 0.026 | −0.066 | −0.177 | −0.308 |
| 10 | 5 | 21.034 | 20.871 | 20.698 | 20.510 | 20.306 | 20.086 | 19.850 | 19.597 | 19.328 |
| 10 | 10 | 41.837 | 41.516 | 41.193 | 40.860 | 40.514 | 40.155 | 39.783 | 39.397 | 38.996 |
| 10 | 15 | 62.616 | 62.146 | 61.680 | 61.208 | 60.727 | 60.236 | 59.734 | 59.220 | 58.694 |
| 10 | 20 | 83.380 | 82.768 | 82.165 | 81.559 | 80.947 | 80.329 | 79.701 | 79.064 | 78.416 |
| 10 | 25 | 104.136 | 103.386 | 102.651 | 101.916 | 101.177 | 100.434 | 99.684 | 98.926 | 98.159 |
| 10 | 30 | 124.889 | 124.006 | 123.142 | 122.281 | 121.418 | 120.552 | 119.682 | 118.805 | 117.920 |
| 10 | 35 | 145.642 | 144.631 | 143.641 | 142.656 | 141.672 | 140.685 | 139.695 | 138.700 | 137.698 |
| 10 | 40 | 166.398 | 165.263 | 164.152 | 163.046 | 161.942 | 160.836 | 159.727 | 158.614 | 157.496 |
| 20 | 0 | 0.230 | 0.184 | 0.125 | 0.050 | −0.042 | −0.152 | −0.279 | −0.424 | −0.586 |
| 20 | 5 | 20.869 | 20.668 | 20.459 | 20.238 | 20.002 | 19.751 | 19.486 | 19.205 | 18.908 |
| 20 | 10 | 41.492 | 41.142 | 40.791 | 40.430 | 40.059 | 39.675 | 39.279 | 38.870 | 38.447 |
| 20 | 15 | 62.105 | 61.612 | 61.124 | 60.631 | 60.129 | 59.619 | 59.098 | 58.566 | 58.022 |
| 20 | 20 | 82.715 | 82.084 | 81.464 | 80.842 | 80.214 | 79.580 | 78.938 | 78.287 | 77.627 |
| 20 | 25 | 103.324 | 102.561 | 101.812 | 101.065 | 100.315 | 99.560 | 98.799 | 98.031 | 97.255 |
| 20 | 30 | 123.937 | 123.045 | 122.172 | 121.302 | 120.431 | 119.557 | 118.679 | 117.794 | 116.903 |
| 20 | 35 | 144.554 | 143.540 | 142.546 | 141.556 | 140.566 | 139.574 | 138.579 | 137.577 | 136.570 |
| 20 | 40 | 165.178 | 164.048 | 162.937 | 161.831 | 160.724 | 159.615 | 158.502 | 157.384 | 156.259 |
| 40 | 0 | 0.034 | −0.098 | −0.234 | −0.383 | −0.544 | −0.718 | −0.906 | −1.108 | −1.324 |
| 40 | 5 | 20.324 | 20.057 | 19.787 | 19.506 | 19.215 | 18.911 | 18.595 | 18.265 | 17.922 |
| 40 | 10 | 40.628 | 40.227 | 39.828 | 39.421 | 39.005 | 38.578 | 38.141 | 37.692 | 37.230 |
| 40 | 15 | 60.945 | 60.413 | 59.888 | 59.358 | 58.821 | 58.277 | 57.723 | 57.160 | 56.586 |
| 40 | 20 | 81.277 | 80.616 | 79.966 | 79.316 | 78.662 | 78.002 | 77.336 | 76.661 | 75.978 |
| 40 | 25 | 101.621 | 100.835 | 100.064 | 99.296 | 98.526 | 97.753 | 96.974 | 96.189 | 95.397 |
| 40 | 30 | 121.977 | 121.071 | 120.184 | 119.300 | 118.415 | 117.528 | 116.637 | 115.741 | 114.838 |
| 40 | 35 | 142.346 | 141.328 | 140.327 | 139.330 | 138.332 | 137.331 | 136.326 | 135.316 | 134.298 |
| 40 | 40 | 162.726 | 161.606 | 160.499 | 159.392 | 158.282 | 157.167 | 156.046 | 154.917 | 153.781 |
| 100 | 0 | −2.228 | −2.544 | −2.847 | −3.149 | −3.452 | −3.757 | −4.068 | −4.384 | −4.705 |
| 100 | 5 | 17.301 | 16.899 | 16.504 | 16.105 | 15.701 | 15.290 | 14.872 | 14.446 | 14.011 |
| 100 | 10 | 36.899 | 36.401 | 35.907 | 35.410 | 34.906 | 34.396 | 33.877 | 33.350 | 32.814 |
| 100 | 15 | 56.550 | 55.946 | 55.351 | 54.753 | 54.150 | 53.542 | 52.927 | 52.305 | 51.675 |
| 100 | 20 | 76.242 | 75.529 | 74.828 | 74.128 | 73.426 | 72.721 | 72.010 | 71.294 | 70.572 |
| 100 | 25 | 95.968 | 95.146 | 94.340 | 93.537 | 92.733 | 91.928 | 91.120 | 90.307 | 89.490 |
| 100 | 30 | 115.721 | 114.796 | 113.887 | 112.981 | 112.075 | 111.167 | 110.255 | 109.339 | 108.418 |
| 100 | 35 | 135.494 | 134.481 | 133.475 | 132.468 | 131.457 | 130.441 | 129.419 | 128.390 | 127.353 |
| 100 | 40 | 155.284 | 154.202 | 153.112 | 152.008 | 150.892 | 149.762 | 148.620 | 147.464 | 146.295 |

Table 22

Thermal expansion coefficient, $\alpha(S, t, p)$, in ppm/K, Eq. (6)

| MPa | °C | $S = 0$ | $S = 5$ | $S = 10$ | $S = 15$ | $S = 20$ | $S = 25$ | $S = 30$ | $S = 35$ | $S = 40$ |
|-----|----|---------|---------|----------|----------|----------|----------|----------|----------|----------|
| 0 | 0 | −67.74 | −47.17 | −28.23 | −10.37 | 6.59 | 22.76 | 38.21 | 52.99 | 67.13 |
| 0 | 5 | 16.03 | 31.98 | 46.95 | 61.27 | 75.03 | 88.29 | 101.09 | 113.47 | 125.43 |
| 0 | 10 | 87.94 | 100.45 | 112.36 | 123.85 | 134.97 | 145.76 | 156.23 | 166.41 | 176.30 |
| 0 | 15 | 150.84 | 160.80 | 170.35 | 179.59 | 188.56 | 197.27 | 205.74 | 213.97 | 221.97 |
| 0 | 20 | 206.80 | 214.80 | 222.48 | 229.91 | 237.12 | 244.11 | 250.89 | 257.46 | 263.83 |
| 0 | 25 | 257.29 | 263.60 | 269.70 | 275.63 | 281.38 | 286.95 | 292.36 | 297.60 | 302.66 |
| 0 | 30 | 303.38 | 307.98 | 312.58 | 317.15 | 321.65 | 326.07 | 330.41 | 334.66 | 338.81 |
| 0 | 35 | 345.89 | 348.44 | 351.41 | 354.62 | 357.99 | 361.47 | 365.04 | 368.68 | 372.38 |
| 0 | 40 | 385.48 | 385.32 | 386.32 | 388.03 | 390.28 | 392.99 | 396.08 | 399.52 | 403.27 |
| 10 | 0 | −30.53 | −11.59 | 5.85 | 22.27 | 37.87 | 52.71 | 66.89 | 80.43 | 93.37 |
| 10 | 5 | 45.64 | 60.31 | 74.12 | 87.32 | 100.02 | 112.27 | 124.10 | 135.54 | 146.59 |
| 10 | 10 | 111.49 | 122.99 | 133.99 | 144.61 | 154.91 | 164.91 | 174.63 | 184.08 | 193.27 |
| 10 | 15 | 169.45 | 178.62 | 187.45 | 196.00 | 204.32 | 212.40 | 220.27 | 227.93 | 235.37 |
| 10 | 20 | 221.29 | 228.67 | 235.78 | 242.67 | 249.35 | 255.83 | 262.12 | 268.22 | 274.13 |
| 10 | 25 | 268.27 | 274.11 | 279.77 | 285.26 | 290.58 | 295.75 | 300.75 | 305.58 | 310.25 |
| 10 | 30 | 311.33 | 315.59 | 319.87 | 324.10 | 328.28 | 332.37 | 336.38 | 340.30 | 344.13 |
| 10 | 35 | 351.17 | 353.54 | 356.31 | 359.31 | 362.46 | 365.72 | 369.05 | 372.45 | 375.89 |
| 10 | 40 | 388.39 | 388.23 | 389.20 | 390.85 | 393.03 | 395.64 | 398.62 | 401.94 | 405.55 |
| 20 | 0 | 4.24 | 21.72 | 37.80 | 52.94 | 67.29 | 80.95 | 93.96 | 106.38 | 118.23 |
| 20 | 5 | 73.54 | 87.04 | 99.76 | 111.95 | 123.68 | 135.00 | 145.93 | 156.49 | 166.71 |
| 20 | 10 | 133.84 | 144.40 | 154.54 | 164.35 | 173.87 | 183.13 | 192.14 | 200.91 | 209.44 |
| 20 | 15 | 187.24 | 195.65 | 203.78 | 211.68 | 219.38 | 226.86 | 234.16 | 241.26 | 248.16 |
| 20 | 20 | 235.24 | 242.01 | 248.56 | 254.92 | 261.09 | 267.08 | 272.89 | 278.52 | 283.98 |
| 20 | 25 | 278.93 | 284.30 | 289.51 | 294.57 | 299.48 | 304.23 | 308.83 | 313.28 | 317.56 |
| 20 | 30 | 319.13 | 323.05 | 326.99 | 330.89 | 334.74 | 338.51 | 342.20 | 345.79 | 349.29 |
| 20 | 35 | 356.45 | 358.61 | 361.18 | 363.96 | 366.88 | 369.91 | 373.01 | 376.17 | 379.37 |
| 20 | 40 | 391.42 | 391.23 | 392.14 | 393.71 | 395.80 | 398.31 | 401.18 | 404.37 | 407.85 |
| 40 | 0 | 66.96 | 81.93 | 95.68 | 108.59 | 120.79 | 132.37 | 143.38 | 153.84 | 163.78 |
| 40 | 5 | 124.44 | 135.88 | 146.70 | 157.07 | 167.07 | 176.71 | 186.03 | 195.03 | 203.73 |
| 40 | 10 | 175.05 | 183.91 | 192.48 | 200.81 | 208.91 | 216.81 | 224.51 | 232.01 | 239.31 |
| 40 | 15 | 220.35 | 227.36 | 234.20 | 240.88 | 247.40 | 253.76 | 259.97 | 266.01 | 271.91 |
| 40 | 20 | 261.45 | 267.08 | 272.56 | 277.91 | 283.11 | 288.16 | 293.06 | 297.82 | 302.42 |
| 40 | 25 | 299.18 | 303.63 | 307.98 | 312.22 | 316.33 | 320.31 | 324.16 | 327.87 | 331.44 |
| 40 | 30 | 334.15 | 337.38 | 340.67 | 343.94 | 347.16 | 350.33 | 353.42 | 356.42 | 359.34 |
| 40 | 35 | 366.85 | 368.58 | 370.72 | 373.07 | 375.58 | 378.18 | 380.87 | 383.61 | 386.39 |
| 40 | 40 | 397.69 | 397.35 | 398.11 | 399.51 | 401.43 | 403.75 | 406.43 | 409.43 | 412.71 |
| 100 | 0 | 208.29 | 218.42 | 227.49 | 235.81 | 243.50 | 250.61 | 257.20 | 263.29 | 268.90 |
| 100 | 5 | 242.47 | 249.54 | 256.18 | 262.48 | 268.48 | 274.21 | 279.66 | 284.86 | 289.80 |
| 100 | 10 | 272.93 | 277.94 | 282.85 | 287.64 | 292.31 | 296.84 | 301.25 | 305.51 | 309.64 |
| 100 | 15 | 300.65 | 304.34 | 308.07 | 311.76 | 315.39 | 318.95 | 322.44 | 325.83 | 329.12 |
| 100 | 20 | 326.28 | 329.13 | 332.05 | 334.96 | 337.83 | 340.65 | 343.39 | 346.06 | 348.65 |
| 100 | 25 | 350.30 | 352.52 | 354.85 | 357.20 | 359.53 | 361.83 | 364.08 | 366.27 | 368.38 |
| 100 | 30 | 373.07 | 374.59 | 376.38 | 378.30 | 380.28 | 382.30 | 384.34 | 386.38 | 388.40 |
| 100 | 35 | 394.84 | 395.35 | 396.49 | 398.01 | 399.79 | 401.78 | 403.95 | 406.26 | 408.69 |
| 100 | 40 | 415.81 | 414.71 | 414.94 | 415.99 | 417.67 | 419.89 | 422.57 | 425.66 | 429.12 |

Table 23

Isothermal compressibility $K(S, t, p)$ in ppm/MPa, Eq. (5)

| MPa | °C | $S = 0$ | $S = 5$ | $S = 10$ | $S = 15$ | $S = 20$ | $S = 25$ | $S = 30$ | $S = 35$ | $S = 40$ |
|-----|----|---------|---------|----------|----------|----------|----------|----------|----------|----------|
| 0 | 0 | 508.84 | 501.73 | 494.94 | 488.36 | 481.93 | 475.65 | 469.49 | 463.43 | 457.48 |
| 0 | 5 | 491.68 | 485.33 | 479.24 | 473.32 | 467.53 | 461.85 | 456.27 | 450.79 | 445.38 |
| 0 | 10 | 478.08 | 472.31 | 466.77 | 461.35 | 456.05 | 450.84 | 445.70 | 440.65 | 435.66 |
| 0 | 15 | 467.32 | 462.02 | 456.89 | 451.88 | 446.95 | 442.10 | 437.31 | 432.58 | 427.91 |
| 0 | 20 | 458.91 | 453.96 | 449.17 | 444.46 | 439.83 | 435.26 | 430.75 | 426.29 | 421.88 |
| 0 | 25 | 452.46 | 447.79 | 443.24 | 438.78 | 434.39 | 430.05 | 425.77 | 421.53 | 417.33 |
| 0 | 30 | 447.69 | 443.22 | 438.87 | 434.60 | 430.39 | 426.24 | 422.13 | 418.08 | 414.06 |
| 0 | 35 | 444.38 | 440.03 | 435.81 | 431.67 | 427.60 | 423.59 | 419.63 | 415.71 | 411.84 |
| 0 | 40 | 442.37 | 438.06 | 433.89 | 429.81 | 425.81 | 421.87 | 418.00 | 414.18 | 410.40 |
| 10 | 0 | 494.63 | 487.94 | 481.49 | 475.21 | 469.07 | 463.06 | 457.18 | 451.41 | 445.76 |
| 10 | 5 | 478.52 | 472.52 | 466.70 | 461.02 | 455.46 | 450.01 | 444.65 | 439.40 | 434.25 |
| 10 | 10 | 465.65 | 460.20 | 454.88 | 449.67 | 444.55 | 439.53 | 434.60 | 429.74 | 424.97 |
| 10 | 15 | 455.41 | 450.38 | 445.46 | 440.63 | 435.87 | 431.19 | 426.58 | 422.04 | 417.57 |
| 10 | 20 | 447.33 | 442.65 | 438.05 | 433.51 | 429.04 | 424.64 | 420.30 | 416.02 | 411.80 |
| 10 | 25 | 441.09 | 436.68 | 432.33 | 428.04 | 423.80 | 419.63 | 415.51 | 411.44 | 407.44 |
| 10 | 30 | 436.43 | 432.22 | 428.07 | 423.97 | 419.92 | 415.93 | 411.99 | 408.11 | 404.29 |
| 10 | 35 | 433.15 | 429.08 | 425.06 | 421.10 | 417.19 | 413.34 | 409.55 | 405.81 | 402.13 |
| 10 | 40 | 431.09 | 427.08 | 423.13 | 419.24 | 415.41 | 411.64 | 407.94 | 404.29 | 400.71 |
| 20 | 0 | 480.97 | 474.67 | 468.52 | 462.51 | 456.63 | 450.88 | 445.26 | 439.75 | 434.37 |
| 20 | 5 | 465.86 | 460.19 | 454.62 | 449.16 | 443.81 | 438.56 | 433.42 | 428.39 | 423.47 |
| 20 | 10 | 453.70 | 448.53 | 443.43 | 438.41 | 433.47 | 428.63 | 423.88 | 419.22 | 414.66 |
| 20 | 15 | 443.95 | 439.19 | 434.46 | 429.80 | 425.20 | 420.68 | 416.24 | 411.89 | 407.62 |
| 20 | 20 | 436.22 | 431.79 | 427.37 | 422.99 | 418.67 | 414.42 | 410.24 | 406.13 | 402.10 |
| 20 | 25 | 430.19 | 426.03 | 421.86 | 417.72 | 413.63 | 409.60 | 405.63 | 401.74 | 397.91 |
| 20 | 30 | 425.66 | 421.70 | 417.72 | 413.77 | 409.87 | 406.02 | 402.23 | 398.51 | 394.86 |
| 20 | 35 | 422.43 | 418.61 | 414.77 | 410.96 | 407.19 | 403.48 | 399.83 | 396.25 | 392.73 |
| 20 | 40 | 420.35 | 416.60 | 412.83 | 409.10 | 405.41 | 401.78 | 398.22 | 394.72 | 391.31 |
| 40 | 0 | 455.14 | 449.55 | 443.95 | 438.42 | 433.00 | 427.69 | 422.52 | 417.50 | 412.62 |
| 40 | 5 | 441.91 | 436.84 | 431.72 | 426.65 | 421.67 | 416.80 | 412.05 | 407.43 | 402.94 |
| 40 | 10 | 431.11 | 426.46 | 421.75 | 417.07 | 412.46 | 407.94 | 403.53 | 399.24 | 395.08 |
| 40 | 15 | 422.33 | 418.05 | 413.67 | 409.31 | 405.01 | 400.79 | 396.66 | 392.65 | 388.76 |
| 40 | 20 | 415.28 | 411.30 | 407.21 | 403.11 | 399.07 | 395.09 | 391.21 | 387.42 | 383.76 |
| 40 | 25 | 409.73 | 406.00 | 402.13 | 398.26 | 394.42 | 390.65 | 386.96 | 383.37 | 379.89 |
| 40 | 30 | 405.48 | 401.95 | 398.26 | 394.56 | 390.89 | 387.28 | 383.75 | 380.32 | 376.99 |
| 40 | 35 | 402.39 | 398.99 | 395.44 | 391.87 | 388.32 | 384.83 | 381.41 | 378.09 | 374.87 |
| 40 | 40 | 400.33 | 397.01 | 393.53 | 390.02 | 386.55 | 383.12 | 379.77 | 376.51 | 373.36 |
| 100 | 0 | 388.25 | 384.41 | 380.13 | 375.78 | 371.47 | 367.29 | 363.30 | 359.52 | 356.00 |
| 100 | 5 | 379.67 | 376.09 | 372.08 | 367.99 | 363.96 | 360.05 | 356.34 | 352.85 | 349.61 |
| 100 | 10 | 372.39 | 369.06 | 365.30 | 361.46 | 357.68 | 354.04 | 350.57 | 347.34 | 344.36 |
| 100 | 15 | 366.29 | 363.19 | 359.65 | 356.03 | 352.47 | 349.04 | 345.79 | 342.77 | 340.00 |
| 100 | 20 | 361.24 | 358.34 | 354.99 | 351.55 | 348.16 | 344.90 | 341.82 | 338.96 | 336.34 |
| 100 | 25 | 357.15 | 354.42 | 351.21 | 347.91 | 344.65 | 341.51 | 338.54 | 335.78 | 333.27 |
| 100 | 30 | 353.92 | 351.33 | 348.23 | 345.03 | 341.85 | 338.78 | 335.87 | 333.16 | 330.69 |
| 100 | 35 | 351.49 | 349.00 | 345.99 | 342.85 | 339.71 | 336.68 | 333.79 | 331.09 | 328.61 |
| 100 | 40 | 349.77 | 347.38 | 344.44 | 341.34 | 338.23 | 335.19 | 332.30 | 329.57 | 327.06 |

Table 24

Adiabatic compressibility, $\kappa(S, t, p)$, in ppm/MPa, Eq. (9)

| MPa | °C | $S = 0$ | $S = 5$ | $S = 10$ | $S = 15$ | $S = 20$ | $S = 25$ | $S = 30$ | $S = 35$ | $S = 40$ |
|-----|----|---------|---------|----------|----------|----------|----------|----------|----------|----------|
| 0 | 0 | 508.54 | 501.58 | 494.89 | 488.35 | 481.93 | 475.62 | 469.39 | 463.24 | 457.18 |
| 0 | 5 | 491.66 | 485.26 | 479.09 | 473.06 | 467.15 | 461.32 | 455.58 | 449.91 | 444.31 |
| 0 | 10 | 477.55 | 471.63 | 465.91 | 460.31 | 454.80 | 449.38 | 444.02 | 438.73 | 433.50 |
| 0 | 15 | 465.76 | 460.23 | 454.88 | 449.63 | 444.47 | 439.37 | 434.34 | 429.36 | 424.44 |
| 0 | 20 | 455.91 | 450.72 | 445.67 | 440.72 | 435.84 | 431.02 | 426.26 | 421.54 | 416.88 |
| 0 | 25 | 447.72 | 442.80 | 438.01 | 433.31 | 428.67 | 424.08 | 419.56 | 415.07 | 410.64 |
| 0 | 30 | 440.98 | 436.29 | 431.71 | 427.21 | 422.77 | 418.39 | 414.06 | 409.77 | 405.53 |
| 0 | 35 | 435.51 | 431.00 | 426.60 | 422.27 | 418.00 | 413.77 | 409.59 | 405.46 | 401.36 |
| 0 | 40 | 431.15 | 426.82 | 422.56 | 418.36 | 414.19 | 410.07 | 405.98 | 401.92 | 397.89 |
| 10 | 0 | 494.57 | 487.93 | 481.49 | 475.17 | 468.97 | 462.88 | 456.88 | 450.98 | 445.17 |
| 10 | 5 | 478.39 | 472.28 | 466.34 | 460.51 | 454.78 | 449.15 | 443.61 | 438.15 | 432.78 |
| 10 | 10 | 464.81 | 459.17 | 453.65 | 448.24 | 442.91 | 437.66 | 432.49 | 427.40 | 422.38 |
| 10 | 15 | 453.42 | 448.17 | 443.02 | 437.95 | 432.95 | 428.03 | 423.17 | 418.38 | 413.66 |
| 10 | 20 | 443.88 | 438.96 | 434.11 | 429.33 | 424.62 | 419.97 | 415.38 | 410.86 | 406.40 |
| 10 | 25 | 435.93 | 431.28 | 426.69 | 422.16 | 417.69 | 413.28 | 408.92 | 404.63 | 400.40 |
| 10 | 30 | 429.35 | 424.93 | 420.56 | 416.24 | 411.98 | 407.77 | 403.61 | 399.52 | 395.48 |
| 10 | 35 | 423.99 | 419.77 | 415.58 | 411.44 | 407.34 | 403.29 | 399.28 | 395.33 | 391.43 |
| 10 | 40 | 419.69 | 415.66 | 411.62 | 407.61 | 403.62 | 399.67 | 395.76 | 391.89 | 388.05 |
| 20 | 0 | 480.97 | 474.64 | 468.43 | 462.33 | 456.33 | 450.45 | 444.66 | 438.99 | 433.43 |
| 20 | 5 | 465.50 | 459.68 | 453.95 | 448.31 | 442.77 | 437.32 | 431.97 | 426.72 | 421.57 |
| 20 | 10 | 452.48 | 447.11 | 441.79 | 436.55 | 431.39 | 426.31 | 421.32 | 416.42 | 411.61 |
| 20 | 15 | 441.52 | 436.53 | 431.57 | 426.67 | 421.83 | 417.07 | 412.38 | 407.78 | 403.26 |
| 20 | 20 | 432.31 | 427.64 | 422.98 | 418.37 | 413.81 | 409.32 | 404.90 | 400.56 | 396.30 |
| 20 | 25 | 424.61 | 420.21 | 415.81 | 411.44 | 407.12 | 402.87 | 398.68 | 394.57 | 390.53 |
| 20 | 30 | 418.22 | 414.05 | 409.87 | 405.71 | 401.60 | 397.54 | 393.55 | 389.63 | 385.78 |
| 20 | 35 | 412.98 | 409.02 | 405.02 | 401.04 | 397.09 | 393.19 | 389.34 | 385.55 | 381.83 |
| 20 | 40 | 408.75 | 404.99 | 401.15 | 397.29 | 393.46 | 389.65 | 385.88 | 382.16 | 378.49 |
| 40 | 0 | 454.84 | 449.10 | 443.34 | 437.63 | 432.02 | 426.52 | 421.14 | 415.90 | 410.80 |
| 40 | 5 | 440.87 | 435.59 | 430.26 | 424.98 | 419.78 | 414.68 | 409.69 | 404.82 | 400.09 |
| 40 | 10 | 429.01 | 424.14 | 419.20 | 414.29 | 409.44 | 404.68 | 400.03 | 395.50 | 391.09 |
| 40 | 15 | 418.95 | 414.44 | 409.84 | 405.24 | 400.71 | 396.25 | 391.89 | 387.65 | 383.52 |
| 40 | 20 | 410.44 | 406.24 | 401.92 | 397.61 | 393.34 | 389.14 | 385.04 | 381.05 | 377.17 |
| 40 | 25 | 403.28 | 399.34 | 395.27 | 391.19 | 387.15 | 383.18 | 379.29 | 375.51 | 371.84 |
| 40 | 30 | 397.30 | 393.59 | 389.72 | 385.84 | 381.98 | 378.19 | 374.48 | 370.87 | 367.36 |
| 40 | 35 | 392.36 | 388.85 | 385.16 | 381.43 | 377.72 | 374.06 | 370.47 | 366.96 | 363.55 |
| 40 | 40 | 388.33 | 385.02 | 381.48 | 377.87 | 374.25 | 370.65 | 367.11 | 363.63 | 360.23 |
| 100 | 0 | 385.35 | 381.22 | 376.67 | 372.05 | 367.49 | 363.07 | 358.84 | 354.84 | 351.10 |
| 100 | 5 | 375.68 | 371.86 | 367.61 | 363.30 | 359.04 | 354.92 | 350.99 | 347.28 | 343.84 |
| 100 | 10 | 367.26 | 363.74 | 359.77 | 355.74 | 351.76 | 347.92 | 344.27 | 340.84 | 337.67 |
| 100 | 15 | 359.96 | 356.70 | 352.98 | 349.20 | 345.46 | 341.86 | 338.45 | 335.26 | 332.32 |
| 100 | 20 | 353.67 | 350.62 | 347.12 | 343.53 | 339.99 | 336.58 | 333.35 | 330.34 | 327.59 |
| 100 | 25 | 348.28 | 345.42 | 342.08 | 338.64 | 335.24 | 331.96 | 328.86 | 325.96 | 323.32 |
| 100 | 30 | 343.70 | 341.01 | 337.80 | 334.47 | 331.16 | 327.95 | 324.90 | 322.06 | 319.44 |
| 100 | 35 | 339.85 | 337.32 | 334.23 | 330.98 | 327.71 | 324.53 | 321.47 | 318.60 | 315.94 |
| 100 | 40 | 336.65 | 334.34 | 331.37 | 328.18 | 324.94 | 321.73 | 318.62 | 315.64 | 312.85 |

Table 25

Isothermal haline contraction coefficient, $\beta(S, t, p)$, in ppm, Eq. (8)

| MPa | °C | $S = 0$ | $S = 5$ | $S = 10$ | $S = 15$ | $S = 20$ | $S = 25$ | $S = 30$ | $S = 35$ | $S = 40$ |
|-----|----|---------|---------|----------|----------|----------|----------|----------|----------|----------|
| 0 | 0 | 827.49 | 806.75 | 800.58 | 796.35 | 792.97 | 790.01 | 787.28 | 784.65 | 782.06 |
| 0 | 5 | 807.85 | 789.37 | 784.16 | 780.71 | 777.99 | 775.63 | 773.45 | 771.35 | 769.26 |
| 0 | 10 | 792.85 | 775.68 | 771.07 | 768.09 | 765.80 | 763.83 | 762.02 | 760.27 | 758.51 |
| 0 | 15 | 781.15 | 764.79 | 760.58 | 757.94 | 755.94 | 754.25 | 752.71 | 751.21 | 749.71 |
| 0 | 20 | 771.85 | 756.06 | 752.14 | 749.76 | 748.00 | 746.54 | 745.22 | 743.94 | 742.66 |
| 0 | 25 | 764.48 | 749.06 | 745.37 | 743.20 | 741.64 | 740.38 | 739.25 | 738.16 | 737.06 |
| 0 | 30 | 758.97 | 743.64 | 740.08 | 738.03 | 736.60 | 735.46 | 734.47 | 733.52 | 732.56 |
| 0 | 35 | 755.71 | 739.90 | 736.22 | 734.11 | 732.66 | 731.53 | 730.54 | 729.62 | 728.70 |
| 0 | 40 | 755.48 | 738.16 | 733.94 | 731.45 | 729.70 | 728.32 | 727.13 | 726.03 | 724.94 |
| 10 | 0 | 813.03 | 793.30 | 787.54 | 783.65 | 780.55 | 777.85 | 775.35 | 772.94 | 770.55 |
| 10 | 5 | 794.98 | 777.28 | 772.42 | 769.24 | 766.75 | 764.60 | 762.62 | 760.70 | 758.79 |
| 10 | 10 | 781.23 | 764.67 | 760.34 | 757.58 | 755.48 | 753.68 | 752.03 | 750.43 | 748.83 |
| 10 | 15 | 770.52 | 754.63 | 750.64 | 748.17 | 746.33 | 744.79 | 743.38 | 742.01 | 740.64 |
| 10 | 20 | 762.00 | 746.56 | 742.83 | 740.59 | 738.97 | 737.63 | 736.43 | 735.26 | 734.08 |
| 10 | 25 | 755.22 | 740.09 | 736.56 | 734.52 | 733.08 | 731.92 | 730.90 | 729.91 | 728.91 |
| 10 | 30 | 750.13 | 735.07 | 731.65 | 729.72 | 728.40 | 727.38 | 726.48 | 725.63 | 724.77 |
| 10 | 35 | 747.12 | 731.59 | 728.05 | 726.08 | 724.74 | 723.72 | 722.84 | 722.02 | 721.20 |
| 10 | 40 | 746.95 | 729.96 | 725.90 | 723.56 | 721.95 | 720.69 | 719.61 | 718.62 | 717.65 |
| 20 | 0 | 799.67 | 780.53 | 775.11 | 771.51 | 768.67 | 766.22 | 763.96 | 761.79 | 759.64 |
| 20 | 5 | 783.05 | 765.77 | 761.17 | 758.21 | 755.95 | 754.01 | 752.24 | 750.53 | 748.81 |
| 20 | 10 | 770.46 | 754.16 | 750.01 | 747.44 | 745.52 | 743.91 | 742.43 | 741.01 | 739.58 |
| 20 | 15 | 760.69 | 744.92 | 741.06 | 738.75 | 737.06 | 735.66 | 734.41 | 733.20 | 731.98 |
| 20 | 20 | 752.91 | 737.49 | 733.86 | 731.74 | 730.25 | 729.04 | 727.97 | 726.94 | 725.91 |
| 20 | 25 | 746.71 | 731.54 | 728.08 | 726.14 | 724.81 | 723.78 | 722.87 | 722.02 | 721.15 |
| 20 | 30 | 742.06 | 726.91 | 723.56 | 721.72 | 720.51 | 719.59 | 718.82 | 718.09 | 717.36 |
| 20 | 35 | 739.32 | 723.70 | 720.24 | 718.35 | 717.13 | 716.22 | 715.46 | 714.77 | 714.08 |
| 20 | 40 | 739.26 | 722.20 | 718.23 | 716.00 | 714.49 | 713.36 | 712.41 | 711.56 | 710.72 |
| 40 | 0 | 776.00 | 756.88 | 751.85 | 748.69 | 746.34 | 744.39 | 742.65 | 741.02 | 739.41 |
| 40 | 5 | 761.87 | 744.30 | 739.96 | 737.37 | 735.51 | 734.01 | 732.70 | 731.48 | 730.27 |
| 40 | 10 | 751.34 | 734.47 | 730.49 | 728.20 | 726.62 | 725.39 | 724.33 | 723.35 | 722.38 |
| 40 | 15 | 743.27 | 726.71 | 722.93 | 720.82 | 719.42 | 718.36 | 717.48 | 716.67 | 715.88 |
| 40 | 20 | 736.88 | 720.49 | 716.86 | 714.91 | 713.66 | 712.75 | 712.02 | 711.36 | 710.72 |
| 40 | 25 | 731.80 | 715.52 | 712.02 | 710.20 | 709.09 | 708.32 | 707.74 | 707.23 | 706.74 |
| 40 | 30 | 728.00 | 711.67 | 708.23 | 706.50 | 705.48 | 704.83 | 704.35 | 703.96 | 703.60 |
| 40 | 35 | 725.85 | 709.01 | 705.45 | 703.66 | 702.62 | 701.97 | 701.51 | 701.15 | 700.81 |
| 40 | 40 | 726.08 | 707.81 | 703.75 | 701.61 | 700.30 | 699.42 | 698.77 | 698.24 | 697.77 |
| 100 | 0 | 726.57 | 698.47 | 692.58 | 689.92 | 688.77 | 688.48 | 688.74 | 689.37 | 690.24 |
| 100 | 5 | 717.28 | 690.38 | 685.08 | 682.89 | 682.16 | 682.27 | 682.91 | 683.90 | 685.12 |
| 100 | 10 | 711.11 | 684.55 | 679.46 | 677.48 | 676.96 | 677.26 | 678.09 | 679.26 | 680.67 |
| 100 | 15 | 706.88 | 680.25 | 675.22 | 673.31 | 672.88 | 673.28 | 674.21 | 675.50 | 677.02 |
| 100 | 20 | 703.80 | 676.95 | 671.92 | 670.06 | 669.67 | 670.14 | 671.15 | 672.52 | 674.14 |
| 100 | 25 | 701.47 | 674.36 | 669.30 | 667.45 | 667.11 | 667.64 | 668.71 | 670.16 | 671.86 |
| 100 | 30 | 699.91 | 672.35 | 667.20 | 665.31 | 664.97 | 665.51 | 666.61 | 668.10 | 669.85 |
| 100 | 35 | 699.49 | 671.02 | 665.58 | 663.51 | 663.03 | 663.47 | 664.50 | 665.94 | 667.65 |
| 100 | 40 | 701.00 | 670.66 | 664.55 | 661.99 | 661.12 | 661.23 | 661.98 | 663.16 | 664.64 |

Table 26

Adiabatic haline contraction coefficient, β' (S , t , p), in ppm, Eq. (11)

| MPa | °C | $S = 0$ | $S = 5$ | $S = 10$ | $S = 15$ | $S = 20$ | $S = 25$ | $S = 30$ | $S = 35$ | $S = 40$ |
|-----|----|---------|---------|----------|----------|----------|----------|----------|----------|----------|
| 0 | 0 | 827.49 | 805.91 | 800.41 | 796.37 | 792.92 | 789.73 | 786.65 | 783.57 | 780.45 |
| 0 | 5 | 807.85 | 789.68 | 784.06 | 780.12 | 776.84 | 773.86 | 770.99 | 768.15 | 765.28 |
| 0 | 10 | 792.85 | 775.90 | 769.98 | 765.97 | 762.71 | 759.81 | 757.05 | 754.34 | 751.61 |
| 0 | 15 | 781.15 | 763.97 | 757.67 | 753.53 | 750.25 | 747.37 | 744.67 | 742.04 | 739.42 |
| 0 | 20 | 771.85 | 753.42 | 746.75 | 742.47 | 739.15 | 736.28 | 733.63 | 731.08 | 728.55 |
| 0 | 25 | 764.48 | 743.99 | 736.94 | 732.53 | 729.15 | 726.29 | 723.68 | 721.19 | 718.74 |
| 0 | 30 | 758.97 | 735.60 | 728.12 | 723.53 | 720.07 | 717.16 | 714.55 | 712.07 | 709.67 |
| 0 | 35 | 755.71 | 728.41 | 720.34 | 715.43 | 711.76 | 708.71 | 705.97 | 703.40 | 700.91 |
| 0 | 40 | 755.48 | 722.82 | 713.82 | 708.31 | 704.20 | 700.77 | 697.70 | 694.81 | 692.02 |
| 10 | 0 | 813.03 | 793.11 | 787.57 | 783.57 | 780.19 | 777.09 | 774.11 | 771.14 | 768.13 |
| 10 | 5 | 794.98 | 777.77 | 772.13 | 768.24 | 765.04 | 762.15 | 759.39 | 756.65 | 753.89 |
| 10 | 10 | 781.23 | 764.76 | 758.83 | 754.87 | 751.70 | 748.88 | 746.22 | 743.60 | 740.98 |
| 10 | 15 | 770.52 | 753.49 | 747.20 | 743.11 | 739.90 | 737.10 | 734.49 | 731.96 | 729.44 |
| 10 | 20 | 762.00 | 743.53 | 736.86 | 732.64 | 729.39 | 726.60 | 724.04 | 721.57 | 719.14 |
| 10 | 25 | 755.22 | 734.59 | 727.56 | 723.21 | 719.92 | 717.13 | 714.61 | 712.21 | 709.86 |
| 10 | 30 | 750.13 | 726.62 | 719.19 | 714.66 | 711.29 | 708.47 | 705.95 | 703.57 | 701.26 |
| 10 | 35 | 747.12 | 719.79 | 711.78 | 706.95 | 703.37 | 700.40 | 697.76 | 695.28 | 692.89 |
| 10 | 40 | 746.95 | 714.47 | 705.54 | 700.11 | 696.08 | 692.73 | 689.75 | 686.95 | 684.24 |
| 20 | 0 | 799.67 | 780.82 | 775.17 | 771.20 | 767.90 | 764.90 | 762.04 | 759.21 | 756.36 |
| 20 | 5 | 783.05 | 766.32 | 760.60 | 756.74 | 753.62 | 750.83 | 748.19 | 745.60 | 742.98 |
| 20 | 10 | 770.46 | 754.05 | 748.05 | 744.13 | 741.03 | 738.31 | 735.77 | 733.28 | 730.80 |
| 20 | 15 | 760.69 | 743.45 | 737.08 | 733.03 | 729.89 | 727.18 | 724.69 | 722.28 | 719.89 |
| 20 | 20 | 752.91 | 734.05 | 727.32 | 723.14 | 719.96 | 717.26 | 714.80 | 712.46 | 710.16 |
| 20 | 25 | 746.71 | 725.61 | 718.54 | 714.22 | 711.00 | 708.31 | 705.90 | 703.62 | 701.40 |
| 20 | 30 | 742.06 | 718.08 | 710.61 | 706.13 | 702.83 | 700.11 | 697.69 | 695.44 | 693.25 |
| 20 | 35 | 739.32 | 711.60 | 703.58 | 698.79 | 695.29 | 692.42 | 689.88 | 687.53 | 685.25 |
| 20 | 40 | 739.26 | 706.58 | 697.62 | 692.24 | 688.28 | 685.02 | 682.13 | 679.43 | 676.83 |
| 40 | 0 | 776.00 | 757.67 | 751.64 | 747.66 | 744.51 | 741.78 | 739.24 | 736.80 | 734.37 |
| 40 | 5 | 761.87 | 744.74 | 738.68 | 734.82 | 731.86 | 729.33 | 727.01 | 724.78 | 722.58 |
| 40 | 10 | 751.34 | 733.89 | 727.56 | 723.64 | 720.70 | 718.22 | 715.98 | 713.86 | 711.77 |
| 40 | 15 | 743.27 | 724.54 | 717.86 | 713.81 | 710.81 | 708.35 | 706.15 | 704.09 | 702.08 |
| 40 | 20 | 736.88 | 716.26 | 709.22 | 705.04 | 702.00 | 699.54 | 697.38 | 695.38 | 693.46 |
| 40 | 25 | 731.80 | 708.79 | 701.43 | 697.12 | 694.04 | 691.58 | 689.46 | 687.52 | 685.68 |
| 40 | 30 | 728.00 | 702.11 | 694.37 | 689.89 | 686.74 | 684.24 | 682.11 | 680.19 | 678.37 |
| 40 | 35 | 725.85 | 696.36 | 688.06 | 683.27 | 679.90 | 677.24 | 674.98 | 672.93 | 671.01 |
| 40 | 40 | 726.08 | 691.91 | 682.67 | 677.25 | 673.39 | 670.30 | 667.64 | 665.22 | 662.92 |
| 100 | 0 | 726.57 | 698.68 | 690.19 | 685.80 | 683.25 | 681.73 | 680.85 | 680.41 | 680.27 |
| 100 | 5 | 717.28 | 689.55 | 681.15 | 676.94 | 674.60 | 673.31 | 672.66 | 672.45 | 672.53 |
| 100 | 10 | 711.11 | 682.28 | 673.68 | 669.44 | 667.14 | 665.91 | 665.35 | 665.23 | 665.42 |
| 100 | 15 | 706.88 | 676.16 | 667.27 | 662.91 | 660.56 | 659.33 | 658.80 | 658.73 | 658.99 |
| 100 | 20 | 703.80 | 670.71 | 661.50 | 657.01 | 654.60 | 653.35 | 652.83 | 652.79 | 653.10 |
| 100 | 25 | 701.47 | 665.68 | 656.14 | 651.49 | 648.99 | 647.70 | 647.17 | 647.14 | 647.46 |
| 100 | 30 | 699.91 | 661.07 | 651.09 | 646.19 | 643.53 | 642.12 | 641.48 | 641.37 | 641.62 |
| 100 | 35 | 699.49 | 657.09 | 646.41 | 641.05 | 638.02 | 636.30 | 635.38 | 634.99 | 634.98 |
| 100 | 40 | 701.00 | 654.22 | 642.30 | 636.07 | 632.32 | 629.94 | 628.40 | 627.41 | 626.78 |

Table 27

Adiabatic lapse rate, $\Gamma(S, t, p)$, in mK/MPa, Eq. (10)

| MPa | °C | $S = 0$ | $S = 5$ | $S = 10$ | $S = 15$ | $S = 20$ | $S = 25$ | $S = 30$ | $S = 35$ | $S = 40$ |
|-----|----|---------|---------|----------|----------|----------|----------|----------|----------|----------|
| 0 | 0 | −4.386 | −3.069 | −1.845 | −0.681 | 0.434 | 1.506 | 2.537 | 3.532 | 4.491 |
| 0 | 5 | 1.061 | 2.124 | 3.132 | 4.102 | 5.041 | 5.953 | 6.839 | 7.701 | 8.541 |
| 0 | 10 | 5.937 | 6.808 | 7.642 | 8.452 | 9.240 | 10.010 | 10.763 | 11.498 | 12.216 |
| 0 | 15 | 10.387 | 11.111 | 11.808 | 12.487 | 13.150 | 13.797 | 14.430 | 15.048 | 15.652 |
| 0 | 20 | 14.515 | 15.124 | 15.712 | 16.283 | 16.840 | 17.383 | 17.913 | 18.429 | 18.933 |
| 0 | 25 | 18.400 | 18.907 | 19.399 | 19.879 | 20.347 | 20.803 | 21.248 | 21.682 | 22.104 |
| 0 | 30 | 22.099 | 22.497 | 22.894 | 23.289 | 23.678 | 24.063 | 24.442 | 24.815 | 25.182 |
| 0 | 35 | 25.657 | 25.915 | 26.203 | 26.508 | 26.825 | 27.150 | 27.482 | 27.820 | 28.162 |
| 0 | 40 | 29.109 | 29.173 | 29.321 | 29.521 | 29.761 | 30.035 | 30.339 | 30.670 | 31.025 |
| 10 | 0 | −1.989 | −0.758 | 0.384 | 1.469 | 2.506 | 3.502 | 4.459 | 5.381 | 6.268 |
| 10 | 5 | 3.034 | 4.025 | 4.964 | 5.868 | 6.744 | 7.595 | 8.422 | 9.226 | 10.008 |
| 10 | 10 | 7.557 | 8.366 | 9.144 | 9.900 | 10.637 | 11.357 | 12.060 | 12.748 | 13.421 |
| 10 | 15 | 11.706 | 12.379 | 13.030 | 13.664 | 14.284 | 14.889 | 15.481 | 16.060 | 16.626 |
| 10 | 20 | 15.574 | 16.142 | 16.690 | 17.224 | 17.745 | 18.252 | 18.747 | 19.230 | 19.700 |
| 10 | 25 | 19.229 | 19.702 | 20.162 | 20.611 | 21.048 | 21.474 | 21.889 | 22.293 | 22.686 |
| 10 | 30 | 22.721 | 23.092 | 23.464 | 23.833 | 24.198 | 24.558 | 24.912 | 25.261 | 25.603 |
| 10 | 35 | 26.090 | 26.329 | 26.599 | 26.885 | 27.184 | 27.491 | 27.806 | 28.126 | 28.451 |
| 10 | 40 | 29.369 | 29.421 | 29.560 | 29.750 | 29.982 | 30.249 | 30.546 | 30.869 | 31.218 |
| 20 | 0 | 0.278 | 1.428 | 2.494 | 3.505 | 4.471 | 5.396 | 6.285 | 7.139 | 7.960 |
| 20 | 5 | 4.910 | 5.831 | 6.705 | 7.548 | 8.365 | 9.158 | 9.928 | 10.678 | 11.407 |
| 20 | 10 | 9.103 | 9.854 | 10.577 | 11.281 | 11.968 | 12.640 | 13.297 | 13.940 | 14.569 |
| 20 | 15 | 12.971 | 13.595 | 14.200 | 14.791 | 15.368 | 15.933 | 16.485 | 17.026 | 17.554 |
| 20 | 20 | 16.594 | 17.120 | 17.631 | 18.128 | 18.612 | 19.085 | 19.546 | 19.995 | 20.432 |
| 20 | 25 | 20.031 | 20.471 | 20.899 | 21.316 | 21.722 | 22.119 | 22.504 | 22.879 | 23.244 |
| 20 | 30 | 23.328 | 23.672 | 24.017 | 24.361 | 24.700 | 25.036 | 25.366 | 25.690 | 26.009 |
| 20 | 35 | 26.518 | 26.736 | 26.987 | 27.254 | 27.535 | 27.824 | 28.122 | 28.425 | 28.733 |
| 20 | 40 | 29.632 | 29.671 | 29.798 | 29.979 | 30.202 | 30.461 | 30.750 | 31.068 | 31.411 |
| 40 | 0 | 4.423 | 5.428 | 6.356 | 7.234 | 8.071 | 8.871 | 9.637 | 10.371 | 11.076 |
| 40 | 5 | 8.364 | 9.158 | 9.914 | 10.643 | 11.350 | 12.036 | 12.703 | 13.352 | 13.983 |
| 40 | 10 | 11.971 | 12.611 | 13.233 | 13.840 | 14.433 | 15.014 | 15.583 | 16.140 | 16.685 |
| 40 | 15 | 15.331 | 15.862 | 16.380 | 16.887 | 17.384 | 17.871 | 18.347 | 18.813 | 19.269 |
| 40 | 20 | 18.509 | 18.956 | 19.392 | 19.818 | 20.233 | 20.638 | 21.033 | 21.418 | 21.792 |
| 40 | 25 | 21.548 | 21.922 | 22.287 | 22.644 | 22.992 | 23.331 | 23.660 | 23.981 | 24.291 |
| 40 | 30 | 24.485 | 24.774 | 25.069 | 25.364 | 25.656 | 25.946 | 26.231 | 26.512 | 26.788 |
| 40 | 35 | 27.348 | 27.523 | 27.734 | 27.966 | 28.213 | 28.471 | 28.738 | 29.013 | 29.295 |
| 40 | 40 | 30.158 | 30.166 | 30.270 | 30.431 | 30.638 | 30.884 | 31.164 | 31.474 | 31.813 |
| 100 | 0 | 13.938 | 14.618 | 15.237 | 15.814 | 16.356 | 16.868 | 17.350 | 17.806 | 18.236 |
| 100 | 5 | 16.452 | 16.947 | 17.419 | 17.873 | 18.310 | 18.732 | 19.139 | 19.532 | 19.910 |
| 100 | 10 | 18.797 | 19.171 | 19.540 | 19.901 | 20.255 | 20.602 | 20.939 | 21.269 | 21.589 |
| 100 | 15 | 21.030 | 21.329 | 21.628 | 21.925 | 22.216 | 22.501 | 22.780 | 23.052 | 23.316 |
| 100 | 20 | 23.190 | 23.441 | 23.694 | 23.944 | 24.190 | 24.431 | 24.666 | 24.895 | 25.116 |
| 100 | 25 | 25.305 | 25.514 | 25.730 | 25.948 | 26.165 | 26.380 | 26.591 | 26.798 | 27.000 |
| 100 | 30 | 27.396 | 27.547 | 27.725 | 27.917 | 28.118 | 28.325 | 28.536 | 28.751 | 28.968 |
| 100 | 35 | 29.481 | 29.536 | 29.659 | 29.822 | 30.015 | 30.235 | 30.476 | 30.738 | 31.017 |
| 100 | 40 | 31.567 | 31.463 | 31.499 | 31.623 | 31.816 | 32.068 | 32.373 | 32.728 | 33.129 |

References

- Alberty, R. A. (2001). Use of Legendre transforms in chemical thermodynamics. *Pure and Applied Chemistry*, 73, 1349–1380.
- Archer, D. G., & Carter, R. W. (2000). Thermodynamic properties of the NaCl + H₂O System. 4. Heat capacities of H₂O and NaCl(aq) in cold-stable and supercooled states. *Journal of Physical Chemistry, B104*, 8563–8584.
- Bacon, S., & Fofonoff, N. (1996). Oceanic heat flux calculation. *Journal of Atmospheric and Oceanic Technology*, 13, 1327–1329.
- Barber, C. R. (1969). The international practical temperature scale of 1968. *Metrologia*, 5, 35–44.
- Barlow, A. J., & Yazgan, E. (1967). Pressure dependence of the velocity of sound in water as a function of temperature. *British Journal of Applied Physics*, 18, 645–651.
- Bigg, P. H. (1967). Density of water in SI units over the range 0–40°C. *British Journal of Applied Physics*, 18, 521–525.
- Blanke, W. (1989). Eine neue Temperaturskala. Die Internationale Temperaturskala von 1990 (ITS-90). *PTB-Mitteilungen*, 99, 411–418.
- Bradshaw, A. (1978). Calculation of the potential temperature of seawater from the effect of pressure on entropy. *Deep-Sea Research*, 25, 1253–1257.
- Bradshaw, A., & Schleicher, K. E. (1970). Direct measurements of thermal expansion of sea water under pressure. *Deep-Sea Research*, 17, 691–706.
- Bradshaw, A., & Schleicher, K. E. (1976). Compressibility of distilled water and seawater. *Deep-Sea Research*, 23, 583–593.
- Bradshaw, A., & Schleicher, K. E. (1986). An empirical equation of state for pure water in the oceanographic region of temperature and pressure determined from direct measurements. *Journal of Chemical and Engineering Data*, 31, 189–194.
- Brewer, P. G., & Bradshaw, A. (1975). The effect of the non-ideal composition of sea water on salinity and density. *Journal of Marine Research*, 33, 157–175.
- Bromley, L. A. (1968). Relative enthalpies of sea salt solutions at 25°C. *Journal of Chemical and Engineering Data*, 13, 399–402.
- Bromley, L. A., Desaussure, V. A., Clipp, J. C., & Wright, J. S. (1967). Heat capacities of sea water solutions at salinities of 1 to 12‰ and temperatures of 2° to 80°C. *Journal of Chemical and Engineering Data*, 12, 202–206.
- Bromley, L. A., Diamond, A. E., Salami, E., & Wilkins, D. G. (1970). Heat capacities and enthalpies of sea salt solutions to 200°C. *Journal of Chemical and Engineering Data*, 15, 246–253.
- Bryden, H. L. (1973). New polynomials for the thermal expansion, adiabatic temperature gradient and potential temperature of sea water. *Deep-Sea Research*, 20, 401–408.
- Caldwell, D. R. (1978). The maximum density points of pure and saline water. *Deep-Sea Research*, 25, 175–181.
- Caldwell, D. R., & Eide, S. A. (1980). Adiabatic temperature gradient and potential temperature correction in pure and saline water: an experimental determination. *Deep-Sea Research*, 27A, 71–78.
- Chen, C. -T., & Millero, F. J. (1976). The specific volume of seawater at high pressures. *Deep-Sea Research*, 23, 595–612.
- Chen, C. -T., & Millero, F. J. (1977). Sound speed of seawater at high pressures. *The Journal of the Acoustical Society of America*, 62, 1129–1135.
- Coplen, T. B. (2001). Atomic weights of the elements 1999. *Pure and Applied Chemistry*, 73, 667–683.
- Cox, R. A., & Smith, N. D. (1959). The specific heat of seawater. *Proceedings of the Royal Society London, Ser. A*, 252, 51–62.
- Del Grosso, V. A. (1970). Sound speed in pure water and seawater. *The Journal of the Acoustical Society of America*, 47, 947–949.
- Del Grosso, V. A. (1974). New equation for the speed of sound in natural waters (with comparison to other equations). *The Journal of the Acoustical Society of America*, 56, 1084–1091.
- Del Grosso, V. A., & Mader, C. W. (1972). Speed of sound in pure water. *The Journal of the Acoustical Society of America*, 52, 1442–1446.
- Doherty, B. T., & Kester, D. R. (1974). Freezing point of seawater. *Journal of Marine Research*, 32, 285–300.
- Dushaw, B. D., Worcester, P. F., Cornuelle, B. D., & Howe, B. M. (1993). On equations for the speed of sound in seawater. *The Journal of the Acoustical Society of America*, 94, 255–275.
- Falkenhagen, H., & Ebeling, W. (1971). *Theorie der Elektrolyte*. Leipzig: S. Hirzel.
- Feistel, R. (1993). Equilibrium thermodynamics of seawater revisited. *Progress in Oceanography*, 31, 101–179.
- Feistel, R. (1998). On the physical chemistry of seawater with deviating ion composition. *Zeitschrift für Physikalische Chemie*, 204, 27–44.
- Feistel, R., & Hagen, E. (1994). Thermodynamic quantities in oceanography. In S. K. Majumdar (Ed.), *The oceans: Physical-chemical dynamics and human impact* (pp. 1–16). Easton: The Pennsylvania Academy of Science.
- Feistel, R., & Hagen, E. (1995). On the GIBBS thermodynamic potential of seawater. *Progress in Oceanography*, 36, 249–327.
- Feistel, R., & Hagen, E. (1998). A Gibbs thermodynamic potential of sea ice. *Cold regions science and technology*, 28, 83–142. corrigendum (1999) 29, 173–176.
- Fofonoff, N. P. (1962). Physical properties of sea-water. In M. N. Hill (Ed.), *The Sea* (pp. 3–30). New York: J. Wiley and Sons.
- Fofonoff, N. P. (1985). Physical Properties of Seawater: A New Salinity Scale and Equation of State of Seawater. *Journal of Geophysical Research*, 90, 3332–3342.

- Fofonoff, N. P., & Millard, R. C. (1983). Algorithms for the computation of fundamental properties of seawater. *Unesco technical papers in marine science*, 44.
- Fujii, K. (1994). Accurate measurements of the sound velocity in pure water under high pressure. *12. Symposium on Thermophysical Properties*, Boulder, Colorado, USA.
- Fujii, K., & Masui, R. (1993). Accurate measurements of the sound velocity in pure water by combining a coherent phase-detection technique and a variable path-length interferometer. *The Journal of the Acoustical Society of America*, 93, 276–282.
- Fujino, K., Lewis, E. L., & Perkin, R. G. (1974). The freezing point of seawater at pressures up to 100 Bars. *Journal of Geophysical Research*, 79, 1792–1797.
- Gill, A. E. (1982). *Atmosphere Ocean Dynamics*. San Diego: Academic Press.
- Gonfiantini, R. (1978). Standards for stable isotope measurements in natural compounds. *Nature*, 271, 534–536.
- Haar, L., Gallagher, J. S., & Kell, G. S. (1988). *NBS/NRC Steam Tables*. Washington, New York, London: Hemisphere Publishing Corp.
- Henderson, S. J., & Speedy, R. J. (1987). Melting Temperature of Ice at Positive and Negative Pressures. *Journal of Physical Chemistry*, 91, 3069–3072.
- IAPWS (1996). *Release on the IAPWS Formulation 1995 for the Thermodynamic Properties of Ordinary Water Substance for General and Scientific Use*. Palo Alto: IAPWS Secretariat. WWW Page, <http://www.iapws.org/release.htm>.
- IAPWS (1997). *Release on the Static Dielectric Constant of Ordinary Water Substance for Temperatures from 238 K to 873 K and Pressures up to 1000 MPa*. Erlangen: IAPWS Secretariat. WWW Page, <http://www.iapws.org/release.htm>.
- Jupp, T., & Schultz, A. (2000). A thermodynamic explanation for black smoker temperatures. *Nature*, 403, 880–883.
- Kell, G. S. (1975). Density, thermal expansibility and compressibility of liquid water from 0 to 150°C: corrections and tables for atmospheric pressure and saturation reviewed and expressed on 1968 temperature scale. *Journal of Chemical and Engineering Data*, 20, 97–105.
- Kell, G. S., & Whalley, E. (1975). Reanalysis of the density of liquid water in the range 0–150°C and 0–1 kbar. *Journal of Chemical Physics*, 62, 3496–3503.
- Krümmel, O. (1893). *Geophysikalische Beobachtungen*. Kiel und Leipzig: Verlag von Lipsius & Tischer.
- Landau, L. D., & Lifschitz, E. M. (1966). *Statistische Physik*. Lehrbuch der Theoretischen Physik Bd.V. Berlin: Akademie-Verlag.
- Landau, L. D., & Lifschitz, E. M. (1974). *Hydrodynamik*. Lehrbuch der Theoretischen Physik Bd.VI. Berlin: Akademie-Verlag.
- Lewis, E. L., & Perkin, R. G. (1981). The practical salinity scale 1978: Conversion of existing data. *Deep-Sea Research*, 28A, 307–328.
- Lewis, E. L., & Randall, M. (1961). *Thermodynamics*. New York, Toronto, London: McGraw-Hill.
- Mamayev, O., Dooley, H., Millard, B., Taira, K., & Morcos, S. (1991). *Processing of oceanographic station data*. Unesco.
- Mamedov, A. M. (1979). O skorosti ultrazvuka v vode v širokom diapazone temperatur i davlenij. *Inzhenerno-Fizicheskij Zhurnal*, 36, 156–160.
- McDougall, T. J. (2003). Potential Enthalpy: A conservative oceanic variable for evaluating heat content and heat fluxes. *Journal of Physical Oceanography*, 33, 945–963.
- McDougall, T. J., Jackett, D. R., Wright, D. G., & Feistel, R. (2003). Accurate and Computationally Efficient Algorithms for Potential Temperature and Density of Seawater. *Journal of Atmospheric and Oceanic Technology*, 20, 730–741.
- Meinen, C. S., & Watts, D. R. (1997). Further evidence that the sound-speed algorithm of Del Grosso is more accurate than that of Chen and Millero. *The Journal of the Acoustical Society of America*, 102, 2058–2062.
- Menaché, M. (1976). Table of absolute density of standard mean ocean water (SMOW) as a function of temperature from 0°C to 40°C. *Unesco technical papers in marine science*, 24, 33–36.
- Millero, F. J. (1978). Freezing point of seawater. *Unesco technical papers in marine science*, 28, 29–35.
- Millero, F. J. (1982). The thermodynamics of seawater. Part I. The PVT properties. *Ocean Science and Engineering*, 7, 403–460.
- Millero, F. J. (1983). The thermodynamics of seawater. Part II. Thermochemical properties. *Ocean Science and Engineering*, 8, 1–40.
- Millero, F. J. (2000). Effect of changes in the composition of seawater on the density-salinity relationship. *Deep-Sea Research I*, 47, 1583–1590.
- Millero, F. J. (2003). Private communication
- Millero, F. J., Chen, C. -T., Bradshaw, A., & Schleicher, K. (1980). A new high pressure equation of state for seawater. *Deep-Sea Research*, 27A, 255–264.
- Millero, F. J., Chen, C. -T., Bradshaw, A., & Schleicher, K. (1981c). Summary of data treatment for the international high pressure equation of state for seawater. *Unesco technical papers in marine science*, 38, 99–192.
- Millero, F. J., Gonzalez, A., & Ward, G. K. (1976a). The density of seawater solutions at one atmosphere as a function of temperature and salinity. *Journal of Marine Research*, 34, 61–93.
- Millero, F. J., Hansen, L. D., & Hoff, E. V. (1973b). The enthalpy of seawater from 0 to 30°C and from 0 to 40 °C salinity. *Journal of Marine Research*, 31, 21–39.
- Millero, F. J., & Kremling, K. (1976c). The densities of Baltic Sea waters. *Deep-Sea Research*, 23, 1129–1138.
- Millero, F. J., & Leung, W. H. (1976b). The thermodynamics of seawater at one atmosphere. *American Journal of Science*, 276, 1035–1077.

- Millero, F. J., & Li, X. (1994). Comments on “On equations for the speed of sound in seawater” [J. Acoust. Soc. Am. 94, 255–275 (1993)]. *The Journal of the Acoustical Society of America*, 95, 2757–2759.
- Millero, F. J., Perron, G., & Desnoyers, J. E. (1973a). Heat capacity of seawater solutions from 5° to 35° and 0.5 to 22‰ chlorinity. *Journal of Geophysical Research*, 78, 4499–4507.
- Millero, F. J., & Poisson, A. (1981a). International one-atmosphere equation of state of seawater. *Deep-Sea Research*, 28A, 625–629.
- Millero, F. J., & Poisson, A. (1981b). Summary of data treatment for the international one atmosphere equation of state for seawater. *Unesco technical papers in marine science*, 38, 19–85.
- Millero, F. J., & Sohn, M. L. (1992). *Chemical Oceanography*. Boca Raton: CRC Press.
- Mohr, P. J., & Taylor, B. N. (1999). CODATA Recommended Values of the Fundamental Physical Constants: 1998. Article simultaneously published in (2000), Review of Modern Physics, 72, 351–495 *Journal of Physical and Chemical Reference Data*, 28, 1713–1852.
- Osborne, N. S., Stimson, H. F., & Ginnings, D. C. (1939). Measurements of heat capacity and heat of vaporization of water in the range 0° to 100°C. *Part of Journal of Research of the National Bureau of Standards*, 23, 197–260.
- Petit, J. P., Tufeu, R., & Le Neindre, B. (1983). Determination of the Thermodynamic Properties of Water from Measurements of the Speed of Sound in the Temperature Range 251.15–293.15 K and the Pressure Range 0.1–350 MPa. *International Journal of Thermophysics*, 4, 35–50.
- Poisson, A., Brunet, C., & Brun-Cottan, J. C. (1980). Density of standard seawater solutions at atmospheric pressure. *Deep-Sea Research*, 27, 1013–1028.
- Poisson, A., & Gadhoumi, M. H. (1993). An extension of the Practical Salinity Scale 1978 and the Equation of State 1980 to high salinities. *Deep-Sea Research I*, 40, 1689–1698.
- Poisson, A., Gadhoumi, M. H., & Morcos, S. (1991). Salinity and density of seawater: Tables for high salinities (42 to 50). *Unesco technical papers in marine science*, 62, 1–85.
- Poisson, A., Lebel, J., & Brunet, C. (1981). The densities of western Indian Ocean, Red Sea and eastern Mediterranean surface waters. *Deep-Sea Research*, 28A, 1161–1172.
- Preston-Thomas, H. (1990). The international temperature scale of 1990 (ITS-90). *Metrologia*, 27, 3–10.
- Rögener, H., & Soll, P. (1980). Beitrag zum Thermodynamischen Meßverfahren—der isentrope Temperatur-Druck-Koeffizient des Wassers. *Brennstoff-Wärme-Kraft*, 32, 472–478.
- Rohde, K. -H. (1966). Untersuchungen über die Calcium-und Magnesiumanomalie in der Ostsee. *Beiträge zur Meereskunde*, 19, 18–31.
- Rossini, F. D., Wagman, D. D., Evans, W. H., Levine, S., & Jaffe, I. (1952). Selected values of chemical thermodynamic properties. *National Bureau of Standards Circular*, 500, 126–128.
- Saunders, P. (1990). The International Temperature Scale of 1990, ITS-90. *WOCE Newsletter*, 10.
- Saunders, P. M. (1995). The Bernoulli function and flux of energy in the ocean. *Journal of Geophysical Research*, 22647–22648.
- Siedler, G. (1998). SI-Einheiten in der Ozeanographie, SI units in oceanography. *Berichte aus dem Institut für Meereskunde an der Christian-Albrechts-Universität Kiel*, 101.
- Siedler, G., & Peters, H. (1986). Properties of seawater. In J. Sündermann (Ed.), (pp. 233–264). *Oceanography*, Landolt-Börnstein New Series V/3a, Berlin, Heidelberg: Springer.
- Siegert, M. J., Ellis-Evans, J. C., Tranter, M., Mayer, C., Petits, J. -R., Salamantin, A., & Priscu, J. C. (2001). Physical, chemical and biological processes in Lake Vostok and other Antarctic subglacial lakes. *Nature*, 414, 603–609.
- Slesarenko, V., & Shtim, A. (1989). Determination of Seawater Enthalpy and Entropy During the Calculation of Thermal Desalination Plants. *Desalination*, 71, 203–210.
- Spiesberger, J. L., & Metzger, K. (1991). A new algorithm for sound speed in seawater. *The Journal of the Acoustical Society of America*, 91, 2677–2788.
- Stimson, H. F. (1955). Heat units and temperature scales for calorimetry. *American Journal of Physics*, 23, 614–622.
- Tanaka, M., Girard, R., Davis, R., Peuto, A., & Bignell, N. (2001). Recommended table for the density of water between 0°C and 40°C based on recent reports. *Metrologia*, 38, 301–309.
- Tillner-Roth, R. (1998). *Fundamental Equations of State*. Aachen: Shaker Verlag.
- Tsunogai, S., Kusakabe, M., Iizumi, H., Koike, I., & Hattori, A. (1979). Hydrographic features of the deep water of the Bering Sea—the Sea of Silica. *Deep-Sea Research*, 26, 641–659.
- Unesco (1981a). Tenth report of the joint panel on oceanographic tables and standards. *Unesco technical papers in marine science*, 36.
- Unesco (1981b). Background papers and supporting data on the practical salinity scale 1978. *Unesco technical papers in marine science*, 37.
- Unesco (1981c). Background papers and supporting data on the international equation of state of seawater 1980. *Unesco technical papers in marine science*, 38.
- Unesco (1985). The international system of units (SI) in oceanography. *Unesco technical papers in marine science*, 45.
- Unesco (1986). Progress on oceanographic tables and standards 1983–1986: Work and recommendations of the Unesco/SCOR/ICES/IAPSO Joint Panel. *Unesco technical papers in marine science*, 50.

- Wagenbreth, H., & Blanke, W. (1971). Die Dichte des Wassers im Internationalen Einheitensystem und in der Internationalen Praktischen Temperaturskala von 1968. *PTB-Mitteilungen*, 81, 412–415.
- Wagner, W., & Pruß, A. (2002). The IAPWS formulation 1995 for the thermodynamic properties of ordinary water substance for general and scientific use. *Journal of Physical and Chemical Reference Data*, 31, 387–535.
- Wagner, W., Saul, A., & Pruß, A. (1994). International equations for the pressure along the melting and along the sublimation curve of ordinary water substance. *Journal of Physical and Chemical Reference Data*, 23, 515–527.
- Warren, B. A. (1999). Approximating the energy transport across oceanic sections. *Journal of Geophysical Research*, 104, 7915–7919.
- Wille, P. (1986). Properties of sea water: acoustical properties of the ocean. In J. Sündermann (Ed.), (pp. 265–382). *Oceanography*, Landolt-Börnstein Vol. V/3a. Berlin, Heidelberg: Springer.
- Wilson, W. D. (1959). Speed of sound in distilled water as a function of temperature and pressure. *The Journal of the Acoustical Society of America*, 31, 1067–1072.

Corrigendum

Corrigendum to: A new extended Gibbs thermodynamic
potential of seawater [Progress in Oceanography
58 (2003) 43–114] ☆

Rainer Feistel *

Baltic Sea Research Institute, D-18119 Warnemünde, Germany

Available online 10 May 2004

Page 46: *The sentence*

The recently published equation of state of McDougall et al. (2003) is a computationally faster but numerically equivalent formulation of FH95 for use in numerical models, restricted to naturally occurring combinations of salinity, temperature and pressure, so-called ‘Neptunian’ waters, and formulated in terms of potential density as function of salinity, potential temperature, and pressure.

must read

The recently published equation of state of McDougall et al. (2003) is a computationally faster but numerically equivalent formulation of FH95 for use in numerical models, restricted to naturally occurring combinations of salinity, temperature and pressure, so-called ‘Neptunian’ waters, and formulated in terms of density as function of salinity, potential temperature, and pressure.

Page 82: *Eq. (53)*

$$S = 1.004867 \cdot c / (\text{g/kg})$$

must read

$$c / (\text{g/kg}) = 1.004867 \cdot S$$

☆ DOI of original article 10.1016/S0079-6611(03)00088-0.

* Tel.: +49-381-5197-152; fax: +49-381-5197-4818.

E-mail address: rainer.feistel@io-warnemuende.de (R. Feistel).